

Abstract

SANCHEZ, ANGELICA. Colloidal Gels of Fumed Silica: Microstructure, Surface Interactions and Temperature Effects. (Under the direction of Prof. Saad A. Khan.)

The interactions of fumed oxides with organic solvents, polymers, and biological systems are of great interest as they can be utilized as viscosity modifiers, fillers or adsorbents when mixed in or in contact with such materials. Fumed silica is of particular interest due to the large surface area that its branched structure provides for establishing interactions with specific matrices or chemical reactive groups. If these small particles are dispersed in an appropriate medium, they can form suspensions, flocculated systems or three-dimensional networks; thus an understanding of how to control this microstructure is of paramount importance, and forms the main thrust of this dissertation. Rheology, a reliable, easy, and readily available technique, is employed not only to characterize the systems but also to study their microstructure and establish correlations that can subsequently be employed to tailor the material for a particular application.

In this work, various types of fumed silica (FS) particles are dispersed in different oligoethers and in high-molecular weight poly(ethylene oxide) PEO and their properties evaluated with the aim to fine tune them for improved performance during end use. In particular, we examine dispersions of hydrophobic and hydrophilic fumed silica in oligoethers of different molecular weights and end group composition at different temperatures by using dynamic rheology. We observe that hydrophilic fumed silica particles form gels in the less polar oligoethers, whereas the hydrophobic ones form a network in all the oligoethers employed. Increasing the temperature irreversibly increases the gel modulus of the system

containing hydrophilic fumed silica in the oligoether that allows for the FS to form a network (poly(ethylene glycol)dimethyl ether PEGdm(250)). We also investigate the effects of fumed silica particle concentration in PEGdm(250); a larger relative change in the gel modulus was observed for the materials containing lower concentration of fumed silica. A “concentration” effect due to polymer adsorption and chemical reaction on the particles’ surface seems to explain this anomalous observation.

We also study how the hydrophobic group length attached on the fumed silica particles affects the rheological properties, in particular the yield stress of the dispersions. Additionally, we take advantage of a material instability known as wall slip to explore how chemical composition of the shearing surface modifies the flow behavior of gels containing particles with different surface functionalities. Dynamic stress sweep experiments with hydrophobic and hydrophilic surfaces suggest that specific interactions between the nanoparticles contained in the gel and the plates’ surface control the extent of wall slip. By combining dynamic mechanical rheology and flow visualization, it has been possible to accurately determine the yield stress of the gels and differentiate between yielding of the material and slipping at the wall.

Mixtures of fumed silica particles, hydrophobic and hydrophilic, have been dispersed in PEGdm(250) and PEG(200), and the effects of temperature on the rheological properties of the systems has been evaluated. In PEGdm(250), the mixtures shows a negative deviation from the log-additive mixing rule within the temperature range studied. This indicates that the two types of particles form independent networks that provide less mechanical stability than each individual component in the system. In PEG(200), the samples containing 100 and 75 % hydrophobic fumed silica, show no significant change in

elastic modulus at different temperatures. In addition, these materials behave more gel-like than their mirror image compositions, i.e., 0 and 25 % hydrophobic fumed silica.

In order to explore the effects of adding a low-molecular weight oligoether to PEO containing hydrophobic and hydrophilic fumed silica, blends of high- and low- molecular weight (MW) PEOs have been prepared by melt and solution mixing. In the composition range studied, the blends containing hydrophilic fumed silica are more susceptible to the presence of the low-MW component. Blends containing more of the high-MW component behave as liquid-like as the low-MW concentration in the blend increases; but the behavior reverses at the 50/50 high- to low-MW composition, where the gel formation mechanism of the fumed silica in the low-MW component dominates and a gel-like behavior is observed. Both hydrophobic and hydrophilic fumed silica show the same trend when dispersed in the mixed-MW PEOs.

Our results are encouraging and, taken together, establish a new approach for designing methods that facilitate processing of these particulate materials and the control of their flow and “at rest” properties while establishing the underlying mechanisms dictating such behavior.

Colloidal Gels of Fumed Silica: Microstructure, Surface Interactions and Temperature Effects

by

Angelica Sanchez

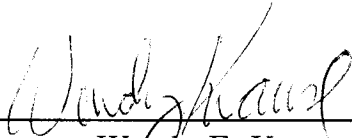
A dissertation submitted to the Graduate Faculty of
North Carolina State University
In partial fulfillment of the requirements of
Doctor of Philosophy

Chemical Engineering

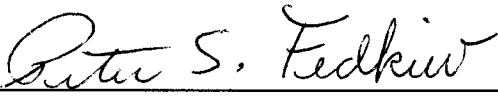
Raleigh, NC 27695

May 2006

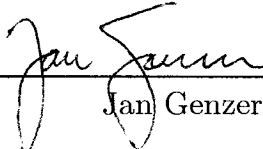
Approved by:



Wendy E. Krause



Peter S. Fedkiw



Jan Genzer



Orlin D. Velev



Saad A. Khan

Chair of Advisory Committee

This work is dedicated to my dad, Luis Alberto, my mom, Gladys and my sisters Laura and Albertina, for their continuous support and encouragement and for giving me so many happy moments.

Biography

Angelica Sanchez was born on June 13, 1972 in Barquisimeto, Venezuela to her parents Luis Alberto and Gladys. After graduating from high-school, she moved to Caracas to attend Simon Bolivar University and in 1995, she received a Bachelor in Materials Engineering majoring in polymers. After finishing her BS, she decided to pursue graduate studies and in 1994 she obtained a Master Scientarium in Materials Engineering from Simon Bolivar University. Following two years of teaching in the Materials Engineering program at Simon Bolivar University and inspired by her mentor, Prof. Alejandro Müller, she decided to continue her graduate studies, and in 2001 was accepted to the Chemical Engineering program at North Carolina State University. Angelica's dissertation research was guided by Prof. Saad Khan. During her time at NC State, Angelica actively participated in several departmental activities, including social chair of the Chemical Engineering Graduate Students Association and Recruiting captain, among others. Upon successful completion of her PhD studies in May 2006, Angelica will join Cabot Corporation as a R&D engineer in Billerica, MA.

Acknowledgments

I would like to acknowledge my advisor Prof. Saad A. Khan for his guidance, support and encouragement. I believe that my experience at NC State as a graduate student has been much more enjoyable because of Dr. Khan's extraordinary personality. His humanity and sense of humor made reports, proposals, papers, and group meetings truly distinct and pleasant experiences (to a certain extent ;). If I had to go through the advisor selection process again, I would certainly choose him as my mentor.

I am grateful to Professors Fedkiw, Genzer, Krause, and Velev for serving on my advisory committee. The Chemical and Biomolecular Engineering department at NC State has a fantastic group of people and I am grateful for the opportunities that I was given during this past five years. I would like to thank Prof. George Roberts for his valuable advice and encouragement during my mentored teaching assistantship. Also, I would like to thank Dr. Fedkiw for his time and dedication, the fruitful discussions and useful comments and suggestions during these past years of research with the Khan and Fedkiw group. I would like to especially thank Dr. Velev for being directly or indirectly, part of my career progress. His enthusiasm and dedication are truly inspiring, even for those who, like me, are not part of his group. I also express my gratitude to Dr. Genzer; thank you very much for the advice and teachings, for the laughs and your friendship.

I would like to recognize the invaluable help that I received from the members of the Khan group (past and present), especially Jeff, Ahmed A., Ahmed E., Jeremy, Collins, Shamsheer, Lauriane, Sachin, Dave (the wave), Joshua, and Annie. It really makes a big difference having someone to discuss a funny result or to just chat for a little bit while the sample is in the rheometer...

I believe that I have had the most wonderful time here at NC State, and I have said thanks to many people who inspired and guided my career; however, this would not have been possible without the company, friendship, support, and encouragement of my friends. I do not think I would ever have enough time to thank Joan (Fabs), my most favorite friend ever, Paulie, and Brian for all the help, laugh, and fun that they provided me since the very first day of grad school; 2001 was a fabulous class. Sometimes I wonder if this would have been as fun without having someone like you guys to share from ice cream to shopping to volleyball, running, coffee breaks (and everything in between). Thanks Jimmy and Jeff for your friendship and for all the fabulous moments that we spent together, and the memories, of course...I miss you guys. I have a very special thank you reserved for Papa, there are so many reasons to thank you... I think that your company, patience, and caring made my last years in Raleigh absolutely terrific. Cooking became much more fun after I met you.

Who would have thought that when the south met the south she liked it so much? Thanks Mosh and Jonny B for smiling and making me smile (and laugh) and for reminding me everyday that boys with good manners rule! This would not have been complete without acknowledging my fantastic roommates, Julie and Quentin. Thank you so much for all the love you gave me and for always making me feel so special. I would like to say thanks to Chris for the espresso times, the fun conversations (even the dorky ones were fun!), and all your help with research, and to April for Chris (hehe), all the fun times with the babes, and your help with finding my way around town.

Table of Contents

List of Figures	xii
List of Tables	xvii
Chapter 1	
Motivation, Goals and Background.....	2
1.1 Motivation and Goals	2
1.2 Background.....	4
1.2.1 Fumed silica: synthesis, characteristics and use.....	4
1.2.2 Colloidal interactions in self-assembled fumed silica nanocomposites.....	7
1.2.3 Rheology as a tool for characterizing self-assembled systems.....	9
1.2.4 Steady shear rheology	10
1.2.5 Dynamic Shear.....	11
1.2.6 Rheology and microstructure	12
1.2.7 Rheology and microstructure of self-assembled fumed systems.....	14
1.3 References.....	17
Chapter 2	
Yield Stress vs. Wall Slip in Colloidal Gels of Fumed Silica: Effects of Geometry Surface Energy on Slip Properties.....	21
Abstract.....	21

2.1	Introduction	22
2.2	Experimental	26
2.2.1	Materials and Methods.....	25
2.2.2	Flow visualization.....	29
2.3	Results and Discussion.....	30
2.3.1	Linear viscoelastic properties of fumed silica gels.....	30
2.3.2	Yield stress vs. wall slip: effects of surface chemistry on slip of FS particulate gels.....	34
2.3.3	Combined flow visualization and mechanical rheology to decipher yield stress and wall slip.....	40
2.4	Conclusions.....	46
2.5	References.....	46
Chapter 3		
	Anomalous Temperature Behavior of Fumed Silica Nanoparticulate Gels in Low-MW Polyethers.....	49
	Abstract.....	51
3.1	Introduction.....	51
3.2	Experimental.....	53
3.2.1	Rheological Characterization.....	55
3.2.2	Extraction and Thermogravimetric Analysis (TGA).....	55

3.3	Results and Discussion.....	56	
3.3.1	Effect of temperature on the dynamic rheological properties of FS gels.....	56	
3.3.2	Temperature sweeps vs. isothermal studies.....	59	
3.3.3	Effect of particle concentration on the dynamic rheological properties of hydrophilic FS gels.....	62	
3.3.4	Chemical reaction vs. physical adsorption.....	66	
3.3.5	Effect of end group type and content on temperature response of hydrophilic FS in polyether dispersions.....	69	
3.4	Conclusions.....	72	
3.5	References.....	73	
Chapter 4			
Effects of Temperature on Polyethers Using Mixtures of Hydrophilic and Hydrophobic Fumed Silicas as Gelling Agents.....			77
Abstract.....			77
4.1	Introduction.....	78	
4.2	Experimental.....	83	
4.3	Results and Discussion.....	84	
4.3.1	Rheological properties of mixed fumed silicas in PEGdm(250).....	84	
4.3.2	Rheological properties of mixed fumed silicas in PEG(200).....	86	

4.3.3	Effects of temperature on the rheological behavior of gels of mixed FS in PEGdm(250)	90
4.4	Conclusions.....	102
4.5	References.....	103
Chapter 5		
	Blends of Low- and High-Molecular Weight Poly(ethylene oxide). Nanocomposites and Composite Polymer Electrolytes.....	107
	Abstract.....	107
5.1	Introduction.....	108
5.2	Experimental.....	111
5.2.1	Rheological Characterization.....	112
5.2.2	Thermal Properties.....	112
5.2.3	PEO Purification.....	113
5.3	Results and Discussion.....	113
5.3.1	Rheological Properties of Mixed-MW systems.....	106
5.3.2	Thermal Properties of mixed-MW systems.....	125
5.3.3	Solution Mixing versus Melt mixing.....	126
5.4	Conclusions.....	129
5.5	References.....	129

Chapter 6

Conclusions and Recommendations.....	133
6.1 Conclusions.....	134
6.1.1 Fumed Silica Forms Gels that Exhibit Yield Stress.....	134
6.1.2 Temperature affects the flow properties of fumed silica gels in an unexpected manner.....	135
6.1.3 Mixtures of hydrophobic and hydrophilic fumed silica particles form independent microstructures when dispersed in a liquid.....	136
6.1.4 Fumed silica acts as a reinforcing filler in blends of high- to low-MW PEO ratio but forms a three-dimensional physical network as the ratio decreases.....	137
6.2 Recommendations.....	138
6.2.1 Biocompatible PEO-silica hybrids.....	138
6.2.2 In-depth study of the dispersibility of fumed silica in formulations to be utilized as composite polymer electrolytes.....	139
6.2.3 Study of the rheological properties of high- and low-molecular weight PEO blends at low temperatures.....	140
6.2.4 Novel organic-inorganic hybrids for use as composite resin cements.....	140
6.3 References.....	141

List of Figures

Figure 1.1. Schematic of fumed or pyrogenic fumed silica formation ^{8, 15}	5
Figure 1.2. Schematic of rheological responses for different types of microstructures: a) non-flocculated, b) flocculated, and c) gel systems.....	13
Figure 2.1. Flow visualization setup showing a schematic of the paint line technique for determining slip velocity.	30
Figure 2.2. Elastic and viscous moduli as a function of frequency for the five dispersions of fumed silica (10wt%) in PEGdm(250).	31
Figure 2.3. Schematic of the proposed interactions between hydrophilic (case A) and hydrophobic (case B and C) fumed silica in slightly polar medium (i.e. in PEGdm(250)).	33
Figure 2.4. Elastic modulus as a function of stress amplitude for (a) A200-C10 and (b) A200-C18 fumed silica in PEGdm(250) at 25 °C.....	35
Figure 2.5. Elastic stress as a function of strain amplitude for (a) A200-C10 and (b) A200-C18 fumed silica dispersions.....	37
Figure 2.6. Effect of the test geometry surface energy on the critical stress for slip for gels of 10 wt% hydrophobic FS in PEGdm(250) as a function of the length of the alkyl chain attached to the surface of the FS particles.....	39
Figure 2.7. van der Waals interaction potential (Vvdw) normalized by kT (k is the Boltzmann constant and T the absolute temperature in K) between FS	

- particles and PDMS covered plates. FS particles are considered to be spherical in shape for the calculations.....40
- Figure 2.8. Snapshots and strain wave form obtained during a stress sweep for gels of A200-C8 in PEGdm(250) tested with hydrophobic and hydrophilic plates at (a) 15 Pa and (b) 31 Pa.42
- Figure 2.9. Snapshots and strain wave form obtained during a time sweep for gels of A200-C8 in PEGdm(250) tested with smooth, serrated, hydrophobic, and hydrophilic plates at different stress amplitudes and time.45
- Figure 3.1. Elastic modulus as a function of frequency for dispersions of hydrophobic (R805) and hydrophilic (A200) fumed silica in PEGdm(250) at 25 and 80 °C.59
- Figure 3.2. Suggested mechanism for PEGdm(250) adsorption on the surface of hydrophilic fumed silica at higher temperature. The arrows identified by (a) and (b) indicate the two suggested hypothesis for increase in the elastic modulus of the A200 gels when thermal energy is provided to the system.59
- Figure 3.3. Temperature sweeps at 0.4 °C/min for dispersions of hydrophobic (R805) and hydrophilic (A200) fumed silica in PEGdm(250). The inset depicts a dynamic time sweep at 80 °C for hydrophilic FS (A200) in PEGdm(250). The dynamic rheological experiments were done in the rheometer at 1 rad/s.60

- Figure 3.4. Temperature sweeps for dispersions of hydrophilic fumed silica (A200) in PEGdm(250) at different concentrations. The dynamic rheological experiments were performed in the rheometer at 1 rad/s.61
- Figure 3.5. Effect of thermal treatment on the rheological properties of various dispersions of hydrophilic fumed silica (A200): (a) Elastic modulus (G') and (b) Normalized elastic modulus ($G'/G'_{t=0}$) vs time at 80 °C. The thermal treatment was performed in the rheometer at 80 °C and 1 rad/s.....64
- Figure 3.6. Elastic modulus versus frequency at 25 and 80 °C for 2 wt% hydrophilic FS (A200) in PEGdm(250)65
- Figure 3.7. Dependence of the elastic modulus on volume fraction for dispersions of hydrophilic (A200) fumed silica in PEGdm(250) at 25 and 80 °C.....67
- Figure 3.8. TGA of fumed silica extracts before and after thermal treatment at 80 °C for 4 h. In all cases the silica was washed and dried several times until constant weight loss was obtained. The temperature scans were conducted at 10 °C/min.66
- Figure 3.9. Derivative of the weight loss (dW/dT) as a function of temperature of fumed silica extracts before and after thermal treatment at 80 °C for 4 h.70
- Figure 3.10. Suggested mechanism for the condensation of PEGdm(250) molecules on the surface of hydrophilic fumed silica upon heating to 80 °C.....72
- Figure 3.11. Effect of PEG end group on the rheological properties of hydrophilic (A200) fumed silica dispersions as a function of temperature. The

rheological experiments were done in the rheometer at 1 rad/s and 0.4 °C/min. The data correspond to two steps, heating (closed symbols) and cooling (open symbols) after the previous step.....72

Figure 3.12. Effect of PEG end group amount on the rheological properties of hydrophilic (A200) fumed silica dispersions as a function of temperature.....73

Figure 4.1. Frequency sweeps of PEGdm(250)+10wt% fumed silica at 25 °C. Results are shown for different blends of hydrophilic (A200) and hydrophobic (R805) fumed silicas. The inset shows the elastic modulus at 1 rad/s as a function of A200 content in the mixture. The dashed line represents the log-additive mixing rule.85

Figure 4.2. Dynamic moduli as a function of frequency at various temperatures for (a)25/75 FS A200/R805 and (b)75/25 FS A200/R805.....87

Figure 4.3. Elastic modulus as a function of strain at various temperatures for (a)25/75 FS A200/R805 and (b)75/25 FS A200/R805. Samples contain 10 wt% FS in PEGdm(250).89

Figure 4.4. Effect of temperature on the critical strain and ultimate modulus before catastrophic failure for gels of 10 wt% mixed FS (A200/R805) in PEGdm(250).92

Figure 4.5. Cohesive energy as a function of temperature for various mixed FS compositions in PEGdm(250). Total content of FS in the colloid is 10 wt%.....94

- Figure 4.6. Effect of fumed silica surface chemistry on the elastic modulus of PEGdm(250)+10wt% FS at different temperatures. The concentration of FS is expressed in g of hydrophilic per g of mixed FS (hydrophilic (A200) + hydrophobic (R805)) in the colloid.93
- Figure 4.9. Dynamic moduli as a function of frequency at various temperatures for (a)25/75 FS A200/R805 and (b)75/25 FS A200/R805.....100
- Figure 4.10. Effect of fumed silica surface chemistry on the elastic modulus of PEG(200)+10wt% FS at different temperatures. The concentration of FS is expressed in g of hydrophilic per g of mixed FS (hydrophilic (A200) + hydrophobic (R805)) in the colloid.....102
- Figure 5.1. Dynamic moduli as a function of frequency for as received and purified PEO 200k at 80 °C.104
- Figure 5.2. Thermal properties of the purified and as received PEO 200k. (a) DSC cooling scans and (b) DSC heating scans. In all cases, the scans were performed at 10 °C/min.105
- Figure 5.3. Dynamic moduli as a function of frequency for PEO 200k without fumed silica and with 10 wt% of hydrophilic (A200) or hydrophobic (R805) fumed silica. The data were collected at 80 °C.107
- Figure 5.4. Elastic and viscous (a) and elastic (b) moduli as a function of frequency for PEO 200k/PEGdm(250) blends + 10 wt% hydrophilic (A200) FS.....120
- Figure 5.5. Elastic and viscous (a) and elastic (b) moduli as a function of frequency for PEO 200k/PEGdm(250) blends + 10 wt% hydrophobic (R805) FS....111

- Figure 5.6. Elastic modulus as a function of PEGdm(250) content in blends of PEO 200k/PEGdm(250) + 10 wt% FS at different frequencies (ω). The closed symbols correspond to the blends containing hydrophilic FS (A200) and the open symbols to the blends containing hydrophobic FS (R805). The connecting lines are added to guide the eye.112
- Figure 5.7. Elastic modulus versus stress amplitude for mixed systems containing hydrophilic (A200) and hydrophobic FS. Experiments were done at 80 °C.124
- Figure 5.8. Effect of mixing method (solution versus melt mixing) on the rheological properties of mixed-MW systems. All the experiments were performed at 80 °C.125
- Figure 5.9. Ionic conductivity as a function of the inverse temperature.....117

List of Tables

Table 1.1. Physical properties of some commercially available fumed silicas.....	6
Table 2.1. Physical properties of commercial and in-house modified FS used in this work.....	28
Table 3.1. Molecular characteristics of the polyethers employed in this work.....	53
Table 4.1. Physical characteristics of the fumed silicas used in this work ¹⁰	84

*1**Motivation, Goals and Background*

1.1 Motivation and Goals

Fumed silica based gels and nanocomposites have been the subject of several research studies¹⁻⁴ due to their importance in applications such as reinforced polymeric systems, membranes, composite polymer electrolytes, and fiber optics cable gels. Fumed silica is an amorphous, non-porous form of silicon dioxide (SiO_2) with a very low density and a powdery appearance. It is prepared by flame hydrolysis of SiCl_4 with the end product consisting of primary spherical particles of ~ 10 nm in diameter which fused together to form branched structures of 100 nm or more (details of this process are presented in Figure 1.1 and section 1.1.2). The native surface is hydrophilic, with silanol groups (Si-OH) being the characteristic functionality. These silanol groups can be replaced by other moieties, so that interactions between particles or particle-medium can be tuned. When such nano particles are added to a continuum phase to prepare a colloidal dispersion, three states of aggregation are likely to occur^{5, 6}: *a*) particulates do not interact with each other (or interactions are minimal) and remain isolated, *b*) fumed silica particles form clusters or flocs, and *c*) a three dimensional network is formed by flocculation of the clusters. The first situation is known as a stable suspension and the last one is usually referred to as a gel.

To design a particular material with desirable properties, an understanding of the intrinsic organization of the system components is required. Colloidal science and technology has suggested interesting approaches to explain the nature of forces governing the system; this however, is not an easy task since there is a large number of factors involved in the particular self-assembly characteristics.

An overarching goal of this project is to combine micro- and macroscopic techniques to evaluate the behavior of fumed silica particles in continuum phases. In particular, low-molecular weight and high-molecular weight poly(ethylene oxide) will be used as the continuous media in which fumed silica particles containing different surface chemistries will be dispersed. These systems have been extensively used^{1, 4, 6-14}; however, a fundamental understanding on the nature of interactions has not been correlated with the observed properties in a systematic fashion that allows for the prediction of a desired particular behavior under both equilibrium and flow circumstances. In particular, several issues remain unresolved. These include:

What are the mechanisms by which fumed silica particles containing different surface chain lengths interact with non-polar solvent media?

How can we tailor the properties of fumed silica gels that are formed by mixing particles with different surface functionalities?

What is an adequate way to prepare fumed silica nanocomposites containing high- and low-molecular weight polyethylene oxides? How does composition influence rheological behavior in a wide range of temperatures, crystallinity?

How is the wall slip phenomenon in fumed silica nanoparticulate gels affected by the surface functionality of both particles and the surface of rheometer plates?

The following sections will briefly go over some general background aspects that are necessary to explain and understand the topics covered in this dissertation. Each chapter however, contains more specific details about the particular issues discussed thereafter.

1.2 Background

1.2.1 Fumed silica: synthesis, characteristics and use

The molecular reaction of silicon tetrachloride (SiCl_4) vapor in a flame of oxygen and hydrogen leads to the formation of an amorphous form of silicon dioxide (SiO_2) through the reaction:



The product, a fluffy, white, amorphous powder with a very low apparent density, is known as “fumed silica” and the synthesis process is referred to as flame hydrolysis (or vapor phase process). As illustrated in Figure 1.1, the flame hydrolysis process initially produces spherical particles of approximately 7 to 14 nm in diameter, which collide while hot and fuse into aggregates of 0.1 μm . These aggregates are branched, chain-like structures, and can be considered as fumed silica primary structure, since the fusion process is irreversible. Further collisions give place to physical entanglement of aggregates to form agglomerates after cooling. Agglomerates are the product of non-specific forces such as dipole-dipole and hydrogen bonding; therefore these can be dispersed by simple mixing^{15, 16}.

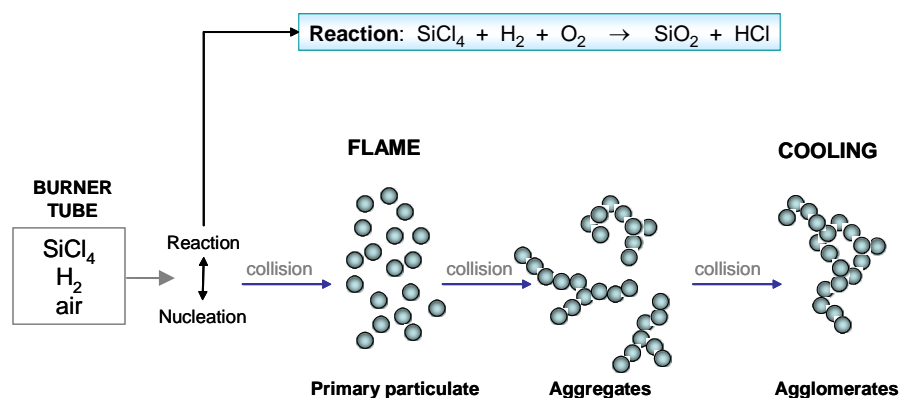


Figure 1.1. Schematic of fumed or pyrogenic fumed silica formation^{8, 15}.

The conditions under which the process takes place allows for the product to have different physical properties, such as particle size, and surface area, among others. Typically primary particle sizes oscillate between 10 to 20 nm, and the surface areas between 100 to 400 m² per g, due to the branched structure of the aggregates. These characteristics give fumed silica interesting and convenient properties as a reinforcing material, as well as thickener agents, due to its ability to create three-dimensional networks¹⁶⁻¹⁸. The native form of fumed silica has a hydrophilic surface chemistry, being that the silanol (Si-OH) and siloxane (Si₂O) functional groups play a major role in the behavior of fumed silica. Silanol density is approximately¹⁷ 2.5 Si-OH per nm², which gives the possibility of interactions through hydrogen bonding not only between particles, but also with solvent media and polymers.

Different synthetic schemes have been employed to modify the surface properties of fumed silica. Surface modification by organofunctional silanes has been used in a variety of applications such as fiber-reinforced nanocomposites and coupling agents, antimicrobials, catalysts, and immobilized enzymes among others. Silylation reactions of fumed silica with

alkyltrialkoxysilanes, $X(\text{CH}_2)_n(\text{SiO})_3$, have been extensively employed to modify the silica surface. The functional group X of the silane coupling agent may be an amine, alcohol, epoxide, or acrylate group capable of interacting with the matrix^{19, 20}. Chlorosilanes have been also employed as silica surface modifiers due to their use as deactivating agents. These reactions provide a way to improve the compatibility between matrix (or solvent medium) and filler in composite materials as well as to effectively modify flow properties in low-molecular weight polymers. As will be described later, this particular property is of paramount importance in composite polymer electrolytes used in lithium batteries applications since high ionic conductivity of low-molecular weight polymers can be combined with the high mechanical properties that the fumed silica networks provide to these materials²¹⁻²⁵.

Based on the versatility, economics, and availability of fumed silica our group has proposed novel composite materials which serve from the interactions (chemical or physical) between solvent media and filler that can be used in lithium batteries applications^{1, 2}. Table 1.q shows some of the commercially available fumed silica types as well as their respective physical properties.

Table 1.1. Physical properties of some commercially available fumed silicas

Fumed silica name	Dominant surface group	OH density (mmol/g)	Silanol (Si-OH) unreacted (%)
A200	Silanol (Si-OH)	0.84	100
R974	Di-methyl (Si-(CH ₃) ₂)	0.42	50
R805	Octyl (Si-(C ₈ H ₁₇))	0.44	52

1.2.2 Colloidal interactions in self-assembled fumed silica nanocomposites

Suspensions of small particles are often called “colloids”. Similar to molecules composed of covalently bonded atoms, the force between colloidal particles can be described by using a potential function $W(r)$, which in the case of spherical molecules separated by a distance r is given by:

$$F = -\frac{dW}{dr} \quad (2)$$

where F is the force between molecules.

The basic forces governing colloidal particle suspensions can be divided into several groups: excluded volume, van der Waals, electrostatic, hydrogen bonding, and hydrophobic^{5, 26}. Excluded volume interactions are a repulsive force that result from crystalline ordering. These types of interactions are short-ranged and they depend on the flexibility of the particles interacting. The second type, van der Waals interactions, arises from attractive dipole-dipole interactions, and can be divided into London or dispersion interactions, Keesom, and Debye forces. In suspensions, van der Waals forces are considered on a continuum basis. The interaction potential between spherical particles A of radius a in a medium B, can be calculated using eqn. 3:

$$W_{vdW} = -\frac{A_H}{12} \left\{ \frac{1}{(x+1)^2 - 1} + \frac{1}{(1+x)^2} + 2 \ln \left[1 - \frac{1}{(1+x)^2} \right] \right\} \quad (3)$$

where A_H is the Hamaker constant, which can be estimated from the Leifshitz theory of dispersion forces in a continuum as:

$$A_H = \frac{3}{4} k_B T \left(\frac{\epsilon_A - \epsilon_B}{\epsilon_A + \epsilon_B} \right)^2 + \frac{3h\nu_e}{16\sqrt{2}} \frac{(n_A^2 - n_B^2)^2}{(n_A^2 + n_B^2)^{3/2}} \quad (4)$$

Where A_H = Hamaker constant

ϵ_i = dielectric constant of material i (particle A or medium B)

n = refractive index

ν_e = main ultraviolet absorption frequency (usually $\sim 3 \times 10^{15} \text{ sec}^{-1}$)

k_B = Boltzmann constant

T = absolute temperature

If r is the distance between the centers of the spheres, and $D = r - 2a$, then x is defined as $D/2a$. As can be seen from eqns. 3 and 4, van der Waals interactions in suspensions yield particle coagulation, with the Hamaker constant a parameter that allows to quantify the strength of the attractive forces between particles^{26, 27}.

The third type of interactions, electrostatics, is present in materials that contain ions; these interactions are usually expressed in terms of the Poisson-Boltzmann equation. Counterion concentration and medium dielectric constant determine the thickness of the double layer formed next to the charged surface. This thickness is defined by the Debye length, which is sensitive to the electrolyte concentration^{26, 27}. A theory that describes net colloidal interactions between particles was proposed by Derjaguin and Landau, and Verwey

and Overbeek in the 1940's. The so-called DLVO theory postulates that the force between two surfaces can be approximated by the sum of electrostatic and van der Waals interactions. Several approaches have been employed to describe the stability of fumed silica particles in both polar and non-polar media. In some cases, DLVO theory holds and can be used to predict interaction potential and stability; however, in some other cases, the theory does not reproduce the behavior obtained experimentally. In these cases, other type of interactions, such as hydrogen bonding and hydrophobic interactions, play an important role in the system and predictions from the theory are not accurate²⁸⁻³¹. Hydrogen bonding is a type of solvation force between electronegative atoms (like oxygen and fluorine) and hydrogen. It is considered as an electrostatic interaction where the H atom is not shared but remains closer to and covalently bound to its parent atom²⁶. It is of considerable importance in colloidal systems since it often induces molecular association. The binding energies in these colloidal systems are of 10 – 40 kJ/mol; this compared with van der Waals interactions binding energies, which are approximately 1 kJ/mol, makes hydrogen bonds a type of interaction considerable strong, though not as strong as covalent or ionic bonds (~ 500 kJ/mol). Additionally, hydrogen bonds are directional and specific, which allows for them to form three-dimensional structures in solids and short-range structures in liquids.

1.2.3 Rheology as a tool for characterizing self-assembled systems

Rheology is a science that studies the deformation of materials as a result of an applied stress. It is useful in characterizing soft condensed matter including complex and structured fluids. This importance in characterizing colloidal systems arises from the fact

that information on the microstructure in equilibrium and under flow conditions can be obtained by using appropriate rheological techniques. Moreover, valuable knowledge on processing and handling of materials can be also obtained from these measurements. Rheological measurements can be performed under steady or dynamic shear mode and depending upon the response of the fluid, the microstructure can be probed.

1.2.4 Steady shear rheology

In steady shear rheology, a sample is deformed by applying a constant shear rate ($\dot{\gamma}$). After an adequate period of time, the shear stress (τ) reaches steady state and a material function, called the apparent viscosity (η), can be determined by taking the ratio between stress and shear rate:

$$\eta = \frac{\tau}{\dot{\gamma}} \quad (5)$$

The behavior of η as a function of $\dot{\gamma}$ or flow curve is used to classify the flow behavior of fluids. If the apparent viscosity does not depend on the applied shear rate, the fluid is known as Newtonian. Fluids that observe a viscosity increase with shear rate are named shear-thickening and those with a decrease in viscosity as a function of shear rate are shear-thinning. Some fluids flow after exceeding a certain stress value; this stress is known as the yield stress and it indicates the susceptibility of the microstructure to breakdown under applied forces^{5, 32}.

1.2.5 Dynamic Shear

Oscillatory shear or dynamic mechanical spectroscopy experiments impose small-amplitude oscillatory shearing to the sample. For example, if a sinusoidal strain (γ) is applied:

$$\gamma = \gamma_o \sin(\omega t) \quad (6)$$

where γ_o is the strain amplitude and ω the frequency of oscillation. The resulting stress τ varies sinusoidally with time and is given by

$$\tau = \tau_o \sin(\omega t + \delta) \quad (7)$$

τ is not necessarily in phase with the applied strain (δ is the phase angle), and if γ_o is small enough (usually $\ll 1$), the stress is represented according to eqn. 8. The regime in which this equation is valid is known to as the linear viscoelastic regime,

$$\tau(t) = \gamma_o \left[G'(\omega) \sin(\omega t) + G''(\omega) \cos(\omega t) \right] \quad (8)$$

$G'(\omega)$ and $G''(\omega)$ are the storage and loss modulus, respectively. The storage modulus is in phase with the strain and is commonly associated with the elastic energy of the material, whereas the loss modulus is in phase with the strain rate and represents the viscous dissipation of that energy⁵. The ratio G''/G' is known as the loss tangent ($\tan \delta$) and is higher than unity for liquid-like materials, and smaller than unity for materials that behave solid-like.

The importance of this type of measurements arises from the fact that at low strain values the “at rest” microstructure can be probed since it is not disrupted by shearing as in

steady shear flow experiments. This is very useful in colloidal systems because the state of aggregation can be associated with the particular rheological response within the linear viscoelastic regime obtained from the dynamic mechanical spectrum of the material, $G'(\omega)$ and $G''(\omega)$.

1.2.6 Rheology and microstructure

In this section, the correlation between rheology and microstructure is addressed. In spite of the fact that rheology as a macroscopic characterization technique cannot specifically elucidate what the nature of the microstructure is, it provides an easily accessible way to correlate this microstructure with the particular responses shown by a system. At this point, it is pertinent to introduce several terms that are commonly used to describe states of aggregation in colloidal systems.

Particles dispersed in a solvent medium possess a non-flocculated or deflocculated microstructure when the forces between particles are negligible. The typical rheological behavior for this type of system is schematized in Figure 1.2(a) where the elastic and viscous moduli are plotted as a function of frequency. It can be seen that for all range of experimentally evaluated frequencies (typically between 0.01 and 100 rad/s) the viscous modulus dominates the rheological response. Similar behavior has been observed for polymer solutions, with a characteristic terminal zone at low frequencies where G' and G'' scale with ω to the power of 2 and 1, respectively. In general, non-flocculated systems can be obtained by stabilizing the particles in such a way that attractive net forces (mainly van der Waals) are overcome by electrostatic or steric stabilization (repulsive forces).

Figure 1.2(b) shows the rheological response of a flocculated dispersion. The elastic modulus and viscosity increase considerably due to particles aggregation or floc formation. A floc is equivalent to an aggregate; it can be disrupted by shear and its strength depends on the magnitude of the attractive force between particles. This aggregation of particles gives a more elastic material with less marked frequency dependence of G' . The limiting case for particles aggregation corresponds to a gel. Figure 1.2(c) shows that when the forces between particles and the concentration allow for the floc size to increase and form a three-dimensional network; G' is completely frequency independent and dominates over G'' . This type of microstructure is known as a gel and it exhibits solid-like behavior, similar to chemically cross-linked polymeric networks.

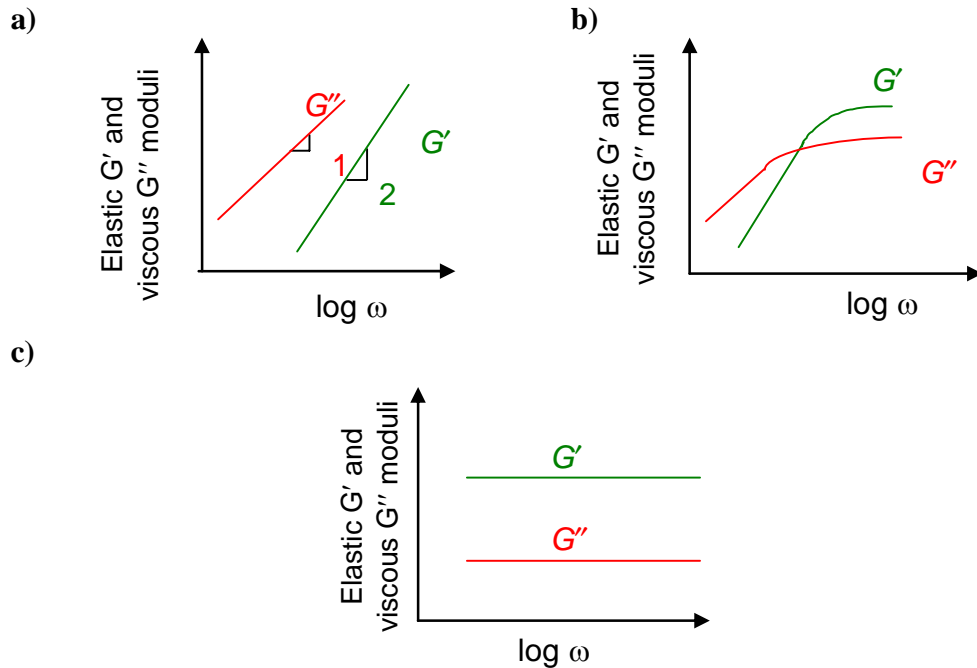


Figure 1.2. Schematic of rheological responses for different types of microstructures: a) non-flocculated, b) flocculated, and c) gel systems.

1.2.7 Rheology and microstructure of self-assembled fumed systems

The literature on fumed silica as thickening agent and reinforcing material in polymeric systems is considerably extensive^{16, 18, 31}. In this section, a review of the most important findings of fumed silica fillers in high-molecular weight polymers as well as in organic liquids is presented. In particular, the relationships between microstructure and rheological properties are highlighted.

The use of fumed silica systems prevails due to the possibility of network (gel-like structure) formation in a variety of solvent media. As was mentioned before, this ability has been extended by the modification of its native surface chemistry through chemical reactions. Early studies focused on low-molecular weight poly(dimethyl siloxane) (PDMS) containing fumed silica^{33, 34}. It was found that the filler imparted thixotropic behavior to the system. The results were interpreted in terms of phenomenological microstructural models of particle interactions through polymer absorption on the silica surface. Khan and Zoeller³ used rheological measurements and light scattering to study samples of polar and nonpolar solvents containing fumed silica with different surface chemistries. They suggested the possibility of three modes of solvent-particles interactions: primary bridging, occurring through hydrogen bonding between unmodified silica particles in mineral oil; secondary bridging, observed in hydrophobic fumed silica particles in poly(propylene glycol), PPG; and no bridging between particles as it was observed for unmodified fumed silica particles in PPG. These systems also exhibited different self-similar (fractal) structures depending on the nature of the solvent.

Raghavan *et al.*⁴ proposed a useful correlation between the elastic modulus of the fumed silica network and surface chains and solvent medium solubility parameter difference. The study comprised a variety of polyether liquids and fumed silica particles with octyl chains tethered to the surface. The results suggested that “reverse steric stabilization” dictated flocculation in the systems, higher elastic modulus was observed in those gels with the larger mismatch in solubility parameters.

Scaling relationships showing the dependence of elastic modulus on fractal dimension of the network and volume fraction have been proposed³⁵⁻³⁷. A power law model described by:

$$G' \sim \phi^n \quad (9)$$

has been suggested, where ϕ is the particle volume fraction and n a parameter used to characterize the mechanism of aggregation.

If the rate at which two particles stick together is lower than the rate of mass transfer, the mechanism is referred to as chemically limited aggregation, and n takes a value of 4.5 ± 0.2 . For diffusion limited cluster-cluster aggregation, n has a value of 4.0 ± 0.5 ³⁸. Khan and Zoeller³ reported a value of $n = 4$ in fumed silica dispersed in mineral oil; this is in excellent agreement with the predicted value of Buscall *et al.*³⁵. Walls³⁹ obtained n value of 4.1 ± 0.4 for colloidal gels of hydrophobic fumed silica ($\sim 50\%$ surface coverage of C_8H_{17}) in poly(ethylene glycol) dimethyl ether (250 M_n), suggesting a diffusion limited cluster-cluster aggregation process. This value was only slightly affected by the presence of salts in

concentrations ranging up to 1.86M, suggesting that the salt does not affect the mechanism of gel formation.

The behavior of fumed silica particles in high-molecular weight polymer matrices is significantly different than that observed in low-molecular weight systems. The high viscosity limits the possibility of interaction between colloidal particles. As such, the volumes required to impact the mechanical properties and flow behavior are higher than those required for molar mass solvents. A limited number of studies have been undertaken on fumed silica/high-molecular weight polymer systems. Zhang and Archer⁴⁰ studied high molecular weight poly(ethylene oxide) (PEO) containing silica nanoparticles. They found that filler particles have a stronger effect on the low-frequency rheological response than at high-frequency values, suggesting that the relaxation dynamics is more affected than the plateau modulus by the presence of silica particles. Thermal annealing of samples after compounding as well as compounding method seem to have an important effect on the microstructure. After annealing two possible situations are suggested, the occurrence of flocculation and the increase of the immobilized PEO layer on the silica particles. Tsagaropoulos and Eisenberg⁴¹ reported a second glass transition temperature (T_g) in a system containing silica particles in high-molecular weight polymers. This transition, which occurred at higher temperature than the bulk polymer, was interpreted in terms of the presence of a low mobility group of chains.

The microstructure and in consequence, the mechanical properties of filled polymers are strongly affected by the nature of the reinforcing particles. Aranguren⁴² reported that poly(dimethyl siloxane) containing silica particles with fewer silanol groups on the surface

formed network structures at higher volume fractions. For polymers capable of interacting with the particles surface through specific interactions such as hydrogen bonding, an increase in viscosity has been reported⁴³. Similar results were reported by Yerian *et al.*⁴⁴ in PEO containing hydrophobic and hydrophilic fumed silica particles. Hydrophilic fumed silica systems are more elastic due to the strongest bridging effect between particles and polymer.

1.3 References

1. Raghavan, S. R.; Riley, M. W.; Fedkiw, P. S.; Khan, S. A., Composite polymer electrolytes based on poly(ethylene glycol) and hydrophobic fumed silica: Dynamic rheology and microstructure. *Chemistry of Materials* 1998, 10, (1), 244-251.
2. Hou, J.; Baker, G. L., Preparation and characterization of cross-linked composite polymer electrolytes. *Chemistry of Materials* 1998, 10, (11), 3311-3318.
3. Khan, S. A.; Zoeller, N. J., Dynamic Rheological Behavior of Flocculated Fumed Silica Suspensions. *Journal of Rheology* 1993, 37, (6), 1225-1235.
4. Raghavan, S. R.; Hou, J.; Baker, G. L.; Khan, S. A., Colloidal interactions between particles with tethered nonpolar chains dispersed in polar media: Direct correlation between dynamic rheology and interaction parameters. *Langmuir* 2000, 16, (3), 1066-1077.
5. Larson, R. G., *The Structure and Rheology of complex Fluids*. Oxford University Press, Inc.: New York, 1999.
6. Raghavan, S. R.; Khan, S. A., Shear-Induced Microstructural Changes in Flocculated Suspensions of Fumed Silica. *Journal of Rheology* 1995, 39, (6), 1311-1325.
7. Barthel, H.; Dreyer, M.; Gottschalk-Gaudig, T.; Litvinov, V.; Nikitina, E., Fumed silica - Rheological additive for adhesives, resins, and paints. *Macromolecular Symposia* 2002, 187, 573-584.

8. Barthel, H.; Rosch, L.; Weis, J., Fumed Silica- Production, Properties, and Applications. In *Organosilicon Chemistry II: From Molecules to Materials*, Auner, N.; Weis, J., Eds. VCH Publishers: Weinheim, Germany, 1996; pp 761-777.
9. Khan, S. A.; Baker, G. L.; Colson, S., Composite Polymer Electrolytes Using Fumed Silica Fillers - Rheology and Ionic-Conductivity. *Chemistry of Materials* 1994, 6, (12), 2359-2363.
10. Khan, S. A.; Maruca, M. A.; Plitz, I. M., Rheology of Fumed Silica Dispersions For Fiberoptic Cables. *Polymer Engineering and Science* 1991, 31, (24), 1701-1707.
11. Raghavan, S. R.; Baker, G. L.; Khan, S. A., Colloidal silica gels for use as novel electrolytes for rechargeable batteries: Synthesis, microstructure and rheology. *Abstracts of Papers of the American Chemical Society* 1998, 216, U601-U601.
12. Raghavan, S. R.; Fussell, G. W.; Khan, S. A., Fumed silica dispersions in polymeric liquids: Evidence for site-specific colloidal interactions. *Abstracts of Papers of the American Chemical Society* 1997, 214, 332-POLY.
13. Raghavan, S. R.; Khan, S. A., Shear-thickening response of fumed silica suspensions under steady and oscillatory shear. *Journal of Colloid and Interface Science* 1997, 185, (1), 57-67.
14. Raghavan, S. R.; Walls, H. J.; Khan, S. A., Rheology of silica dispersions in organic liquids: New evidence for solvation forces dictated by hydrogen bonding. *Langmuir* 2000, 16, (21), 7920-7930.
15. Legrand, A. P., *The Surface Properties of Silicas*. John Wiley & Sons: London, 1998.
16. Iler, R. K., *The Chemistry of Silica: Solubility, Polymerization, Colloid and Surface Properties, and Biochemistry*. John Wiley & Sons: New York, NY, 1979; p xxiv, 866.
17. Basic Characteristics of Aerosil; Degussa Technical Bulletin No. 11; Degussa Corp.: Akron, OH, 1993.
18. Mathias, J.; Wannemacher, G., Basic Characteristics and Applications of Aerosil. *Journal of Colloid and Interface Science* 1988, 125, 61-68.
19. Leyden, D. E., Silanes, surfaces, and interfaces: proceedings of the Silanes, Surfaces, and Interfaces Symposium Snowmass, Colorado, June 19-21, 1985. Gordon and Breach: New York, 1986; p xi, 599.

20. Joseph, R.; Zhang, S. M.; Ford, W. T., Structure and dynamics of a colloidal silica poly(methyl methacrylate) composite by C-13 and Si-29 MAS NMR spectroscopy. *Macromolecules* 1996, 29, (4), 1305-1312.
21. Scrosati, B.; Croce, F.; Panero, S., Progress in lithium polymer battery R&D. *Journal of Power Sources* 2001, 100, (1-2), 93-100.
22. Liu, Y.; Lee, J. Y.; Hong, L., Functionalized SiO₂ in poly(ethylene oxide)-based polymer electrolytes. *Journal of Power Sources* 2002, 109, (2), 507-514.
23. Walls, H. J.; Riley, M. W.; Fedkiw, P. S.; Spontak, R. J.; Baker, G. L.; Khan, S. A., Composite electrolytes from self-assembled colloidal networks. *Electrochimica Acta* 2003, 48, (14-16), 2071-2077.
24. Walls, H. J.; Zawodzinski, T. A. J., Anion and Cation Transference Number by Electrophoretic NMR of Polymer Electrolytes Sum to Unity. *Journal of Electrochemical Society Letters* 2000, 3, (7), 321-324.
25. Walls, H. J.; Zhou, J.; Yerian, J. A.; Fedkiw, P. S.; Khan, S. A.; Stowe, M. K.; Baker, G. L., Fumed silica-based composite polymer electrolytes: synthesis, rheology, and electrochemistry. *Journal of Power Sources* 2000, 89, (2), 156-162.
26. Israelachvili, J. N., *Intermolecular and Surface Forces*. 2nd ed.; Academic Press London: London, 1991; p xxi, 450.
27. Evans, D. F.; Wennerström, H., *The colloidal domain: where physics, chemistry, biology, and technology meet*. 2nd ed.; Wiley-VCH: New York, 1999; p xl, 632.
28. Russel, W. B., Review of the Role of Colloidal Forces in the Rheology of Suspensions. *Journal of Rheology* 1980, 24, (3), 287-317.
29. Metzner, A. B., Rheology of Suspensions in Polymeric Liquids. *Journal of Rheology* 1985, 29, (6), 739-775.
30. Vincent, B.; Kiraly, Z.; Emmett, S.; Beaver, A., The Stability of Silica Dispersions in Ethanol Cyclohexane Mixtures. *Colloids and Surfaces* 1990, 49, (1-2), 121-132.
31. Chen, M.; Russel, W. B., Characteristics of Flocculated Silica Dispersions. *Journal of Colloid and Interface Science* 1991, 141, (2), 564-577.
32. Macosko, C. W., *Rheology: Principles, Measurements and Applications*. VCH: New York, NY, 1994.

33. Kosinski, L. E.; Caruthers, J. M., Rheological Properties of Poly(Dimethylsiloxane) Filled with Fumed Silica.2. Stress-Relaxation and Stress Growth. *Journal of Non-Newtonian Fluid Mechanics* 1985, 17, (1), 69-89.
34. Kosinski, L. E.; Caruthers, J. M., The effect of molecular weight on the rheological properties of poly(dimethylsiloxane) filled with fumed silica. *Rheologica Acta* 1986, 25, 153-160.
35. Buscall, R.; Mills, P. D. A.; Goodwin, J. W.; Lawson, D. W., Scaling Behavior of the Rheology of Aggregate Networks Formed from Colloidal Particles. *Journal of the Chemical Society-Faraday Transactions I* 1988, 84, 4249-4260.
36. Rueb, C. J.; Zukoski, C. F., Viscoelastic properties of colloidal gels. *Journal of Rheology* 1997, 41, (2), 197-218.
37. Shih, W. H.; Shih, W. Y.; Kim, S. I.; Liu, J.; Aksay, I. A., Scaling Behavior of the Elastic Properties of Colloidal Gels. *Physical Review A* 1990, 42, (8), 4772-4779.
38. Buscall, R.; Mills, P. D. A.; Yates, G. E., Viscoelastic Properties of Strongly Flocculated Polystyrene Latex Dispersions. *Colloids and Surfaces* 1986, 18, (2-4), 341-358.
39. Walls, H. J. Colloidal Silica Gels as Composite Electrolytes: Rheology and Ion Transport. Ph.D. Thesis, North Carolina State University, Raleigh, NC, 2002.
40. Zhang, Q.; Archer, L. A., Poly(ethylene oxide)/silica nanocomposites: Structure and rheology. *Langmuir* 2002, 18, (26), 10435-10442.
41. Tsagaropoulos, G.; Eisenberg, A., Dynamic-Mechanical Study of the Factors Affecting the 2 Glass- Transition Behavior of Filled Polymers - Similarities and Differences with Random Ionomers. *Macromolecules* 1995, 28, (18), 6067-6077.
42. Aranguren, M. I.; Mora, E.; Degroot, J. V.; Macosko, C. W., Effect of Reinforcing Fillers On the Rheology of Polymer Melts. *Journal of Rheology* 1992, 36, (6), 1165-1182.
43. Torro-Palau, A. M.; Fernandez-Garcia, J. C.; Orgiles-Barcelo, A. C.; Ferrandiz-Gomez, T. D.; Martin-Martinez, J. M., Rheological properties of polyurethane adhesives containing silica as filler: Influence of the nature and surface chemistry of silica. *Macromolecular Symposia* 2001, 169, 191-196.

44. Yerian, J. A. Nanocomposite polymer electrolytes: Modulation of mechanical properties using surface-functionalized fumed silica. Ph.D. Thesis, North Carolina State University, Raleigh, NC, 2003.

2

*Yield Stress vs. Wall Slip in Colloidal Gels
of Fumed Silica: Effects of Geometry
Surface Energy on Slip Properties*

Abstract

A combination of dynamic oscillatory experiments and flow visualization with a CCD camera is employed to evaluate the yield stress of colloidal silica (fumed) gels in low-molecular weight polyether poly(ethylene glycol)dimethyl ether (PEGdm(250)). In particular, the combination of dynamic rheology with the paint mark technique, enables us differentiate between slip and yielding. We explore how the chemical composition of the shearing surface modifies the flow behavior of gels containing particles with different surface functionalities. To do this, a set of hydrophobic FS particles was dispersed in PEGdm(250) and the effect of the testing geometry surface energy on the slip properties of the gels used as a tool to evaluate the role that colloidal interactions play during flow. Dynamic time and stress sweep experiments flow visualization suggest that specific interactions between the nanoparticles in the gel and the plates' surface control the extent of slip. We found that in the case of hydrophobic FS gels sheared on hydrophobic surfaces, the wall slip occurs but it is delayed with respect to the hydrophilic or smooth (stainless steel) geometry. These results shed new light into the processing and microstructural dynamics of complex nanoparticulate gels.

To be submitted to Journal of Rheology

Authors: A.M. Sanchez and S.A. Khan

2.1 Introduction

Complex fluids have gained special interest over the past years not only because of the appearance of new synthetic materials, but also due to the development of multicomponent systems which combine specific properties of the individual components. In addition, the possibility to utilize and promote interactions among the components is of particular interest, as those interactions allow for the development of responsive systems, materials that can be specifically tuned so that they perform differently based on the interactions dominating the microstructure, among others. The mechanisms of assembly and the role that those interactions play under particular events add on to this interest as they dictate the fluid behavior under many circumstances ¹

Whether during processing these complex fluids into end products or during their performance in a particular application, such materials are submitted to flow and deformation; therefore, a deep understanding of the fluid response under stress or deformation is of paramount importance from both manufacturing and research standpoints.

Our group has been involved in the research of some of these complex fluids systems and their flow properties for the past few years. Moreover, the dynamic and steady flow properties of fumed silica suspensions have been extensively investigated as these can be employed in various fields such as composite polymer electrolytes ²⁻⁴, paints, fiber optics cable gels, and reinforced polymeric systems among others ⁵⁻⁸.

Fumed silica is an amorphous, non-porous form of silicon dioxide (SiO_2) with a very low density and a powdery appearance. It is prepared by flame hydrolysis of SiCl_4 with the end product consisting of primary spherical particles of ~10 nm in diameter which fused

together to form branched structures of 100 nm or more^{9, 10}. The native surface is hydrophilic, with silanol groups (Si-OH) being the characteristic functionality. These silanol groups can be replaced by other moieties, so that interactions between particles or particle-medium can be tuned.

Under certain circumstances, usually dictated by the solvent media and surface chemistry of the fumed silica particles, these suspensions flocculate and form gels, i.e., solid-like materials^{5, 6, 11-13}, which can flow at a specific shear rate/stress. In these situations, characterizing the stress or shear rate at which the material starts to flow, namely finding the yield stress, is of primary significance as this is a signature property which determines the processing and application windows. Numerous studies have emphasized the necessity to establish a method or protocol to accurately characterize the yield stress of a complex fluid as experimental artifacts, inherent to either the sample or the type of geometry, can lead to erroneous values of such property.

One of the most common sources of error during yield stress determination of solid-like suspensions is the occurrence of wall slip¹⁴⁻¹⁷ or wall depletion effects as referred to by Barnes¹⁴. The migration of particles away from the geometry solid surfaces has been attributed to the hydrodynamic and entropic forces that result when the bulk is submitted to flow¹⁴. Reliable measurements have been obtained by modifying the walls surface, especially roughening by sandblasting or machining specific shapes onto the plates or cylinders¹⁸. Walls *et al*⁶ suggested chemically altering the surface of the rheometer plates as a way to prevent slip from occurring; they reported that by using hydrophobic test geometry surfaces, wall slip could be reduced in gels of hydrophobic (octyl-modified) fumed

silica particles whereas hydrophilic test geometry surfaces resembled the behavior obtained with smooth geometries. Princen¹⁹ reported that by treating the surface of the concentric cylinders geometry, reproducible flow data for concentrated oil-in-water emulsions was obtained. Moreover, the aqueous phase of the emulsion wetted the surface and this is kept separate from the adjacent layer of oil droplets by a thin aqueous film. This allowed them to study not only the rheological properties of the emulsion but also those of the wall film. Léger *et al.*²⁰ used near-field laser velocimetry to measure the local velocity of a polymer melt at the solid-polymer interface. By “decorating” the surface, i.e., by controlling the chemistry of the surface through grafting, the authors found that the slip velocity was strongly dependent on the molecular weights of the bulk and surface chains, and surface density. In addition, more recent studies of hexadecane on modified sapphire surfaces made by Pit *et al.*²¹ show that the strength of the fluid-surface interactions and the roughness at molecular scale control slip at the wall. The no slip boundary condition is maintained for incomplete fluorinated monolayer surface while the lyophobic surfaces promoted slip, indicating that both adhesion and roughness at molecular level control the extension of slippage.

Based on the aforementioned works, we propose that the wall depletion effect occurring in most rheometers and viscometers be used as a tool to study the role of interactions between the fluid (or fluid components) and the walls of the geometry. Moreover, a particular surface could be tailored to reduce or promote wall depletion effects and this modification used to establish correlations between interactions within the bulk and with the surface. Additionally, as Walls *et al.*⁶ previously established, differentiating

between wall slip and yield stress is, even with the existent technologies for slip prevention, an unresolved issue. This follow-up paper uses an approach that not only allows to accurately determine the yield stress in colloidal gels, but also establishes a way of interpreting wall slip in terms of specific interactions between the surface (of the test geometry) and the nature of the tested material.

In order to study the effects of test geometry surface energy on the occurrence and development of wall depletion, a series of fumed silica gels were sheared on surfaces with very different surface energies, i.e. high surface energy or hydrophobic and low surface energy or hydrophilic. The occurrence of wall slip as well as the time dependence of wall slip at various stress values were evaluated for each surface and compared to the results obtained with serrated plates by using the paint mark method suggested by Aral and Kalyon²². A different approach from the traditional steady flow measurements was employed to examine wall slip. Our approach entailed the use of dynamic measurements, in particular, dynamic oscillatory stress and/or time sweeps, simultaneously with the images collected from a CCD camera during the course of the experiments.

2.2 Experimental

2.2.1 Materials and Methods

Silica dispersions were prepared by mixing five types of fumed silica (FS) nanoparticles, each of them having a different surface chemistry, into Poly(ethylene glycol)dimethyl ether, PEGdm(250) (Sigma, Mw~250 g/mol). Native hydrophilic fumed silica, Aerosil A200, was provided by Degussa and employed as the starting material for the

FS surface modification. A200 has a surface area of $200 \text{ m}^2/\text{g}$, a particle size of 12 nm ²³, and a surface silanol (Si-OH) content of $2.5 \text{ Si-OH groups}/\text{nm}^2$ ²⁴. Hydrophobic fumed silicas were synthesized in our laboratory by substituting surface Si-OH moieties through chlorosilylation reactions. Three different alkyl chains were attached on the surface of A200: decyl (A200-C10), dodecyl (A200-C12), and octadecyl (A200-C18) alkyl chains. Commercial octyl-modified fumed silica, Aerosil R805, was also obtained from Degussa. The details of the surface modification are described elsewhere²⁵ and the physical characteristics of both commercial and in-house modified fumed silicas are listed in Table 2.1. The dispersions were prepared by high-shear mixing 10 wt% of previously vacuum-dried fumed silica (3 days, $120 \text{ }^\circ\text{C}$) in the solvent; the resulting product was kept in vacuum for 2 h in order to extract air bubbles, and the samples were used within 24 h of their preparation.

Dynamic rheology experiments were performed in a stress-controlled rheometer TA Instruments AR2000 at $25 \text{ }^\circ\text{C}$. In order to examine the effect of rheometer plate surface hydrophobicity on gel rheology a procedure based on that described by Walls and co-workers¹⁶ was used to coat the plates with poly(dimethyl siloxane) PDMS which was later on modified to obtain different surface energy. However, in this work, poly(dimethyl siloxane) PDMS model networks were used instead of commercial Sylgard-184 as a way to control composition and degree of crosslinking. The PDMS networks were prepared, as suggested by Patel *et al.*²⁶ by vigorously mixing the needed amounts of crosslinker (tetrakis(dimethylsiloxy)silane), vinyl-terminated PDMS, $M_w = 49000 \text{ g/mol}$, and platinum catalyst (cis-dichlorobis(diethyl sulfide) platinum(II)) for approximately 5 min. After applying vacuum to extract air bubbles, films of $\sim 1 \text{ mm}$ thickness were allowed to fully

crosslink at room temperature for 1 week. The parallel plate test geometry was coated with the PDMS model network films and tested under adequate dynamic oscillatory shear conditions in order to verify that the shear stress required to detach the PDMS film from the plates surface exceeded the maximum shear stress employed during all stress sweeps applied to our samples by at least 50X. PDMS model network films have a water contact angle of 109° , which indicates that the surface is hydrophobic. In order to decrease the surface energy and obtain our second test geometry surface type, i.e. to render the surface hydrophilic, PDMS networks were treated in a UVO chamber (Jetlight Company, Inc. model 42) for 30 min²⁷. The resulting water contact angle was less than 15° , indicating that the surface had successfully changed its surface energy. In order to avoid surface reconstruction and therefore changes in the contact angle²⁷, hydrophilic PDMS films were used within 5 h of applying the UV treatment. Furthermore, the contact angle was measured after conducting the experiments and compared to the original values. In all cases, the measured contact angle values were the same within experimental error.

FS gels in PEGdm(250) were tested on four different parallel plate geometries, each of them differing in its surface properties. In the subsequent sections, stainless steel plates will be referred to as “smooth” geometry, sandpaper-covered plates as “serrated”; PDMS-covered plates and UV-treated PDMS-covered plates will be referred to as “hydrophobic” and “hydrophilic”, respectively. The results reported in this work were reproducible within a relative error of less than 10%. In order to provide a standard mechanical history for all samples, dynamic time, stress, and frequency sweeps were preceded by a frequency sweep

going from 0.4 – 40 rad/s at a stress within the sample linear viscoelastic regime and followed by a 15 min delay, a protocol we have ahead established for this system¹⁶.

Table 2.1. Physical characteristics of the commercial and in-house modified fumed silica used in this work

Fumed silica	Surface group	Fraction of unreacted Si-OH (%) ^(a)
A200	Si-OH	100.0 ± 0.2
A200-C8	-C ₈ H ₁₇	52.0 ± 0.1
A200-C10	-C ₁₀ H ₂₁	50.5 ± 0.1
A200-C12	-C ₁₂ H ₂₅	61.1 ± 0.1
A200-C18	-C ₁₈ H ₃₇	61.1 ± 0.2

^(a) determined by thermogravimetric analysis TGA

2.2.2 Flow visualization

Direct visualization of the slip phenomenon was facilitated by using a CCD camera (see Figure 2.1). A straight line was painted from the top to the bottom plate, and the onset of slip was registered as the stress (or time) at which the paint mark lost connectivity with the moving plate (top)²². It is important to mention that the slip phenomenon observations were done during dynamic oscillatory sweeps (time or stress); therefore, we combined direct visualization with evaluation of the strain waveform in order to determine wall slip and distinguish it from yield stress²⁸. This approach allowed us to obtain clear interpretation of the experimental results and appropriate insight as to whether a sample was yielding or slipping.

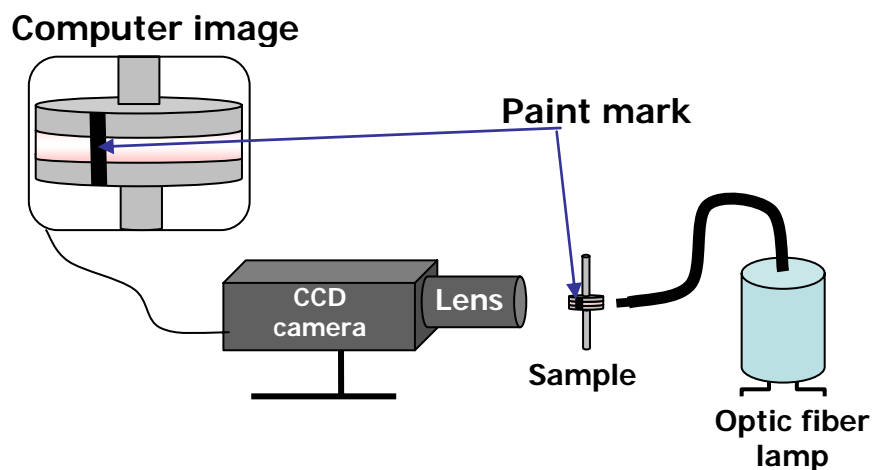


Figure 2.1. Flow visualization setup showing a schematic of the paint line technique for determining slip velocity.

2.3 Results and Discussion

2.3.1 Linear viscoelastic properties of fumed silica gels

Prior to examining the slip behavior of FS gels on different surfaces, we examine in Figure 2.2 the frequency spectra and dynamic moduli of 5 different fumed silicas dispersed in PEGdm(250). These silicas differ in the attached surface moieties going from 100% silanol groups (A200) to 8, 10, 12, and 18 carbon atoms for the A200-C8, A200-C10, A200-C12, and A200-C18, respectively. In all cases, the elastic modulus (G') is higher than the viscous modulus (G'') (only shown for the A200 gel for clarity) and the frequency dependence of G' is minimal.

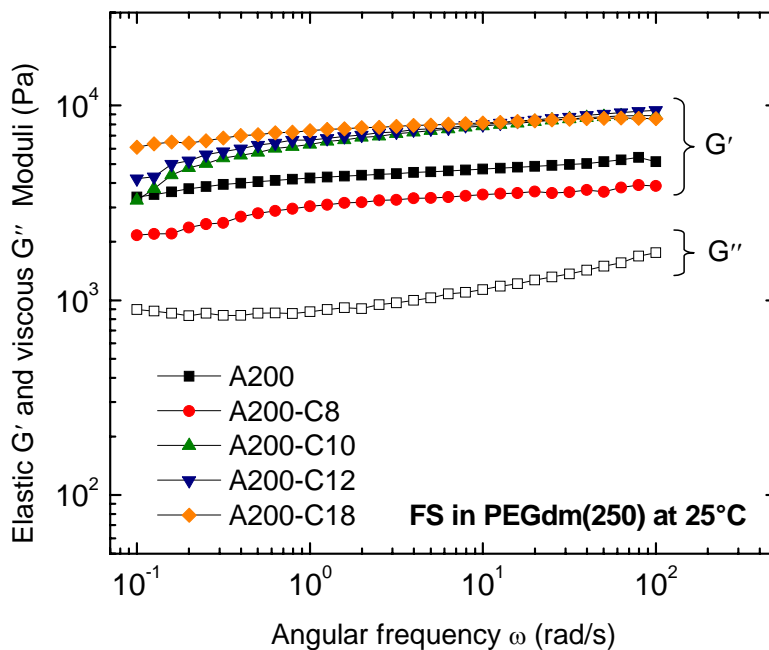


Figure 2.2. Elastic and viscous moduli as a function of frequency for the five dispersions of fumed silica (10wt%) in PEGdm(250).

This is characteristic of a gel-like behavior resulting from flocculation of the FS particles into a three-dimensional physical network. For the hydrophobic FS gels (alkyl terminated FS particles), as the hydrophobicity of the silica particles increases, i.e., as the length of the aliphatic chain tethered to the surface is increased, the gel modulus also becomes larger and more frequency independent. These results can be explained in terms of the predominant type of interactions occurring in the systems. For instance, native hydrophilic fumed silica A200 forms a gel in PEGdm(250) mainly due to the fact that by end-capping the poly(ethylene glycol) molecule with non-polar methyl groups, the ability of the solvent to interact with the hydrophilic fumed silica surface is weakened. Therefore, the particles interact with each other through hydrogen bonding as a way of minimizing the

energy in the system. As a result, a network of A200 particles physically linked through the surface silanol groups is formed and the system behaves like a gel.

For the hydrophobic FS particles, as the chain length of tethered molecules increases from C-8 to C-18, both van der Waals interactions and reverse steric stabilization dominate the gel formation mechanism⁵. It is noticeable that G' of A200-C10 and A200-C12 FS gels are very close to each other; however, for the longest alkyl chain-modified FS employed in this work, A200C-18, there seems to be an additional contribution to the gel modulus provided by the attached chains. If the chains are in the crystalline state, as it has been suggested by Snyder and Allara²⁹ for a monolayer on a silicon wafer, the rigidity of the system will increase by the presence of an additional layer of a crystalline corona on the FS particles. Allara *et al.*³⁰ showed that for disordered monolayers of alkyl chains a distinct change in surface wetting behavior occurred for chains between 14 and 17 carbon atoms. This was attributed to ordering (crystallization) of the chains and increase of chain extension. If this is the case, as it was mentioned before, for A200-C18 particles, the effective radius will increase by about 2.2 nm; this will in turn increase the effective volume fraction as well as the rigidity of the particles.

Figure 2.3 shows a schematic describing the proposed interaction schemes for the results observed in Figure 2.2. When hydrophilic fumed silica is dispersed in a slightly polar solvent such as PEGdm(250) (poor hydrogen bonding ability), *case A*, a network forms through interactions among the particles which get close enough to form hydrogen bonding with themselves. *Case B* corresponds to the situation where short alkyl chains, covering ~50% of the silica surface, shield some of the remaining Si-OH groups and the solvent does

not solvate the surface of the particles. Interactions between the hydrophobic chains govern the gel formation mechanism. Finally, *case C* corresponds to highly hydrophobic particles where the longer alkyl chains not only shield the Si-OH groups completely, but also increase the effective particle size, especially if the chains are capable of crystallizing.

The results shown in this section suggest that the elastic modulus of hydrophobic FS particles increases with increasing the alkyl chain length of the modified FS; this behavior is more noticeable at lower frequencies and attributed to an additional increase in the rigidity of the particles given by the fact that the longer chains are capable of crystallizing. In addition, reverse steric stabilization seems to be the governing mechanism in the gel formation process for gels of longer alkyl-covered fumed silica nanoparticles in PEGdm(250).

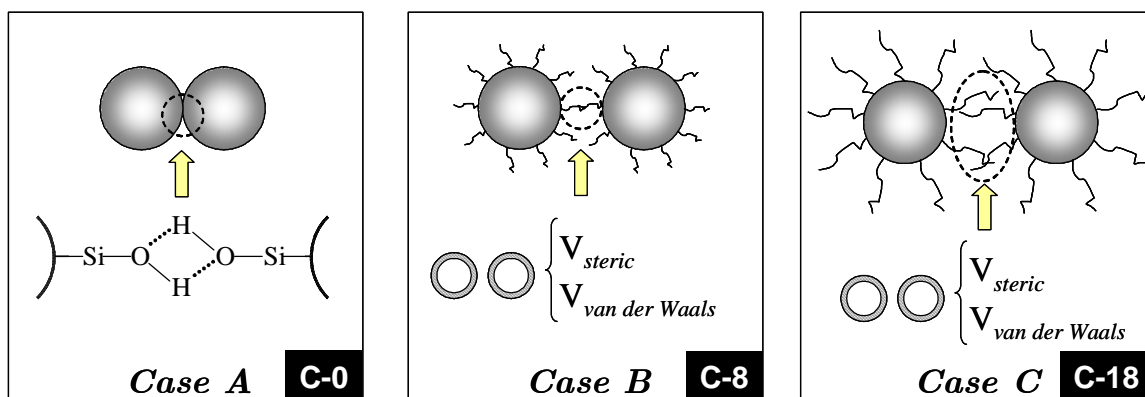


Figure 2.3. Schematic of the proposed interactions between hydrophilic (*case A*) and hydrophobic (*case B* and *C*) fumed silica in slightly polar medium (i.e. in PEGdm(250)).

2.3.2 Yield stress *vs.* wall slip: effects of surface chemistry on slip of FS particulate gels

Walls *et al*¹⁶ suggested that specific interactions between the fumed silica particles contained in the tested gel and the surface of the testing geometry help to prevent the occurrence of wall slip. In view of these results, we evaluate the effect of surface chemistry on slip by using hydrophobic, hydrophilic, smooth, and serrated test geometry surfaces for all the hydrophobic fumed silica particulate gels described in the previous section. In addition, the effect of the particles surface chemistry was also evaluated, i.e., the effect of hydrophobic chains attached to the surface of the FS particles on the slip properties. Figure 2.4 (a and b) shows the elastic modulus as a function of applied stress amplitude for gels of A200-C10 and A200-C18 in PEGdm(250) measured with different test geometry surfaces. Gels containing A200-C8 and A200-C12 behave similarly; thus the results are not shown. A constant G' at low stress values followed by a drop after a certain stress is reached is observed.

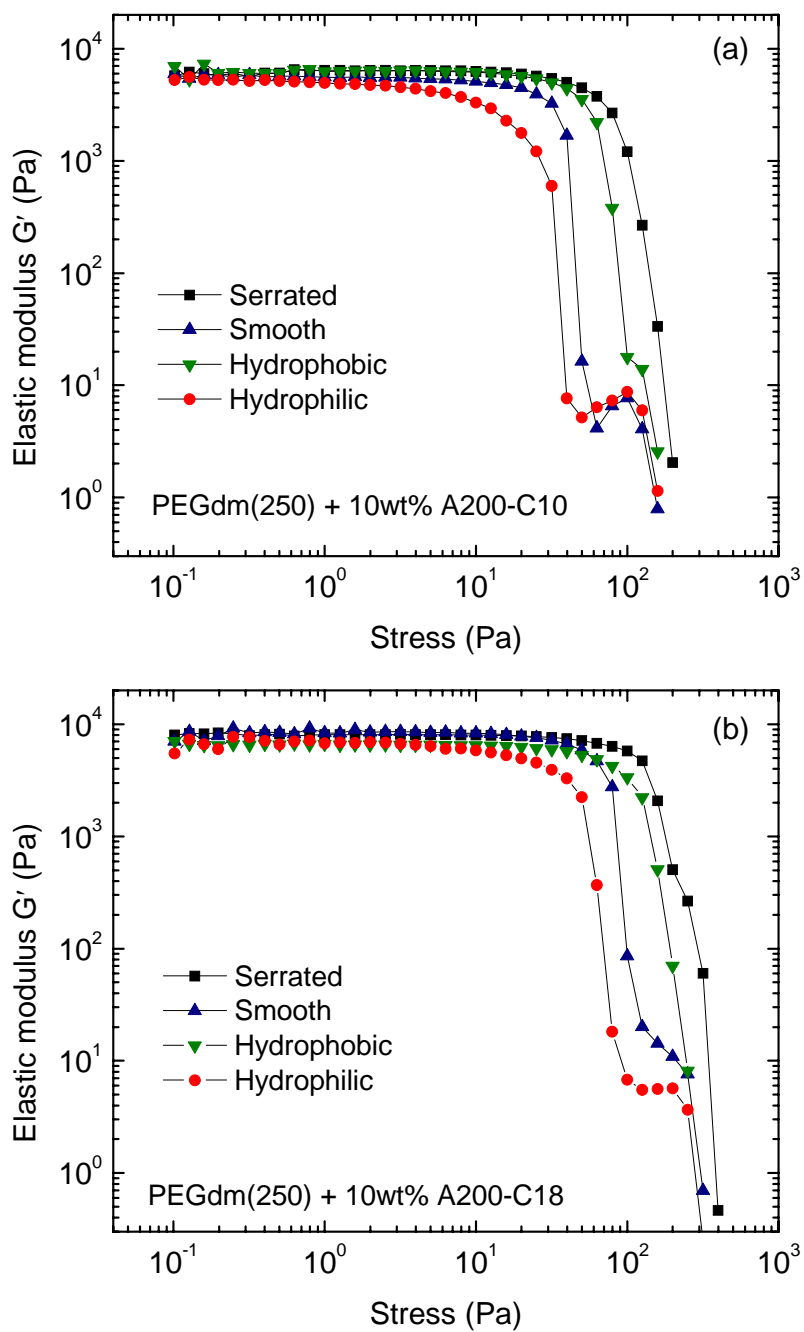


Figure 2.4. Elastic modulus as a function of stress amplitude for (a) A200-C10 and (b) A200-C18 fumed silica in PEGdm(250) at 25 °C.

This behavior is characteristic of structured/complex fluids that shear-thin after high enough stress is applied, and indicates the end of the linearity of the rheological response

due to deformation and breakdown of the microstructure (i.e., yielding). Though G' is the same for all geometries in the linear region, the rheological response obtained with the four surfaces after the critical stress is overcome differs considerably. When roughened surface plates are employed, a continuous decrease of G' with stress amplitude is observed; however, with smooth, hydrophobic and hydrophilic surfaces, G' drops in a “two-step” fashion. This behavior has been previously observed and it is ascribed to as wall slip^{14, 31}. In colloidal systems, wall slip has been explained in terms of the presence of a particle-lean layer with different flow behavior than the bulk; the material next to the wall deforms more than the bulk leading to misinterpretation of the observed flow behavior.

To further examine the effects of the length of alkyl chains tethered to the FS particles on yield behavior and how this is influenced by the test geometry surface chemistry, we show in Figure 2.5 the in-phase component of the stress as a function of the strain amplitude for gels of hydrophobic FS particles (A200-C8, A200-C10, A200-C12, and A200-C18). By determining the point at which the elastic stress reaches its maximum value, we determined the yield stress of the materials (see Figure 2.5). This approach is referred to as the elastic stress method for determination of the yield stress^{32, 33} and it has been suggested as an alternative to steady shear flow methods for determining yield stress since it is less subjective, it is based on simple and reliable experiments (dynamic oscillatory), and closely matches the results obtained with steady stress methods^{16, 33}. In all cases, the values obtained with the serrated geometry were considered to be the more accurate or the “control values” as slippage is mechanically prevented¹⁵. We observe that the yield stress is the

lowest for the hydrophilic geometry; however, the hydrophobic test geometry gives yield stress values that are closer to the ones obtained with the “control” geometry.

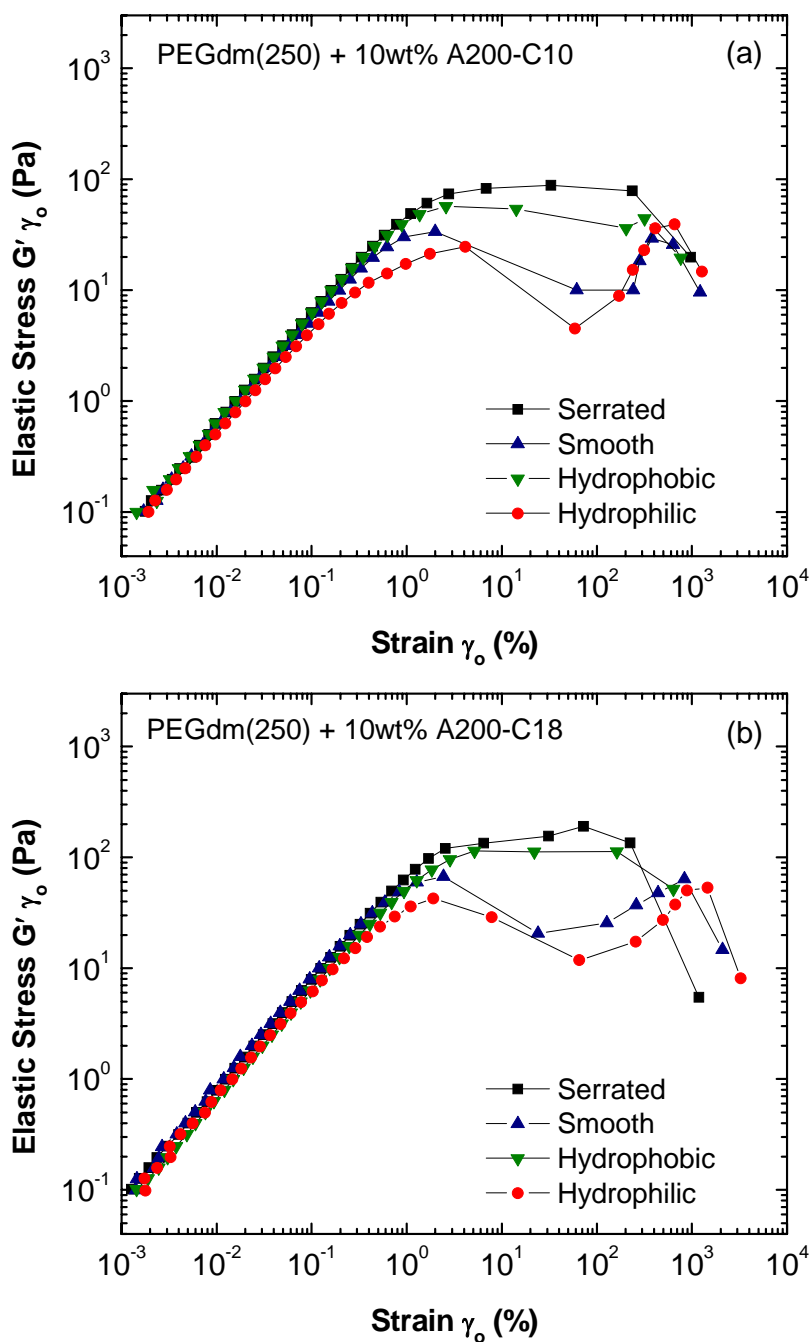


Figure 2.5. Elastic stress as a function of strain amplitude for (a) A200-C10 and (b) A200-C18 fumed silica dispersions

Figure 2.6 summarizes the yield stress values obtained for all the FS gels when tested using hydrophobic and hydrophilic plates. We observe that as the sample starts to get closer to the “slipping regime” or closer to the “yielding point” (we discuss slip *vs.* yield in subsequent section), whichever occurs first, the hydrophobic particles remain “affixed” to the hydrophobic surface up to stress values that are higher than those observed with the hydrophilic plates. We interpret these observations in terms of the attraction developed between the alkyl chains covering the surface of the FS particles and the hydrophobic test geometry. Conversely, when the interactions are not favored such as in the case of hydrophilic plates and hydrophobic FS particles, where the interaction potential is expected to be repulsive, the particles do not stick to the surface and the estimated yield stress value is even lower than that obtained with the regular geometry surfaces, which are slightly hydrophobic (water contact angle θ of 56°).

Figure 2.7 shows an example of the calculated van der Waals interaction potential for gels of octyl-modified FS particles in PEGdm(250) as a function of the separation distance between the particles and the surface. It can be seen that the van der Waals interaction potential (V_{vdW}) of hydrophobic PDMS surface and hydrophobic FS particles (A200-C8, A200-C10, A200-C12, and A200-C18) is attractive (negative V_{vdW}), while that of the hydrophilic PDMS and hydrophobic FS particles is repulsive (positive V_{vdW}). Likewise, hydrophilic PDMS and FS A200 show attractive V_{vdW} , while the opposite is observed for hydrophilic PDMS and hydrophobic FS. These calculations support our explanation as to why the hydrophobic particles prefer to segregate from the plate-sample interface to the bulk when the plates are covered with a hydrophilic material and vice versa.

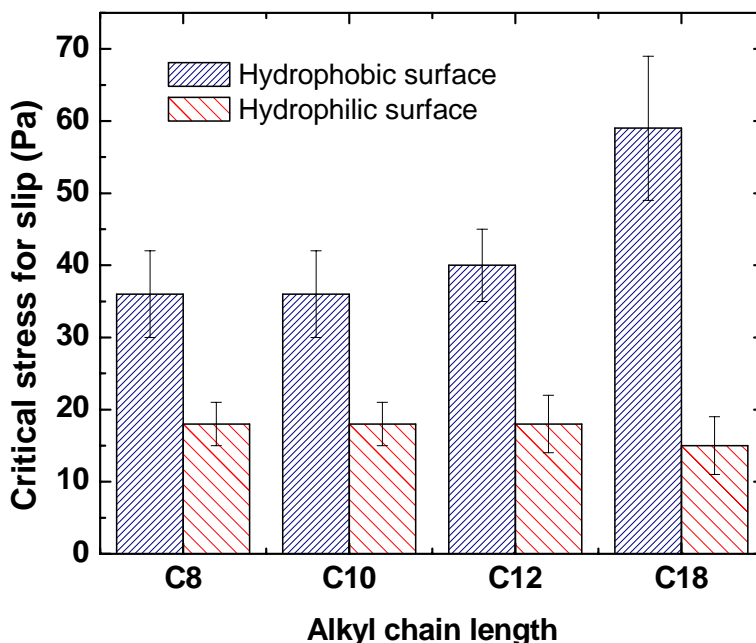


Figure 2.6. Effect of the test geometry surface energy on the critical stress for slip for gels of 10 wt% hydrophobic FS in PEGdm(250) as a function of the length of the alkyl chain attached to the surface of the FS particles.

It is important to mention that even though the values plotted in this figure have several sources of error and should be considered with caution (due to estimations of the Hamaker constant values and interfacial energy), the observed trend is correct; hydrophobic particles are attracted to the hydrophobic surface and repelled from the hydrophilic one and this effect is clearly reflected in the critical stress for slip values shown in Figure 2.6. Based on these results, we believe that the strength and nature of the interactions between the testing material and the geometry are responsible for the formation of the particle-lean layer in the colloidal gels studied. This is, the particle-lean layer will form at earlier stages of the stress sweep experiment when the dominant attraction is repulsive or when the strength of the attractive interaction is low, and at later stages of the experiment if the opposite

situation is observed. If we can find an easy method capable of predicting the occurrence of wall slip in a systematic and reliable way, we will have a tool to study the strength of interactions and predict the specific behavior of the material during processing or when a stress or strain field is applied. The next section describes our approach to finding this method and the results we gathered from it.

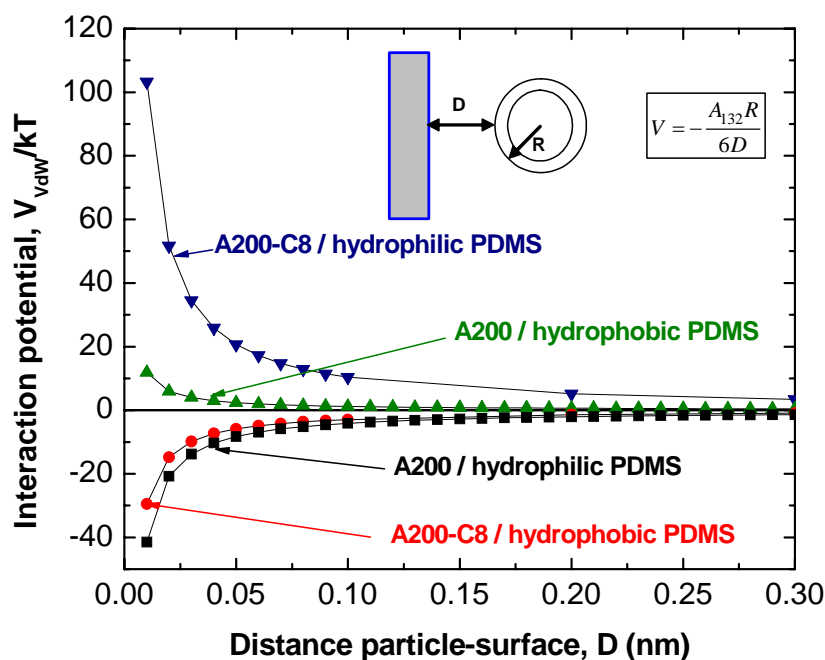


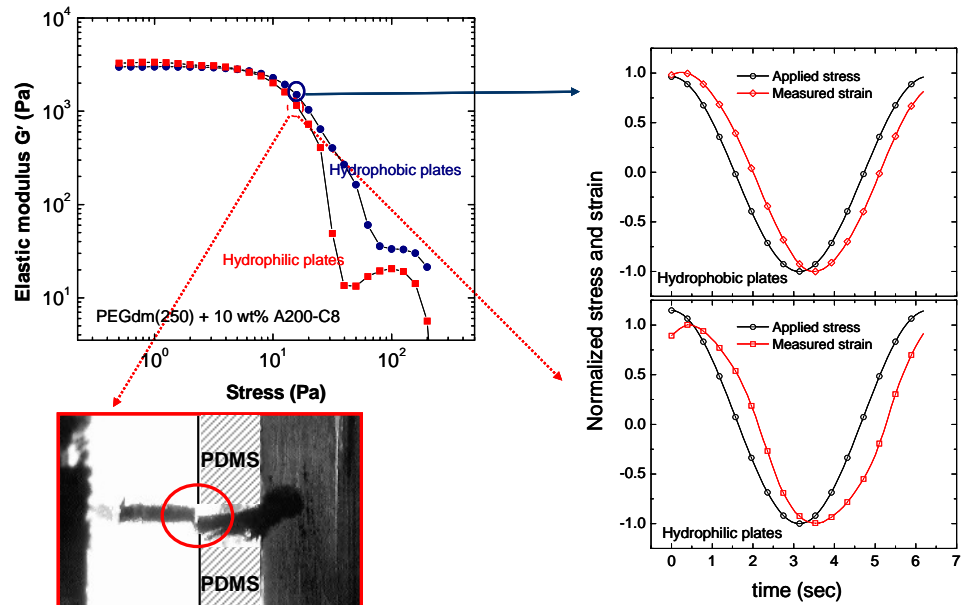
Figure 2.7. van der Waals interaction potential (V_{vdw}) normalized by kT (k is the Boltzmann constant and T the absolute temperature in K) between FS particles and PDMS covered plates. FS particles are considered to be spherical in shape for the calculations.

2.3.3 Combined flow visualization and mechanical rheology to decipher yield stress and wall slip

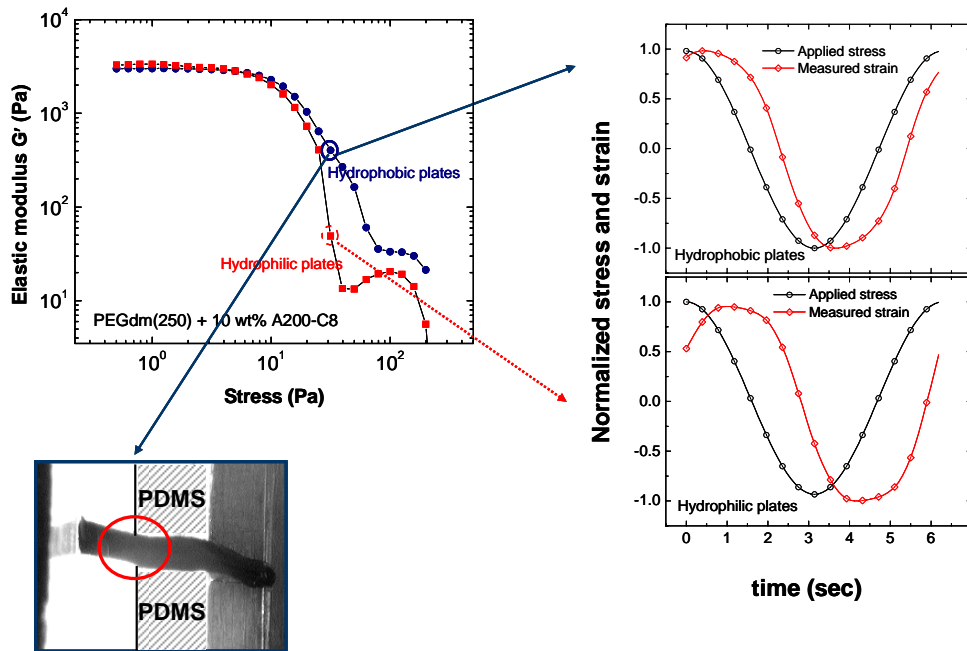
Aral and Kalyon²² first suggested the use of a very simple yet useful method to determine wall slip. As illustrated in Figure 2.1, the continuity of a paint mark going from

the rheometer's top to the bottom plate is employed as an indicator of zero velocity at the wall (no-slip boundary condition) while a stress or time sweep experiment is conducted. We suggest simultaneously using this simple method and a dynamic oscillatory stress (or strain) experiment, such as the yield stress determination by the elastic stress, to measure and evaluate the occurrence of wall slip. Due to the fact that during a dynamic oscillatory experiment, a *sinusoidal* stress is commanded and the corresponding sinusoidal strain wave is obtained, the onset of wall slip is considered to be the maximum stress amplitude (τ_0) at which the mark is no longer continuously deformed by the moving plate. At this point, the no-slip boundary condition is no longer satisfied and the velocity at the plate is different from the bulk velocity.

Figure 2.8 shows an example of a FS gel experiencing wall slip on hydrophobic and hydrophilic plate geometries. The snapshots correspond to the point at which the maximum stress amplitude occurred and the wave form is showed for the complete oscillation at the indicated stress amplitude. Figure 2.8a shows that for a stress value that is within 15% of the linear regime (stress < 10 Pa), the hydrophobic plates do not exhibit a marked deformation of the paint line (image not shown) and the strain wave shape remains sinusoidal. The hydrophilic plates on the other hand, show not only a non-sinusoidal strain wave but also a disruption in the paint line continuity.



(a) Stress = 15 Pa



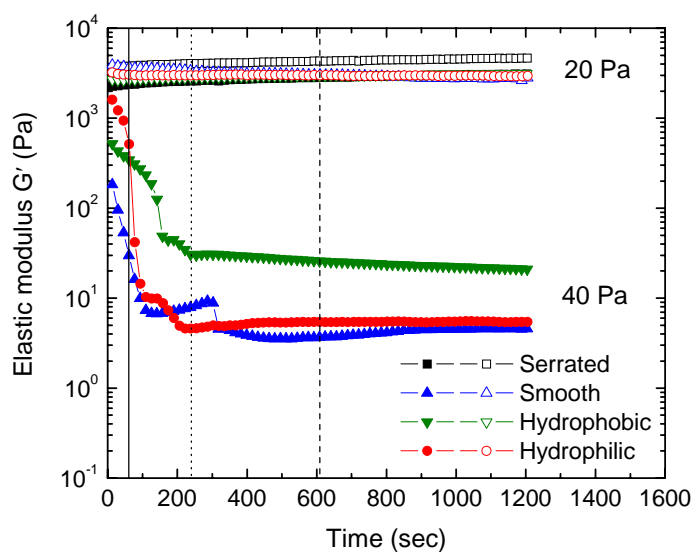
(b) Stress = 31 Pa

Figure 2.8. Snapshots and strain wave form obtained during a stress sweep for gels of A200-C8 in PEGdm(250) tested with hydrophobic and hydrophilic plates at (a) 15 Pa and (b) 31 Pa.

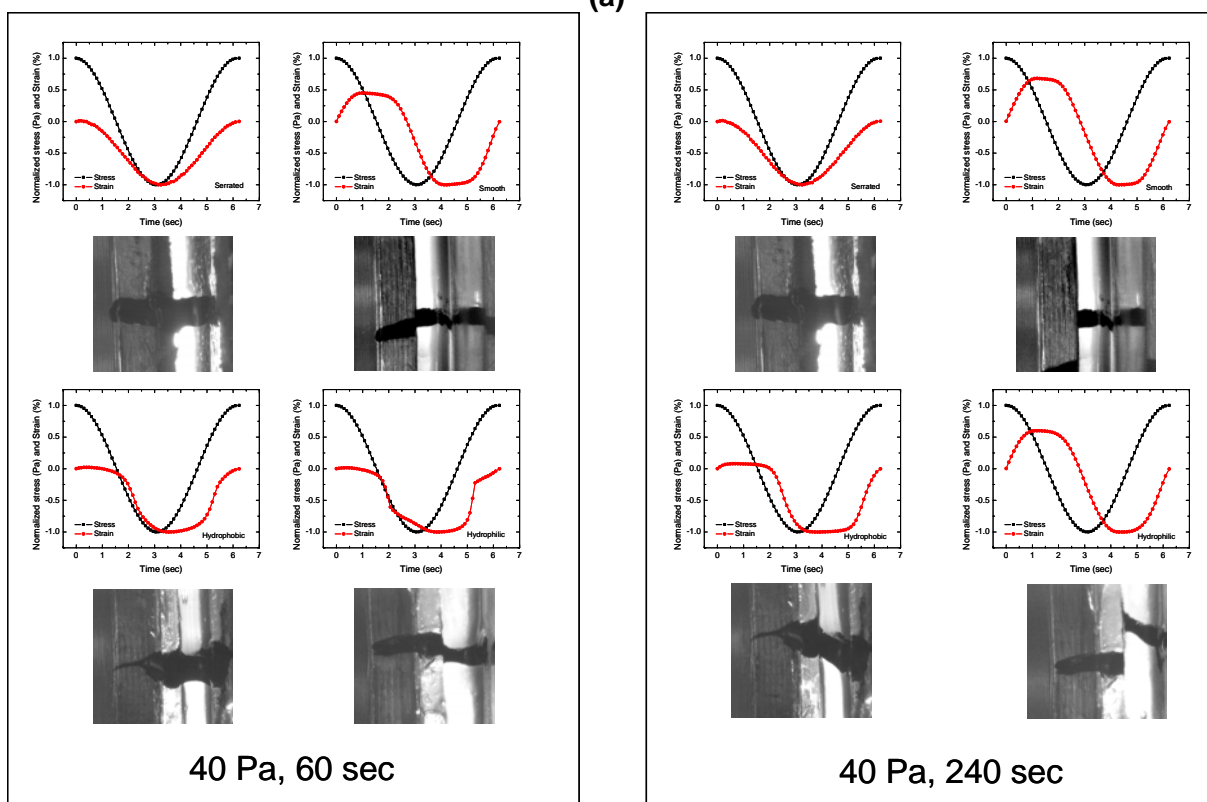
At a higher stress values (Figure 2.8b), the deformation exerted on the sample is higher and the hydrophobic plates show a non-sinusoidal behavior. It is interesting to note that even though the deformation is higher and the wave non-sinusoidal, the sample is not slipping as indicated by the continuity in the now more deformed paint line. If we compare the strain wave obtained using hydrophilic plates at the same stress value of 31 Pa (see Figure 2.8b), the strain wave is highly non-sinusoidal and the paint line has completely broken into three parts: the top and bottom plates and the middle part corresponding to the sample. These results indicate that our technique is of practical use as it visually states that either slippage or yielding is occurring. That is, for systems that exhibit yield stress such as gels of FS in PEGdm(250), it is possible to obtain a non-sinusoidal wave shape when the sample is either above its yield point or if the material exhibits wall slip²⁸. By adding the paint mark, not only we can distinguish between slip and flow of the gels but also accurately determine the onset of slip under a particular set of conditions, i.e., stress, temperature, frequency.

To this point, we have analyzed the effects of the plates' surface energy in terms of prevention of wall slip as the stress amplitude is varied. In view of this situation, we decided to perform oscillatory *time* sweep experiments at different stress values, covering stress regions below and above the yield stress. These experiments would indicate if the surface effects are still observed after the material has been deformed to the point where not only the elasticity of the material is responsible for the behavior, but also the viscous component is adding to the response (disruption of the flocs).

Figure 2.9 shows oscillatory time sweep experiments for two different stress values (above and below the yield stress) along with snapshots and wave shapes at specific times (indicated by the dashed lines) for the two stress values. The time sweep experiments at two different stress amplitudes plot is showed in Figure 9a. At 20 Pa, the wave shapes are sinusoidal for all the testing surfaces (data not shown). In addition, a constant stress value as a function of time is observed and no breaks in the paint mark are evident for either one of the geometries. At higher stress values (40 Pa), however, the wave shapes are non-sinusoidal for the hydrophilic, hydrophobic and serrated geometries, but the paint mark shows no disruptions for the serrated geometry. It is also interesting to notice that the material sheared on the hydrophobic plates shows paint mark breakdown at later times, in contrast with the hydrophilic and smooth plates, which observe complete detachment of the fluid from the wall. If a longer time is analyzed (Figure 9c) the hydrophobic plate result is similar to the one obtained with the hydrophilic and smooth plates, indicating that the strength between the bulk (specifically, the FS particles) and the surface is preventing or retarding the particle-lean layer formation and in consequence the slippage of the material. These results suggest again that the properties of the testing surface have a strong effect on the behavior of particulate gels and that our technique is useful to distinguish between slippage and yielding.



(a)



(b)

Figure 2.9. Snapshots and strain wave form obtained during a time sweep for gels of A200-C8 in PEGdm(250) tested with smooth, serrated, hydrophobic, and hydrophilic plates at different stress amplitudes and time.

2.4 Conclusions

We have studied gels of hydrophobic and hydrophilic fumed silica particles in PEGdm(250), a solvent medium that allows for both types of particles to aggregate and form a three-dimensional network. Though different mechanisms are responsible for gel formation, a common response is observed when the gels are sheared on surfaces that have been specifically treated to show high and low surface energy (hydrophilic and hydrophobic, respectively). If the testing surface (rheometer plates) has the ability of interacting in a more attractive way with the surface of the particles contained in the gel, these interactions will prevent the slippage of the material and prevail until the applied shear stress overcomes them. In addition, we have effectively combined two techniques, dynamic oscillatory measurements and flow visualization with a CCD camera to determine the onset and occurrence of slip during a stress sweep experiment as well as during a time sweep. These results have potential application in the exact determination of the material yield stress, which is necessary in numerous processing and end use circumstances.

2.5 References

1. Tadros, T. F., Correlation of viscoelastic properties of stable and flocculated suspensions with their interparticle interactions. *Advances in Colloid and Interface Science* 1996, 68, 97-200.
2. Raghavan, S. R.; Riley, M. W.; Fedkiw, P. S.; Khan, S. A., Composite polymer electrolytes based on poly(ethylene glycol) and hydrophobic fumed silica: Dynamic rheology and microstructure. *Chemistry of Materials* 1998, 10, (1), 244-251.

3. Fan, J.; Raghavan, S. R.; Yu, X. Y.; Khan, S. A.; Fedkiw, P. S.; Hou, J.; Baker, G. L., Composite polymer electrolytes using surface-modified fumed silicas: conductivity and rheology. *Solid State Ionics* 1998, 111, (1-2), 117-123.
4. Walls, H. J.; Zhou, J.; Yerian, J. A.; Fedkiw, P. S.; Khan, S. A.; Stowe, M. K.; Baker, G. L., Fumed silica-based composite polymer electrolytes: synthesis, rheology, and electrochemistry. *Journal of Power Sources* 2000, 89, (2), 156-162.
5. Raghavan, S. R.; Hou, J.; Baker, G. L.; Khan, S. A., Colloidal interactions between particles with tethered nonpolar chains dispersed in polar media: Direct correlation between dynamic rheology and interaction parameters. *Langmuir* 2000, 16, (3), 1066-1077.
6. Raghavan, S. R.; Walls, H. J.; Khan, S. A., Rheology of silica dispersions in organic liquids: New evidence for solvation forces dictated by hydrogen bonding. *Langmuir* 2000, 16, (21), 7920-7930.
7. Khan, S. A.; Maruca, M. A.; Plitz, I. M., Rheology of Fumed Silica Dispersions For Fiberoptic Cables. *Polymer Engineering and Science* 1991, 31, (24), 1701-1707.
8. Riley, M.; Fedkiw, P. S.; Khan, S. A., Transport properties of lithium hectorite-based composite electrolytes. *Journal of the Electrochemical Society* 2002, 149, (6), A667-A674.
9. Basic Characteristics of Aerosil; Degussa Technical Bulletin No. 11; Degussa Corp.: Akron, OH, 1993.
10. Iler, R. K., *The Chemistry of Silica: Solubility, Polymerization, Colloid and Surface Properties, and Biochemistry*. John Wiley & Sons: New York, NY, 1979; p xxiv, 866.
11. Raghavan, S. R.; Fussell, G. W.; Khan, S. A., Fumed silica dispersions in polymeric liquids: Evidence for site-specific colloidal interactions. *Abstracts of Papers of the American Chemical Society* 1997, 214, 332-POLY.
12. Chen, M.; Russel, W. B., Characteristics of Flocculated Silica Dispersions. *Journal of Colloid and Interface Science* 1991, 141, (2), 564-577.
13. Ramakrishnan, S.; Gopalakrishnan, V.; Zukoski, C. F., Clustering and mechanics in dense depletion and thermal gels. *Langmuir* 2005, 21, (22), 9917-9925.

14. Barnes, H. A., A Review of the Slip (Wall Depletion) of Polymer-Solutions, Emulsions and Particle Suspensions in Viscometers - Its Cause, Character, and Cure. *Journal of Non-Newtonian Fluid Mechanics* 1995, 56, (3), 221-251.
15. Barnes, H. A.; Nguyen, Q. D., Rotating vane rheometry - a review. *Journal of Non-Newtonian Fluid Mechanics* 2001, 98, (1), 1-14.
16. Walls, H. J.; Caines, S. B.; Sanchez, A. M.; Khan, S. A., Yield Stress and Wall Slip Phenomena in Colloidal Silica Gels. *Journal of Rheology* 2003, 47, (4), 847-868.
17. Roberts, G. P.; Barnes, H. A., New measurements of the flow-curves for Carbopol dispersions without slip artefacts. *Rheologica Acta* 2001, 40, (5), 499-503.
18. Nickerson, C. S.; Kornfield, J. A., A "cleat" geometry for suppressing wall slip. *Journal of Rheology* 2005, 49, (4), 865-874.
19. Princen, H. M., Rheology of foams and highly concentrated emulsions. II. Experimental study of the yield stress and wall effects for concentrated oil-in-water emulsions. *Journal of Colloid and Interface Science* 1985, 105, (1), 150-71.
20. Leger, L.; Hervet, H.; Massey, G.; Durliat, E., Wall slip in polymer melts. *Journal Of Physics-Condensed Matter* 1997, 9, (37), 7719-7740.
21. Pit, R.; Hervet, H.; Leger, L., Direct experimental evidence of slip in hexadecane: Solid interfaces. *Physical Review Letters* 2000, 85, (5), 980-983.
22. Aral, B. K.; Kalyon, D. M., Effects of temperature and surface roughness on time-dependent development of wall slip in steady torsional flow of concentrated suspensions. *Journal of Rheology (New York, NY, United States)* 1994, 38, (4), 957-72.
23. Degussa, T. B. Aerosil as a thickening agent for liquid systems; Degussa Technical Bulletin No. 23; Degussa Corp.: Akron, OH, 1993.
24. Hou, J.; Baker, G. L., Preparation and characterization of cross-linked composite polymer electrolytes. *Chemistry of Materials* 1998, 10, (11), 3311-3318.
25. Sanchez, A. M. North Carolina State University, Raleigh, 2006.
26. Patel, S. K.; Malone, S.; Cohen, C.; Gillmor, J. R.; Colby, R. H., Elastic modulus and equilibrium swelling of poly(dimethylsiloxane) networks. *Macromolecules* 1992, 25, (20), 5241-51.

27. Efimenko, K.; Wallace, W. E.; Genzer, J., Surface modification of Sylgard-184 poly(dimethyl siloxane) networks by ultraviolet and ultraviolet/ozone treatment. *Journal of Colloid and Interface Science* 2002, 254, (2), 306-315.
28. Yoshimura, A. S.; Prudhomme, R. K., Wall Slip Effects on Dynamic Oscillatory Measurements. *Journal of Rheology* 1988, 32, (6), 575-584.
29. Snyder, R. G.; Strauss, H. L.; Elliger, C. A., Carbon-hydrogen stretching modes and the structure of n-alkyl chains. 1. Long, disordered chains. *Journal of Physical Chemistry* 1982, 86, (26), 5145-50.
30. Allara, D. L.; Parikh, A. N.; Judge, E., The existence of structure progressions and wetting transitions in intermediately disordered monolayer alkyl chain assemblies. *Journal of Chemical Physics* 1994, 100, (2), 1761-4.
31. Kalyon, D. M.; Yaras, P.; Aral, B.; Yilmazer, U., Rheological behavior of a concentrated suspension: a solid rocket fuel simulant. *Journal of Rheology* (New York, NY, United States) 1993, 37, (1), 35-53.
32. Pai, V. B.; Khan, S. A., Gelation and rheology of xanthan/enzyme-modified guar blends. *Carbohydrate Polymers* 2002, 49, (2), 207-216.
33. Yang, M. C.; Scriven, L. E.; Macosko, C. W., Some Rheological Measurements on Magnetic Iron-Oxide Suspensions in Silicone Oil. *Journal of Rheology* 1986, 30, (5), 1015-1029.

3

*Anomalous temperature behavior of fumed
silica nanoparticulate gels in low-MW
polyethers*

Abstract

Dispersions of hydrophilic and hydrophobic fumed silica (FS) nanoparticles in various molecular weight (MW) polyethers are systematically studied in order to understand the factors dictating the nature and magnitude of colloidal interactions in the systems. In particular, dynamic rheological experiments were employed to characterize the effects of temperature on the properties of the dispersions. We find that the elastic modulus of hydrophilic FS in PEGdm(250) gels irreversibly increases after heating up from 25 to 80 °C, whereas the elastic modulus of hydrophobic FS in PEGdm(250) reversibly decreases with temperature. The effects of time and FS concentration are also evaluated for samples that have been thermally treated and compared to those tested at room temperature. At 80 °C, the elastic modulus of the hydrophilic FS in PEGdm(250) increased as a function of time and reaches a plateau value after ~200 min. At lower concentrations of hydrophilic FS in PEGdm(250) (starting at 2 wt%), the magnitude of change in elastic modulus with temperature becomes larger. Thermogravimetric analysis of FS particles that are washed and dried before and after the thermal treatment suggests that a condensation reaction between the silanol groups on the FS surface and the PEGdm(250) molecules takes place upon heating. The amount and type of end groups present in the PEGs used in this study seems to dictate the occurrence of this reaction. Hydrophilic FS in PEGdm(500), which contains a smaller amount of end groups, does not show a marked increase in modulus with temperature. In contrast, PEGdm(250) does show reaction.

To be submitted to Langmuir

Authors: A.M. Sanchez and S.A. Khan

3.1 Introduction

The interactions of fumed oxides with organic solvents, polymers and biological systems are of great interest as they can be utilized as viscosity modifiers, fillers or adsorbents when mixed in or in contact with such materials^{1, 2}. Fumed silica FS, is of particular interest due to the large surface area that its branched structure provides^{3, 4}. If these small particles are dispersed in an adequate medium, they form suspensions, flocculated systems or networks; thus an understanding of how to control this microstructure is of paramount importance.

Extensive research involving FS dispersions has been conducted; recently, alternative novel applications such as fiber optic cables and composite polymer electrolytes, our major research effort in the past years, have gained special importance⁵⁻¹⁰. From processing and end use standpoints, of special interest is an understanding of how the equilibrium, at rest, and flow properties of colloidal composites change with various conditions to which the material is exposed to. In this regard, most of the research conducted has focused on properties at room temperature.

Depending on the type of interactions present in a colloidal system, a change in temperature can dramatically modify the microstructure leading to a complete different behavior during flow or at rest. In other words, the material's ability to flow, intrinsically related to its relaxation time spectrum, goes through a broad spectrum ranging from milliseconds (solution-like fluids) to infinity such as the times encountered in chemically crosslinked networks¹¹. Moreover, if the equilibrium microstructure takes longer to develop,

temperature is one of the external variables that can be used to accelerate development of the equilibrium (or final) microstructure.

Zhang and Archer¹⁰ found that the rheological properties of 600kg/mol poly(ethylene oxide) (PEO)/colloidal silica nanocomposites change dramatically with temperature. At 75 °C, the elastic modulus increased with time and reached a plateau after 200 sec. If the samples had been previously annealed (several days at 75 °C under nitrogen atmosphere), the change in elastic modulus was very little compared to the variation in fresh samples. The authors suggested evolution of the microstructure to a final equilibrium state corresponding to an immobilized layer thickness of the order of $R_g \sim N^{0.5}$; where R_g corresponds to the radius of gyration of the polymer molecules and N is the degree of polymerization. The higher elastic modulus after annealing was attributed to higher effective particle volume fraction resulting from the increase in the immobilized layer thickness.

Other work dealing with adsorption of polymers from solution, specifically adsorption of PEO in silica, recognize the effects that the solvent and molecular weight (MW) of the PEO have on the resulting adsorbed polymer layer¹²; the specific adsorption increases from benzene > chloroform > water > methanol >> dioxane > dimethylformamide. Chloroform behaved differently from the other solvents evaluated; the strong dependence of solubility on MW dictates the specific adsorption on the silica surface for this particular solvent. The authors suggest that specific adsorption of PEO on silica follows a power-law relationship with MW. These studies, however, do not include the temperature effects as the adsorption isotherms were performed at 20 °C. Maitra *et al.*¹³ concluded that a heat treatment step

was required to obtain maximum PEO coverage when grafting low-MW PEO (~ 375 g/mol) onto high-surface area (380 m²/g) fumed silica. Moreover, a gel was obtained after the thermal treatment and the occurrence of a chemical bond was corroborated by thermogravimetric analysis experiments.

It can be seen that in spite of the efforts made in the characterization of microstructure and flow properties of colloidal systems containing silica, very few studies have dealt with temperature effects, suggesting a need for a better understanding of these phenomena. In order to provide insight on this particular area, we prepared colloidal dispersions of hydrophobic and hydrophilic fumed silica and tested them under oscillatory shear at temperatures ranging from 25 to 80 °C. The results are analyzed in terms of how the colloidal interactions change and affect the properties of the materials. A rather unusual and unexpected result dealing with the change of materials elasticity with temperature is discussed and an explanation is provided based on the characterization of the particulate material after specific thermal treatments. We foresee an alternative, simple and inexpensive way of tuning the rheological properties of silica nanoparticulate systems that experience flocculation at room temperature.

3.2 Experimental

A total of four polyethers differing in the amount and type of end group content were used as the continuous media for the fumed silica dispersions. Poly(ethylene glycol) dimethyl ether (two different molecular weights), poly(ethylene glycol) methyl ether, and poly(ethylene glycol) were obtained from Aldrich and used as received. The molecular weight, molecular structure and viscosity at 25 °C of these polyethers are listed in Table 3.1.

Table 3.1. Molecular characteristics of the polyethers employed in this work.

Material/Name	Molecular structure	n ⁽¹⁾	MW (g/mol)	Viscosity ⁽²⁾ (Pa-s)
Poly(ethylene glycol) dimethyl ether/ PEGdm(250)	$\text{H}_3\text{C}-\left(\text{O}-\underset{\text{H}_2}{\text{C}}-\underset{\text{H}_2}{\text{C}}\right)_n-\text{O}-\text{CH}_3$	5.6	250	0.007
Poly(ethylene glycol) dimethyl ether/ PEGdm(500)	$\text{H}_3\text{C}-\left(\text{O}-\underset{\text{H}_2}{\text{C}}-\underset{\text{H}_2}{\text{C}}\right)_n-\text{O}-\text{CH}_3$	11.4	500	0.025
Poly(ethylene glycol) methyl ether/ PEGm(350)	$\text{H}-\left(\text{O}-\underset{\text{H}_2}{\text{C}}-\underset{\text{H}_2}{\text{C}}\right)_n-\text{O}-\text{CH}_3$	7.9	350	0.027
Poly(ethylene glycol)/ PEG(400)	$\text{H}-\left(\text{O}-\underset{\text{H}_2}{\text{C}}-\underset{\text{H}_2}{\text{C}}\right)_n-\text{OH}$	9.0	400	0.023

(1) Number of repeating units in the polymeric chain. (2) Measured at 25 °C.

Two types of fumed silica (FS) nanoparticles were kindly donated by Degussa. Hydrophilic FS (A200) has a primary particle size of 12 nm and a surface area of 200 m²/g, while hydrophobic FS (R805) has a primary particle size of 12 nm and 150 m²/g³. The main difference between these two types of FS nanoparticles relies in their surface chemistry. The surface of the hydrophilic material contains mainly silanol groups (~ 2.5 Si-OH/nm²), whereas 50% of the R805 surface has been decorated with octyl chains, rendering the particles hydrophobic^{3, 4}. Though the primary particles are in the order of nm, the aggregation process that takes place during the flame hydrolysis synthesis makes the length scale of the aggregates slightly larger (~0.1-0.5 μm) and mechanically unbreakable. This feature is unique to these amorphous SiO₂ particles as it creates structure and controls the surface area¹. The composites were prepared by high-shear mixing at 6000 rpm in a Silverson SL2 mixer (Silverson Machines, Chesham, U.K.), the previously dried FS (at 110 °C, under vacuum) in the liquid oligoethers. Once mixed, the samples were degassed under

vacuum to extract the bubbles formed in the previous step and the materials were tested within 24 hours of their preparation.

3.2.1 Rheological Characterization

The dynamic rheological experiments were performed in a stress-controlled rheometer AR-G2 (TA Instruments) using 20 and 40 mm diameter parallel plate geometries. The rheometer is equipped with a Peltier control system that allows accurate control (± 0.1 °C) of the temperature between 10 – 90 °C. All the experiments were conducted within the linear viscoelastic region of deformation at each temperature. A pre-shear step (between 0.4-40 rad/s at 25 °C) followed by a recovery step (20 min at zero shear) was applied to each sample in order to establish a uniform shear history, a protocol established based on a previous work on this area¹⁴.

3.2.2 Extraction and Thermogravimetric Analysis (TGA)

FS dispersions were treated under different conditions (iso- and dynamic thermal treatments to be mentioned in the discussion section), washed three times with acetonitrile, methanol, acetone, and water, filtered, and dried under vacuum at 100 °C. All solvents were obtained from Aldrich, and used as received. Prior to characterization, the extracted FS powder was characterized by thermogravimetric analysis (TGA). The temperature heating scans were done in a TGA Q500 (TA Instruments) from 25 – 1000 °C, at 10 °C/min under nitrogen atmosphere. The resulting weight loss as a function of temperature trace was employed to quantify the content of organics in the sample.

3.3 Results and Discussion

3.3.1 Effect of temperature on the dynamic rheological properties of FS gels

Figure 3.1 shows the elastic modulus as a function of frequency for two types of FS in PEGdm(250) at different temperatures. In this particular case, the formulations differ only in the surface chemistry of the FS particles dispersed in the oligoether. For the two types of FS and two temperatures shown, all samples exhibit gel-like behavior, as the elastic modulus (G') is higher than the viscous modulus (G'') (only shown for the hydrophobic FS gels at 80 °C for clarity) and frequency independent^{7, 9, 11}. This characteristic signature indicates that the FS particles form a three-dimensional network with an infinite relaxation time.

For the hydrophobic FS (R805) gel, G' (or gel modulus) at 80 °C is lower than that at 25 °C, and the frequency independent behavior of G' observed at the lower temperature becomes slightly frequency dependent ($G'_{(80)} \sim \omega^{0.2}$). A decrease in the solvent viscosity and an increase in the particle mobility as a consequence of the higher thermal energy can possibly explain the observed reduction in the elastic modulus for the R805 gels. The viscosity of the matrix in which the particles are dispersed (PEGdm(250) in this case) goes from 7.0 mPa-s at 25 °C to 2.4 mPa-s at 80 °C causing the material, as a whole, to decrease its resistance to deformation as temperature increases. Moreover, the higher thermal energy not only increases the Brownian motion of the particles, but also decreases the interaction potential among the particles driven by dispersion forces in this particular case^{7, 15}.

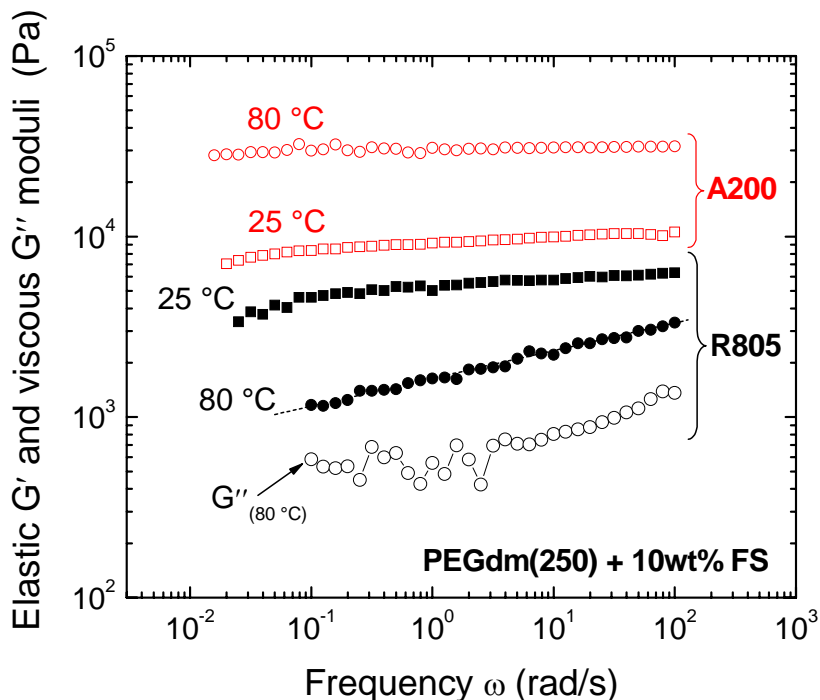


Figure 3.1. Elastic modulus as a function of frequency for dispersions of hydrophobic (R805) and hydrophilic (A200) fumed silica in PEGdm(250) at 25 and 80 °C.

If we take a look at the gels of hydrophilic FS (A200), a very different and unexpected behavior is observed upon heating to 80 °C. The gel modulus at 80 °C is higher than that observed at 25 °C, indicating that the gel becomes stronger after enough heat is provided. If we compare the gel formation mechanism for hydrophobic and hydrophilic FS particles dispersed in PEGdm(250), a solvent medium with low hydrogen bonding ability, we would expect for the gel which forms through hydrogen bonding among the particles (hydrophilic) to become more susceptible to deformation, i.e., to show a lower elastic modulus at higher temperatures. However, the results presented in Figure 3.1 indicate that neither the decrease in hydrogen bonding strength nor the decrease in viscosity of the continuous phase with temperature dominates the rheological response of the hydrophilic FS (A200) gels in PEGdm(250).

We suggest two hypotheses to explain this anomalous behavior. First, as the temperature increases and the particles become more mobile, the PEGdm(250) molecules are more amenable to surround or be in contact with the surface of the silica particles, given that the physical interactions among them become weaker. If this occurs, there will be less PEGdm(250) molecules in the solvent phase and more on the FS surface (entrapped within the agglomerates or aggregates). This will effectively increase the volume fraction thereby making the gel become stronger¹⁶ (see Figure 3.2 line (a)). Whether the concentration effect involves a chemical reaction, physical adsorption of the oligomer molecules on the surface or both, remains unanswered at this point and will be discussed in detail later on.

Our second hypothesis suggests that bridging between particles caused by the PEGdm(250) molecules is responsible for the increase in the elastic modulus at higher temperature (Figure 3.2 line (b)). If the particle aggregates are connected to each other by bridging chains, the network strength would increase since the newly formed larger aggregates would be more difficult to deform. This hypothesis also requires for the oligomer chains to chemically react with the silanol groups available on the surface of the FS particles or to physically adsorb onto it. These two hypotheses are summarized schematically in Figure 3.2. As previously mentioned, both cases give as a result stronger networks, thus higher elastic modulus. In the following sections, we will discuss our interpretation of this unexpected, interesting phenomenon through additional experiments conducted on the FS gels.

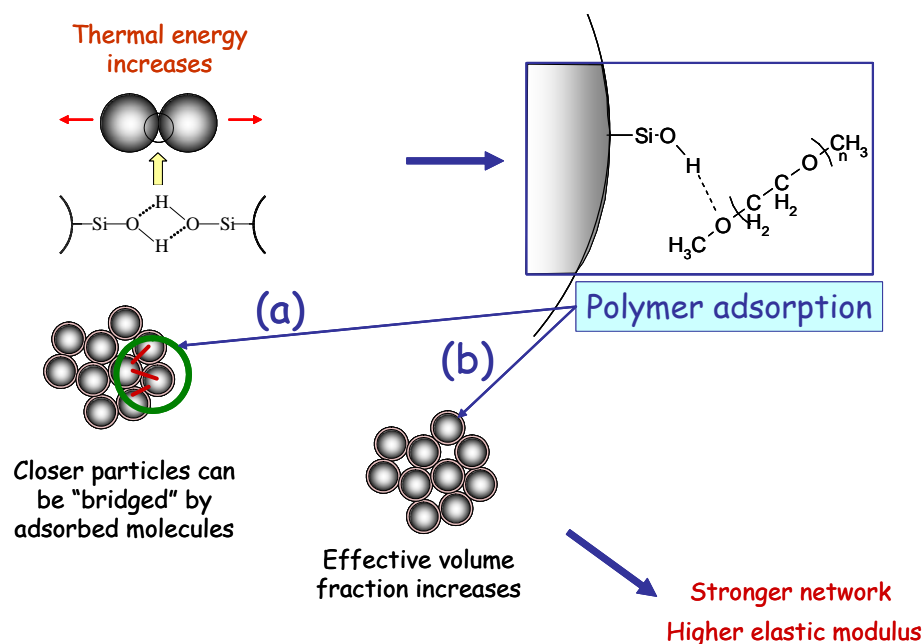


Figure 3.2. Suggested mechanism for PEGdm(250) adsorption on the surface of hydrophilic fumed silica at higher temperature. The arrows identified by (a) and (b) indicate the two suggested hypothesis for increase in the elastic modulus of the A200 gels when thermal energy is provided to the system.

3.3.2 Temperature sweeps *vs.* isothermal studies

Even though an increase in the elastic modulus of the hydrophilic FS gels after isothermal treatments at temperatures between 25 and 80 °C is observed, we are interested in investigating if the change in elastic modulus with temperature is a continuous phenomenon or if there is a specific transition temperature for this change to occur. In order to study this effect, we performed dynamic temperature sweeps at 0.4 °C/min. At this rate, the temperature varied slowly enough so that the rheological measurements were always under steady conditions. Figure 3.3 shows the elastic modulus as a function of temperature for gels of hydrophobic and hydrophilic FS in PEGdm(250). We observe that for hydrophobic FS gels, the elastic modulus progressively decreases with temperature, while

for hydrophilic FS gels the opposite trend is observed. These results indicate that the gel modulus of FS in PEGdm(250) changes continuously as temperature increases and it is rather a function of time at a particular temperature. This effect can be clearly seen in the inset of Figure 3.3, where the change in elastic modulus as a function of time at 80 °C for hydrophilic FS in PEGdm(250) is shown. It can be seen that G' increases and reaches a plateau after ~200 min. The time effect will be discussed in detail in the next section; however it is important to note that G' reaches an equilibrium value as has been observed for adsorption of high- and low-MW polymers on silica from solution^{10, 12, 17}.

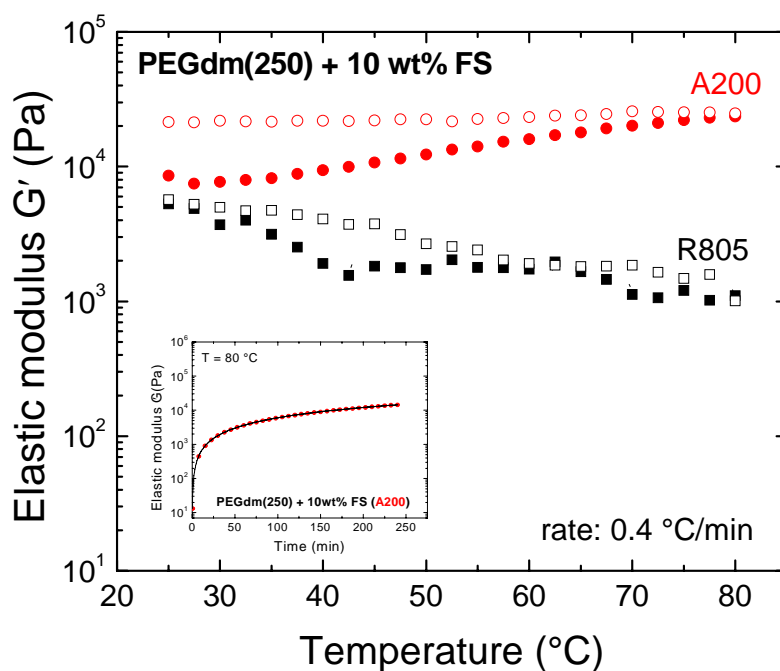


Figure 3.3. Temperature sweeps at 0.4 °C/min for dispersions of hydrophobic (R805) and hydrophilic (A200) fumed silica in PEGdm(250). The inset depicts a dynamic time sweep at 80 °C for hydrophilic FS (A200) in PEGdm(250). The dynamic rheological experiments were done in the rheometer at 1 rad/s.

Another interesting feature that can be seen from this figure is that as the samples are cooled down following a first heating step, the elastic modulus of hydrophilic FS gels, unlike the hydrophobic FS ones, does not return to its initial value. In fact, G' remains at the same value reached during the heating step. The fact that the elastic modulus remains at a constant value after the thermal treatment has been applied by either heating at a controlled rate or isothermally treating the sample at a specific temperature, indicates that the process is not reversible and that the network strength is not affected by temperature. Once again, a distinction between chemical reaction and physisorption of the PEGdm(250) molecules on the silica surface can not be made at this stage but will be clarified in later sections. Highly interactive polymer-particle systems, such as the one discussed in this work, can show higher levels of physisorption and in this cases the binding is strong enough to be considered irreversible¹⁰. Additionally, PEO can displace interfacial water from the silica surface^{1, 17, 18}, which indicates the level of affinity of this material for silica. If we consider the change in G' to be an indication of the amount of chains that adsorb on the surface, our thermal treatment seems to increase the affinity of PEGdm(250) for the silica, thus lowering the amount of PEGdm(250) chains in the continuous phase making the FS volume fraction effectively higher. Please, note that re-testing a sample that has been subjected to a cycle of heating and cooling results in a slight increase in modulus (data not shown); however, after the third cycle there are not further changes in G').

3.3.3 Effect of particle concentration on the dynamic rheological properties of hydrophilic FS gels

Previous works indicate that the adsorption of PEO occurs easily when the viscosity of the medium is lower^{1, 12, 17}. As a result, adsorption of high-MW polymers on silica or other surfaces, tend to be conducted in solution^{1, 12, 17}. In our case, the situation is different; the solvent and adsorbate are one and the same, and accessibility to the surface is not limited by the polyether molecular weight (i.e., length of the chain) since the number of monomer units in PEGdm(250) is small (5-6 monomer units). In view of this situation, the mobility of the polyether chains is only limited by the amount of particles dispersed. We therefore examined the effect of fumed silica concentration, and monitored the change in G' as a function of temperature and time.

Figures 3.4 and 3.5 show, respectively, dynamic oscillatory temperature and time sweeps for various concentrations of hydrophilic FS (A200) in PEGdm(250). The elastic modulus of the less concentrated FS dispersions is lower than that for the more concentrated ones (up to 15 wt% in this work) indicating that a denser three-dimensional network forms when there are more particles that are also closer to each other. For all FS concentrations, the behavior is similar to the one discussed previously for 10 wt% A200 dispersion; G' increases during the heating step and remains constant after the cooling step (see Figure 3.4). It is interesting to note that for the 2 wt% FS in PEGdm(250) material, G' shows a slight increase upon cooling with respect to the value attained at 80 °C. This is possibly due to the fact that in this case, the material is a very weak gel^{7, 8} (see Figure 3.6) and the contribution of the continuous medium to the overall elastic response of the material plays a

more important role. In other words, since the viscosity of the continuous phase increases as the temperature decreases, the overall rheological response reflects this viscosity change. This contribution, however, is not as important as the concentration effect taking place as a result of the temperature treatment, which can be clearly seen in Figure 3.6.

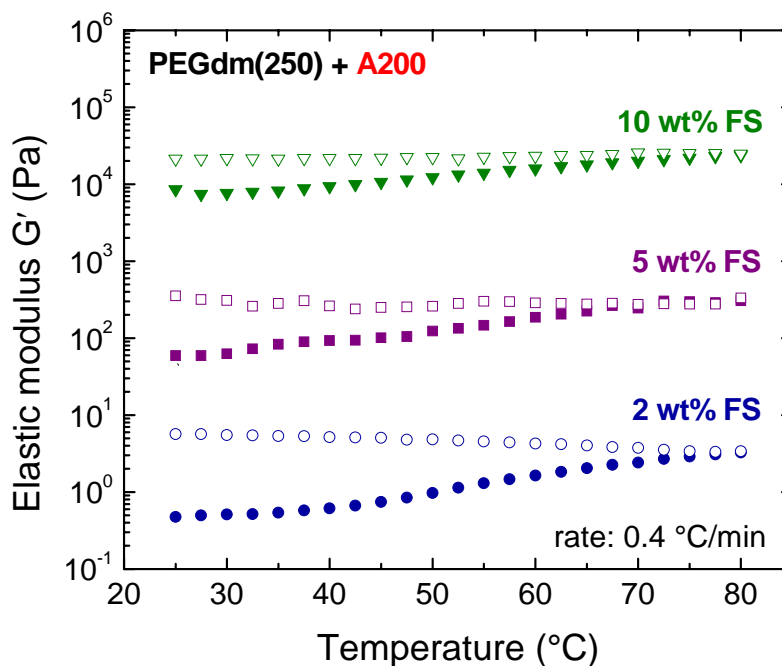


Figure 3.4. Temperature sweeps for dispersions of hydrophilic fumed silica (A200) in PEGdm(250) at different concentrations. The dynamic rheological experiments were performed in the rheometer at 1 rad/s.

Here, the elastic modulus after the thermal treatment at 80 °C is independent of frequency and the magnitude of the viscous contribution (G'') becomes smaller in contrast with G'' of the same material before the thermal treatment. Figure 3.5 shows an increase of the elastic modulus followed by a plateau region as time progresses for various concentrations of hydrophilic FS in PEGdm(250) at 80 °C.

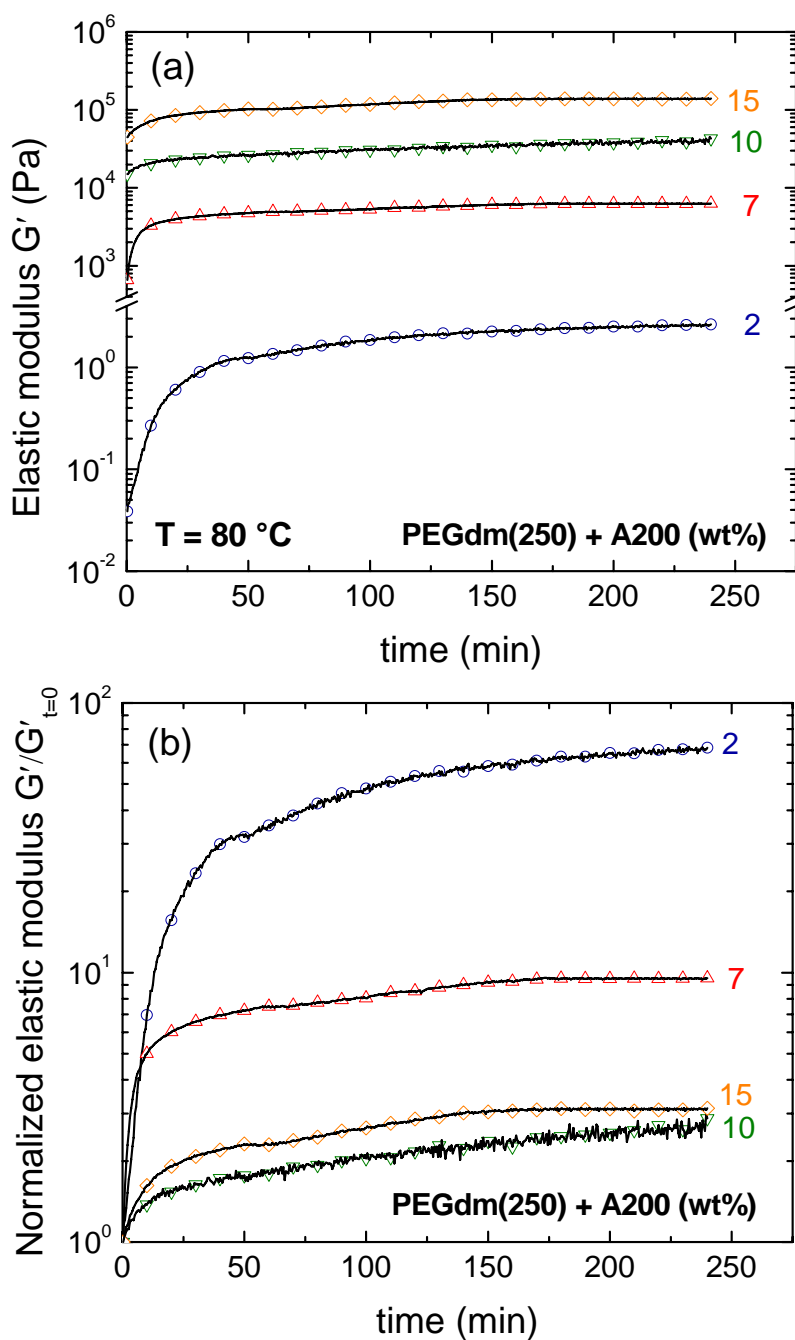


Figure 3.5. Effect of thermal treatment on the rheological properties of various dispersions of hydrophilic fumed silica (A200): (a) Elastic modulus (G') and (b) Normalized elastic modulus ($G'/G'_{t=0}$) vs time at 80 °C. The thermal treatment was performed in the rheometer at 80 °C and 1 rad/s.

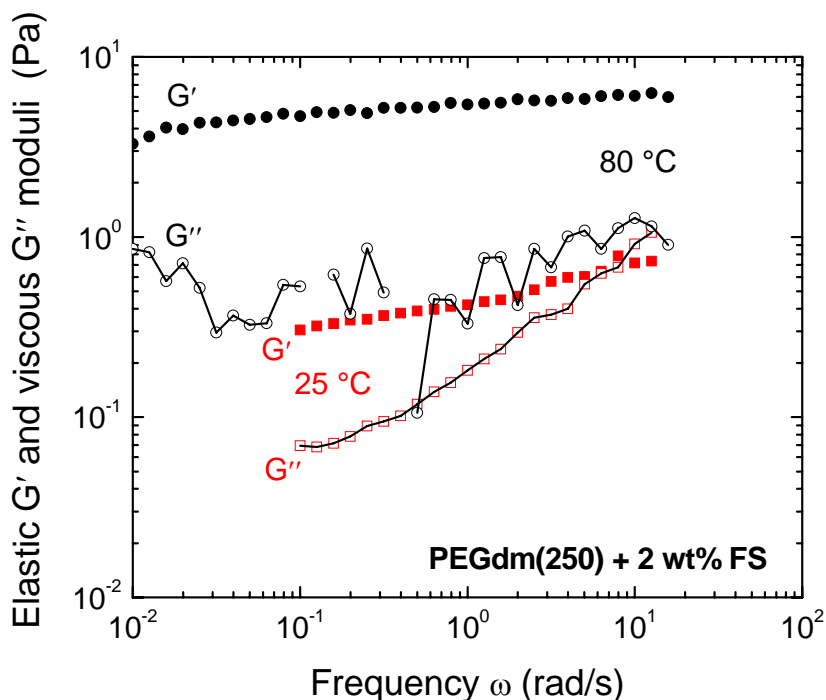


Figure 3.6. Elastic modulus versus frequency at 25 and 80 °C for 2 wt% hydrophilic FS (A200) in PEGdm(250).

The effect of fumed silica concentration is better illustrated in Figure 3.5(b), where we normalized the elastic modulus by its initial value ($G'_{t=0}$) to quantify the magnitude of change in elasticity. It can be seen that the dispersions containing lower amounts of FS exhibit a larger change in elasticity. We interpret these results in terms of the larger effective surface area available for the PEGdm(250) molecules to adsorb. As the FS aggregates get closer, because of the larger number present in the system, the accessibility of the polymer chains to the surface of the FS particles is limited. Consequently, a smaller number of chains can effectively be in contact with the surface and the concentration effect is less than for those cases where the adsorption is not hindered by the presence of numerous aggregates. This indicates that for the elastic modulus to change, closer proximity of the FS

aggregates is not required and this result leans us towards the first suggested hypothesis, where bridging of the FS particles by PEGdm(250) chains is not necessary for the elastic modulus to increase.

Figure 3.7 summarizes the dependence of G' on particle concentration at 25 and 80 °C. A power-law scaling relationship is observed, indicating that at each temperature, the rheological properties are governed by the fractal (self-similar) nature of the FS particle arrangement. Moreover, the self-similar structures are the same for all the dispersions at each temperature¹⁹. A very interesting feature is also noted for gels of A200 FS at 25 °C; the power-law exponent is higher than that obtained for these materials at 80 °C. Additionally, in both cases, the values are slightly higher than the ones suggested by Buscall²⁰, Shih¹⁹, Khan and Zoeller¹⁶, Saint-Michel²¹ and others for colloidal systems well beyond the percolation threshold. Although we can not assign a mechanism of aggregation with certainty (i.e., reaction limited cluster-cluster aggregation vs. diffusion limited cluster-cluster aggregation), at 25 °C, particle aggregation seems to be driven by the physical interactions (hydrogen bonding) among particles.

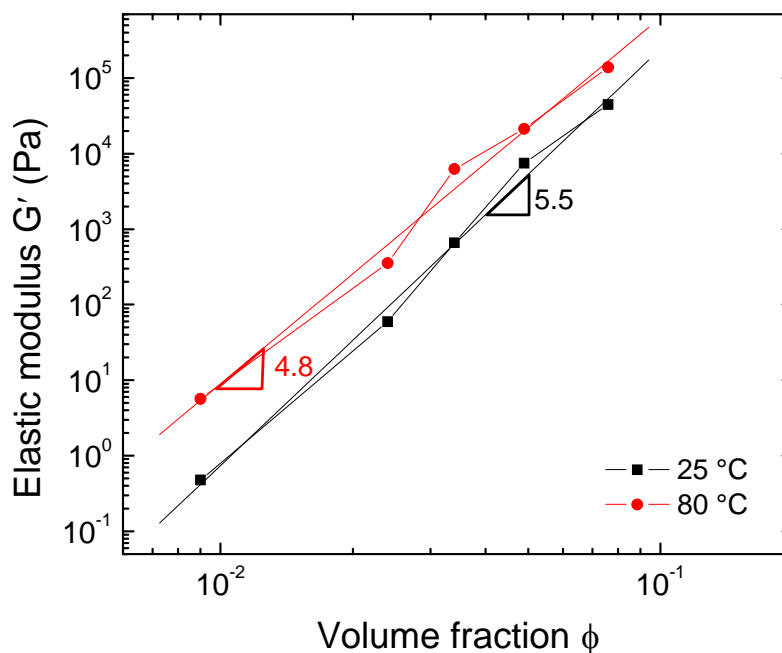


Figure 3.7. Dependence of the elastic modulus on volume fraction for dispersions of hydrophilic (A200) fumed silica in PEGdm(250) at 25 and 80 °C

3.3.4 Chemical reaction *vs.* physical adsorption

The rheological experiments discussed to this point, allow us to understand and evaluate the mechanical properties of FS gels before and after the samples are submitted to thermal treatments, which can easily happen during processing or end use and somehow correlate them with the microstructure. These experiments, however, do not provide clear evidence that helps us understand if the polyether chains physically adsorb to the FS surface or if there is a chemical reaction involved. In order to obtain more insight about this interesting temperature effect, samples of fresh and thermally treated hydrophilic FS (A200) gels were extracted with acetonitrile, methanol and water to remove the continuous medium,

i.e., the polyether. After repeated washing steps and drying under vacuum at room temperature, the remaining FS extract was tested by thermogravimetric analysis (TGA). The results are shown in Figure 3.8 as weight loss as a function of temperature. It can be seen that the thermally treated sample exhibited a higher weight loss than the one that was not thermally treated.

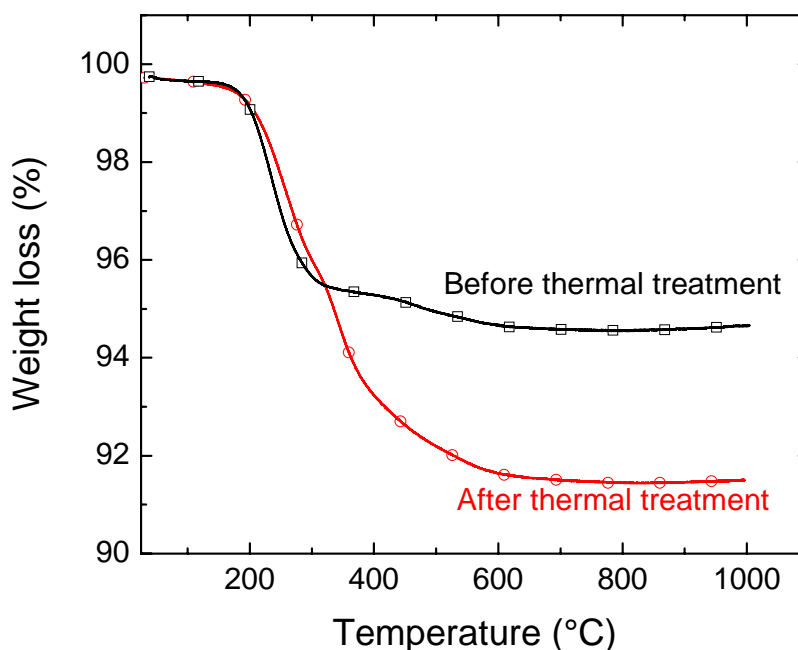


Figure 3.8. TGA of fumed silica extracts before and after thermal treatment at 80 °C for 4 h. In all cases the silica was washed and dried several times until constant weight loss was obtained. The temperature scans were conducted at 10 °C/min.

Although repeated washing steps (until the observed weight loss value remained constant) were conducted, both samples show the presence of organic material that degrades approximately at the same temperature. The trace corresponding to the thermally treated sample not only shows a higher weight loss, but also a different shape as the degradation mechanism takes place. This difference is more clearly seen in Figure 3.9, where the derivative of the weight loss with respect to temperature (dW/dT) is plotted as a function of

temperature. A secondary peak at ~ 340 °C and a broader change in weight loss as a function of temperature is observed for the thermally treated sample. In contrast, the untreated sample shows a single degradation step that occurs in a narrower temperature range. These two signals are attributed to the presence of PEGdm(250) molecules that are physically adsorbed (low temperature signal) and chemically reacted (high temperature signal) with the silanol groups present on the FS surface, respectively. Similar results were observed by Maitra¹³ after modifying FS particles with PEO-silane, where the PEO segment contained 6-9 repeating units. In this case, a low-temperature shoulder at ~ 250 °C in the dW/dT trace was observed and attributed to desorption of low-MW monomers. A higher temperature peak observed at ~ 375 °C was attributed to the degradation of high-MW and crosslinked species formed after silanol condensation¹³. Based on this evidence, we conclude that hydrophilic FS gels undergo a chemical reaction upon heating to 80 °C and this reaction is responsible for the increase in the elasticity of the gels.

Figure 3.10 shows a schematic of the proposed condensation reaction between the silanol groups on the FS surface and the ether oxygen of the PEGdm(250) chains. Evidence of adsorption and reaction of the ether oxygen in PEO and the silanol groups on silica surface was given by Fontana several years ago²². More recent works on grafting of PEO chains (MW = 1800 g/mol) on silica²³ suggest that the grafting of PEG molecules occurs through esterification reaction. It is important to mention that in our case, the amount of chemically reacted PEGdm(250) molecules is much lower compared to the physically adsorbed molecules. Therefore, the attached molecules are just enough to concentrate the dispersion and not to create a hydrophobic corona on the FS surface. This explains the fact

that the hydrophilic FS in PEGdm(250) gels become stronger and not a suspension of sterically stabilized particles in PEGdm(250) due to matching of the refractive indices of the corona layer and the solvent medium¹⁵.

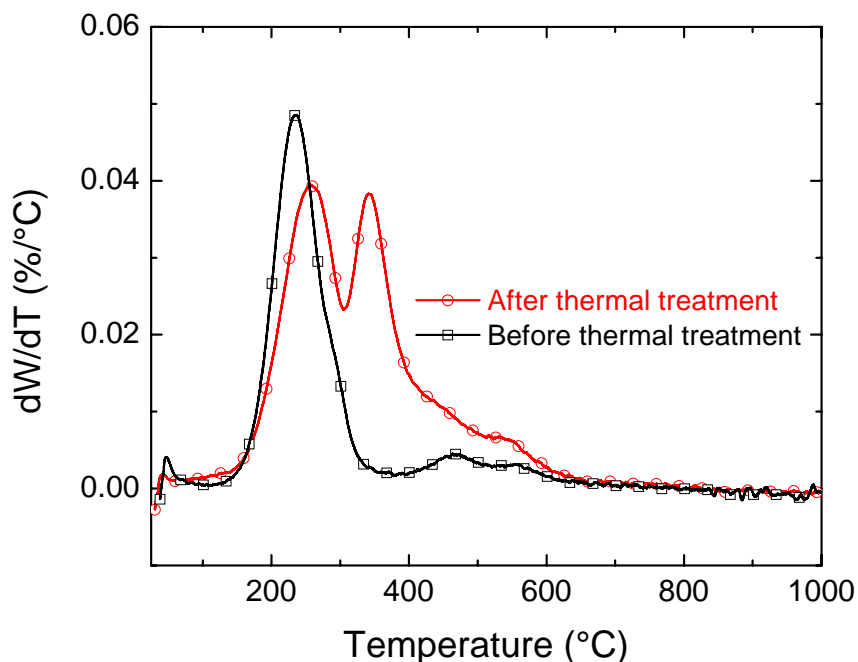


Figure 3.9. Derivative of the weight loss (dW/dT) as a function of temperature of fumed silica extracts before and after thermal treatment at 80 °C for 4 h.

3.3.5 Effect of end group type and content on temperature response of hydrophilic FS in polyether dispersions

While hydrophilic FS A200 forms gels in PEGdm(250), PEGdm(500) and PEGm(350), a suspension-like behavior is obtained when it is dispersed in PEG(400). As explained in previous studies^{9,16}, the ability of the solvent media to form hydrogen bonding plays a major role in the mechanism of gel formation. Native hydrophilic FS particles with

silanol groups on the surface preferentially interact with PEG, a solvent with strong hydrogen bonding formation ability and the particles stay away from each other to favor this type of interaction. This solvation effect stabilizes the system and a suspension of FS particles is obtained. If the hydroxyl groups are substituted by methyl groups, one end in the case of PEG_m and both ends for PEG_{dm}, the molecules are not prone to hydrogen bonding with the FS surface and the particles prefer to maximize the interactions with each other rather than with the medium. This results in a FS network with a very large elastic component.

Figure 3.11 illustrates the behavior of hydrophilic FS dispersions in PEG and its methyl-substituted analogs as a function of temperature. The elastic modulus of A200 in PEG(400) decreases reversibly with temperature, whereas in PEG_m(350) a higher G' is observed followed a heating and cooling cycle. We attribute these results to the difference in the amount of end groups available as well as to the fact that in PEG(400), the reaction does not alter the microstructure noticeably since the particles are not in close proximity to each other and the chains solvate the FS surface sites even at lower temperatures. This hypothesis is verified in Figure 3.12, where we plot the elastic modulus as a function of temperature for A200 in PEG_{dm}(500). It can be seen that the gel modulus slightly decreases as temperature increases and the initial gel modulus is value is almost recovered upon cooling from 80 °C. Because the PEG_{dm}(500) molecule is longer than the PEG_{dm}(250), the amount of end groups (-OCH₃) available for the condensation reaction to occur is considerably less and the effective volume fraction remains the same, as opposed to the previously mentioned concentration effect occurring in PEG_{dm}(250).

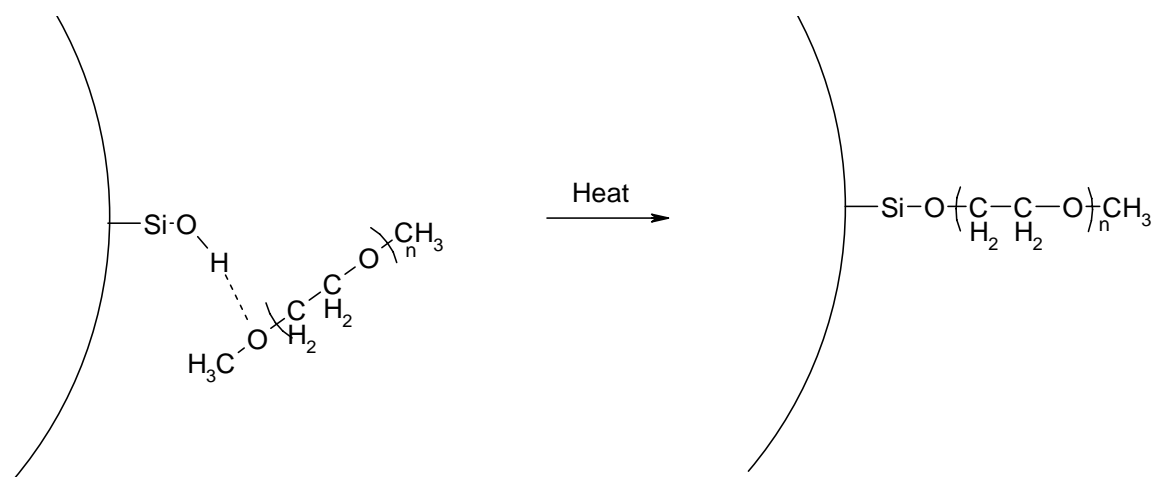


Figure 3.10. Suggested mechanism for the condensation of PEGdm(250) molecules on the surface of hydrophilic fumed silica upon heating to 80 °C.

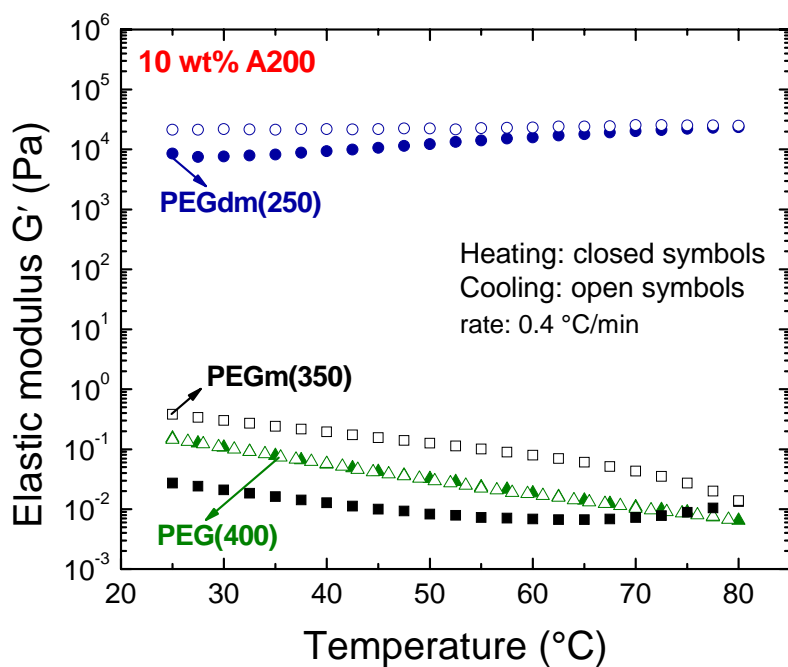


Figure 3.11. Effect of PEG end group on the rheological properties of hydrophilic (A200) fumed silica dispersions as a function of temperature. The rheological experiments were done in the rheometer at 1 rad/s and 0.4 °C/min. The data correspond to two steps, heating (closed symbols) and cooling (open symbols) after the previous step.

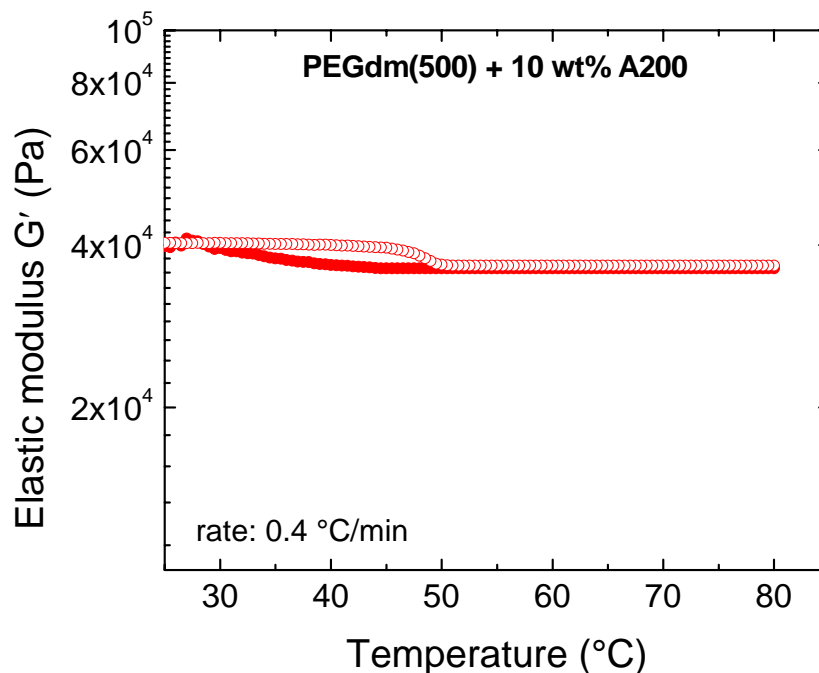


Figure 3.12. Effect of PEG end group amount on the rheological properties of hydrophilic (A200) fumed silica dispersions as a function of temperature.

3.4 Conclusions

In this study, we investigated the effects of temperature on various dispersions of FS in PEG and its methyl-substituted analogs. Dynamic rheological experiments are able to capture differences in the elasticity of the materials that, along with thermogravimetric analysis explain the changes occurring in the systems. An anomalous temperature behavior is observed for gels of hydrophilic FS (A200) in PEGdm(250). The elastic modulus, which characterizes the strength of the physical network, irreversibly increases upon heating to 80 °C. If 50% of the FS surface is covered with hydrophobic moieties (octyl chains in the case of R805), the gels behave differently. In this case, the gel modulus decreases as the temperature increases and the original value is recovered upon cooling. Physical adsorption as well as a condensation reaction between the silanol groups available (and easily

accessible) on the hydrophilic FS surface increases the effective volume fraction. This concentration effect is responsible for the increase in elastic modulus of the temperature treated materials. If the PEGdm(250) is substituted by a longer molecule such as PEGdm(500), the modulus decreases upon heating and the initial value is recovered upon cooling. The larger amount of end groups available in PEGdm(250), thus seems to play a role in the condensation reaction that makes the system effectively more concentrated. These results indicate that the rheological properties of FS gels in low-MW polyethers can thereby be tailored by a simple thermal treatment if the proper combination of hydrophilicity and of the FS particles and solvent polarity are chosen.

3.5 References

1. Iler, R. K., *The Chemistry of Silica: Solubility, Polymerization, Colloid and Surface Properties, and Biochemistry*. John Wiley & Sons: New York, NY, 1979; p xxiv, 866.
2. Legrand, A. P., *The Surface Properties of Silicas*. John Wiley & Sons: London, 1998.
3. *Basic Characteristics of Aerosil*; Degussa Technical Bulletin No. 11; Degussa Corp.: Akron, OH, 1993.
4. *Hydrophobic Aerosil: Manufacture, Properties and Applications*; Degussa Technical Bulletin No. 6; Degussa Corp.: Akron, OH, 1991.
5. Raghavan, S. R.; Baker, G. L.; Khan, S. A., Colloidal silica gels for use as novel electrolytes for rechargeable batteries: Synthesis, microstructure and rheology. *Abstracts of Papers of the American Chemical Society* 1998, 216, U601-U601.
6. Raghavan, S. R.; Fussell, G. W.; Khan, S. A., Fumed silica dispersions in polymeric liquids: Evidence for site-specific colloidal interactions. *Abstracts of Papers of the American Chemical Society* 1997, 214, 332-POLY.
7. Raghavan, S. R.; Hou, J.; Baker, G. L.; Khan, S. A., Colloidal interactions between particles with tethered nonpolar chains dispersed in polar media: Direct correlation

- between dynamic rheology and interaction parameters. *Langmuir* 2000, 16, (3), 1066-1077.
8. Raghavan, S. R.; Khan, S. A., Shear-Induced Microstructural Changes in Flocculated Suspensions of Fumed Silica. *Journal of Rheology* 1995, 39, (6), 1311-1325.
 9. Raghavan, S. R.; Walls, H. J.; Khan, S. A., Rheology of silica dispersions in organic liquids: New evidence for solvation forces dictated by hydrogen bonding. *Langmuir* 2000, 16, (21), 7920-7930.
 10. Zhang, Q.; Archer, L. A., Poly(ethylene oxide)/silica nanocomposites: Structure and rheology. *Langmuir* 2002, 18, (26), 10435-10442.
 11. Larson, R. G., *The Structure and Rheology of complex Fluids*. Oxford University Press, Inc.: New York, 1999.
 12. Howard, G. J.; McConnell, P., Adsorption of Polymers at the solution-solid interface. Polyethers in silica. *The Journal of Physical Chemistry* 1967, 71, (9), 2974-2981.
 13. Maitra, P.; Ding, J.; Huang, H.; Wunder, S. L., Poly(ethylene oxide) silanated nanosize fumed silica: DSC and TGA characterization of the surface. *Langmuir* 2003, 19, 8994-9004.
 14. Walls, H. J.; Caines, S. B.; Sanchez, A. M.; Khan, S. A., Yield Stress and Wall Slip Phenomena in Colloidal Silica Gels. *Journal of Rheology* 2003, 47, (4), 847-868.
 15. Israelachvili, J. N., *Intermolecular and Surface Forces*. 2nd ed.; Academic Press London: London, 1991; p xxi, 450.
 16. Khan, S. A.; Zoeller, N. J., Dynamic Rheological Behavior of Flocculated Fumed Silica Suspensions. *Journal of Rheology* 1993, 37, (6), 1225-1235.
 17. Voronin, E. F.; Gun'ko, V. M.; Guzenko, N. V.; Pakhlov, E. M.; Nosach, L. V.; Leboda, R.; Skubiszewska-Zieba, J.; Malysheba, M. L.; Borysenko, M. V.; Chuiko, A. A., Interaction of poly(ethylene oxide) with fumed silica. *Journal of Colloid and Interface Science* 2004, 279, 326-340.
 18. Gun'ko, V. M.; Mironyuk, I. F.; Zarko, V. I.; Turov, V. V.; Voronin, E. F.; Pakhlov, E. M.; Goncharuk, E. V.; Leboda, R.; Skubiszewska-Zieba, J.; Janusz, W.; Chibowski, S.; Levchuk, Y. N.; Klyueva, A. V., Fumed silicas possessing different

- morphology and hydrophilicity. *Journal of Colloid and Interface Science* 2001, 242, (1), 90-103.
19. Shih, W. H.; Shih, W. Y.; Kim, S. I.; Liu, J.; Aksay, I. A., Scaling Behavior of the Elastic Properties of Colloidal Gels. *Physical Review A* 1990, 42, (8), 4772-4779.
 20. Buscall, R.; Mills, P. D. A.; Goodwin, J. W.; Lawson, D. W., Scaling Behavior of the Rheology of Aggregate Networks Formed from Colloidal Particles. *Journal of the Chemical Society-Faraday Transactions I* 1988, 84, 4249-4260.
 21. Saint-Michel, F.; Pignon, F.; Magnin, A., Fractal behavior and scaling law of hydrophobic silica in polyol. *Journal of Colloid and Interface Science* 2003, 267, 314-319.
 22. Fontana, B. J., The configuration of an adsorbed polymeric dispersant by infrared studies. *Journal of Physical Chemistry* 1963, 67, 2360-2362.
 23. Hommel, H.; Legrand, A. P.; Balard, H.; Papirer, E., Influence of chain length on conformation of poly(ethylene glycol) chains grafted on silica. *Polymer* 1983, 24, 959-963.

4

Effects of Temperature on Polyethers Using Mixtures of Hydrophilic and Hydrophobic Fumed Silicas as Gelling Agents

Abstract

The rheological behavior of mixed colloidal particles containing different surface functionalities in low-molecular weight polyethers is examined. In particular, the effects of temperature on mixtures of hydrophilic and hydrophobic fumed silica in different proportions, in poly(ethylene glycol) dimethyl ether and poly(ethylene glycol) are investigated to determine how the presence of various colloidal particles of different surface functionalities affect the rheology and microstructure of the dispersions. In poly(ethylene glycol) dimethyl ether, a gel-like structure is formed for all the samples regardless of the hydrophilic to hydrophobic filler ratio. Likewise, temperature does not cause the materials to transition from solid-like to liquid-like behavior. The presence of colloidal particles with opposite surface activities (high-surface energy or hydrophilic *vs.* low-surface energy or hydrophobic) in the mixed-fumed silica phase dilutes the reinforcing effect of the individual components as evidenced by the negative deviation from the log-additive mixing rule. On the contrary, mixed-fumed silicas in poly(ethylene glycol) exhibit a synergistic behavior for the elastic modulus of the colloids. The modulus goes through a maximum at 50/50 hydrophilic/hydrophobic FS within the temperature range evaluated. In poly(ethylene glycol)dimethyl ether, blends containing 75% of one of the FS resemble the behavior of the major component: an increase of modulus with temperature for blends containing larger amounts of hydrophilic FS and a slight decrease in elastic modulus for those containing larger amounts of the hydrophobic kind. In poly(ethylene glycol) only 25% of hydrophobic fumed silica is necessary to obtain a rheological solid-like response.

To be submitted to Journal of Colloid Interface Science

Authors: A.M. Sanchez, S. Ilias, and S.A. Khan

4.1 Introduction

Colloidal particles are of great interest in several areas such as coatings, adhesives, printing inks, display and photonic devices, and biological systems, among others. Often, these particles are used to obtain desirable rheological properties of the solvent media in which they are dispersed, and a variety of states, ranging from stable suspensions to elastic networks. The magnitude of particle-particle interaction potential and the concentration of particles dispersed in the solvent are the main factors determining the state of aggregation¹⁻³. The interaction potential, which includes long-ranged repulsive electrostatic forces, short-ranged attractive van der Waals forces, and specific interactions such as hydrogen bonding, can be affected by pH, surfactant additives, particle size, random thermal forces, and externally imposed shear. If the proper balance between these factors is chosen, a physical network of particles suspended in a liquid is obtained. This aggregation state is particularly attractive, as in certain applications such as composite polymer electrolytes, it is possible to preserve the chemical properties of the liquid where the particles are dispersed and at the same time tune the flow properties of the colloid.

Composite polymer electrolytes based on oligomers of poly(ethylene oxide), PEO and fumed silica (FS) particles are an example of systems in which the chemical properties of the liquid are desired but its physical nature adds limitations to its use in the application. Oligomers of PEO have the ability to solvate ions (i.e. lithium ions) and this makes it a good candidate for an electrolyte in lithium battery applications⁴⁻⁸. Additionally, their low-molecular weight (MW) makes possible for this material to achieve reasonable ionic

conductivities at low temperatures. At the same time, as oligomers of low-MW, their viscosities range from 5-10 mPa-s which makes them incapable of sustaining large deformations without flowing. If a physical network can be formed in these liquid matrices, the physical integrity of the electrolyte material can be preserved. Previous research shows that gel electrolytes of FS in oligoethers exhibit decoupling of electrochemical and mechanical properties⁵.

Fumed silica is an amorphous form of silicon dioxide (SiO_2) obtained by flame hydrolysis. The resulting primary particles, spheres of approximately 7 to 14 nm in diameter, can collide while hot and fuse into aggregates of $\sim 0.1 \mu\text{m}$. These aggregates are branched, chain-like structures, and can be considered as the fumed silica primary structure, since the fusion process is irreversible^{9, 10}. Further collisions give place to physical entanglement of aggregates to form agglomerates after cooling. Agglomerates are the product of non-specific forces such as dipole-dipole and hydrogen bonding; therefore these can be dispersed by simple mixing. The native form of fumed silica has a hydrophilic surface chemistry, being that the silanol (Si-OH) and siloxane (Si_2O) functional groups play a major role in the behavior of fumed silica. These moieties can be modified with various groups such as alkyl chains (to render the particles hydrophobic), and a variety of surface functionalities is obtained.

Often in certain applications such as paints, two or more types of particles are mixed to comply with the end product demands. For example, in the specific case of paint formulations, titanium dioxide particles provide opacity to the paint, while poly(methyl methacrylate) particles give the paint its required adhesive properties. While there has been

some research dealing with mixtures of particles, different particle sizes has been among the most studied parameters¹¹⁻¹⁴. Very little work has been done on particles that do not behave as hard spheres and that have very different interaction potential. Since the interaction potential along with the particle size play a major role in the state of aggregation in colloidal systems, an understanding of the behavior of colloids containing mixtures of particles with very different interaction capabilities is of particular interest. In this work, we suggest combining hydrophobic and hydrophilic FS particles into one material as a way of improving the gel strength, specifically gel modulus and yield stress, in a broad temperature range and without having to modify the interaction potential through expensive or complicated procedures.

The mechanism of gel formation depends largely on the type of solvent, the surface chemistry of the colloidal particles, and temperature. Hydrophilic fumed silica in non-polar solvent media with no hydrogen-bonding ability such as mineral oil¹⁵ and poly(dimethyl siloxane) forms a stable gel at room temperature^{16, 17}. On the contrary, in strongly hydrogen-bonding liquids, a solvation layer around the hydrophilic silica particles forms. The solvation layer thus stabilizes the particles and a suspension, resembling the behavior of a viscous fluid, is obtained. If the solvent is just weakly hydrogen-bonding, then the silica particles flocculate and a physical network is obtained¹⁸.

Hydrophobic fumed silica particles form gels in polar solvents either by van der Waals interactions and/or reverse steric stabilization due to the mismatch in solubility parameter between hydrophobic coronas of adjacent particles and the medium^{19, 20}. In non-polar media, stable suspensions of silica particles have been obtained by matching the

refractive indexes of the hydrophobic layer that is attached to the surface of the silica particle and that of the solvent where the particles are dispersed²¹.

Changes in temperature or solvent quality readily induce flocculation; therefore, the necessity of including this variable as an important part of our analysis. Previous studies of hydrophilic fumed silicas in non-polar liquids such as mineral oil and n-hexadecane show that the effect of temperature on gel modulus depends on the surface chemistry of the colloidal particles. Temperature has negligible effects on hydrophilic fumed silica in non-polar solvents. Because the solvency of hydrophilic fumed silica in these solvents does not increase significantly as temperature increases, the elastic network formed stays relatively unchanged. Conversely, increasing the temperature from 25 °C to 70 °C decreases the elastic modulus (G') of hydrophobic fumed silica in polar solvents such as mineral oil and hexadecane²². This occurs because as the temperature increases, the non-polar liquid is able to better solvate the hydrophilic silica particles, which leads to decreased attraction between particles. The gel network is disrupted as van der Waals and steric interactions between particles are weakened and this results in a lower elastic modulus. Additionally, the contribution of the solvent medium with lower viscosity as temperature increases, may play an important role in the overall rheological response (see §3.3.1 of Chapter 3).

In polar liquids, the effects of temperature on the behavior of hydrophilic FS are different than what is observed in non-polar liquids. The interaction potential between particles and particle-medium change and so does the reactivity of certain groups present in the solvent molecules towards the silanol groups available in the FS surface. In Chapter 3, these effects were discussed for poly(ethylene glycol) dimethyl ether (PEGdm), a solvent

with low hydrogen-bonding ability. As temperature increases, the ether oxygens available in the molecule are capable of chemically reacting with the silanol groups on the FS surface. This reaction increases the effective volume fraction and the system becomes stronger, as evidenced by the higher elastic modulus observed after heating up to 80 °C.

Based on the results obtained by our research group in the past years and with the aim to find alternative, inexpensive ways of improving the strength of fumed silica gels (which can be potentially used in lithium batteries), we investigated the rheological properties of mixtures of hydrophobic and hydrophilic fumed silica nanoparticles in PEGdm(250) and poly(ethylene glycol) PEG(200), a highly hydrogen bonding medium. We propose that by evaluating the properties of mixed FS gels at elevated temperatures (> 30 °C), hydrogen bonding, the principal mechanism of gel formation for hydrophilic FS particles in PEGdm(250), could be screened and the contribution of the hydrophobic fumed silica phase evaluated. If these interactions can be subtracted, we would be able to tell whether the network is an addition of the two fumed silicas or if they interfere antagonistically with each other when forming the gel. In the case of PEG(200) where hydrophilic fumed silica does not form a three-dimensional network, the presence of the hydrophobic silica can play an important role if a solid-like behavior is required as a function of temperature. This knowledge is of interest in understanding the behavior of mixed colloidal particles in a specific solvent medium.

4.2 Experimental

We used two types of fumed silica (FS) nanoparticles, native hydrophilic A200 and hydrophobic R805 (kindly donated by Degussa). The physical characteristics of these two types of particles are shown in Table 4.1. Basically, they differ in their surface chemistry; R805 is prepared by attaching octyl chains to the surface of A200. The silica dispersions were prepared by shear mixing (Silverson SL2) previously vacuum-dried (3 days at 120 °C) nanoparticles in the solvent medium. Poly(ethylene glycol) dimethyl ether, was employed as one of the solvent media. This material has a molecular weight (MW) of 250 g/mol and it will be referred to as PEGdm(250). PEGdm(250) has a Newtonian viscosity of 7 mPa-s at 25 °C; it was obtained from Sigma and used as received. The other solvent employed, Poly(ethylene glycol), has a MW of 200 g/mol and a Newtonian viscosity of 50 mPa-s at 25 °C. Adequate amounts of A200 and R805 (at fixed ratios) were weighed to compose 10 wt% of the FS phase in either PEGdm(250) or PEG(200) dispersions. Various A200 to R805 ratios, 100/0, 75/25, 50/50, 25/75, and 0/100 were prepared. After mixing, the materials were degassed under vacuum to extract any bubbles created during the mixing step and the samples were used within 24h of their preparation.

A TA Instruments ARG2 stress-controlled rheometer was used to conduct a series of stress and frequency sweeps, at several temperatures going from 25 °C to 80 °C. 20 mm parallel plate geometry (or 40 mm for low torque signals) was the preferred geometry to test the materials. The dynamic shear experiments were done within the linear viscoelastic region of deformation. To reduce the variability of results among samples, a standard shear history was imposed to all the materials. This procedure consisted of a frequency sweep

between 0.4 rad/s and 40 rad/s (within the linear viscoelastic region of deformation) followed by a 15 min delay prior to the experiment of interest, i.e. stress, time or frequency sweep. The results presented in this work were reproducible within less than 10% error.

Table 4.1. Physical characteristics of the fumed silicas used in this work¹⁰

Fumed silica	Main surface group	Primary particle diameter (nm)	Surface area (m²/g)	Fraction of unreacted silanols (mol%)
A200	Silanol Si-OH	12	200	100
R805	Octyl -C ₈ H ₁₇	12	150	52

4.3 Results and Discussion

4.3.1 Rheological properties of mixed fumed silicas in PEGdm(250)

Figure 4.1 shows the elastic modulus (G') as a function of frequency for several hydrophilic (A200)/hydrophobic (R805) FS mixtures in PEGdm(250) at 25 °C. In all cases, the colloids contain 10wt% FS. It can be seen that all the materials exhibit gel-like, as G' is independent of frequency and lower than the viscous modulus G'' (not shown here for clarity). This result indicates that hydrophobic, hydrophilic fumed silicas, and their mixtures form a flocculated, three-dimensional network structure (3D network) in PEGdm(250) regardless of the presence of a secondary particle type with different surface chemistry.

Though all the materials behave solid-like, the strength of the gels, characterized by the elastic modulus (often times referred to as gel modulus), is lower for the mixed systems

than for the samples with only either A200 or R805. Similar results were obtained by Yerian²³ for mixtures of hydrophilic and hydrophobic FS at concentrations ranging from 5 wt% to 20 wt%. He attributed this behavior to the hydrophobic fumed silica diluting the number of effective interactions occurring amongst the hydrophilic FS particles in the solvent.

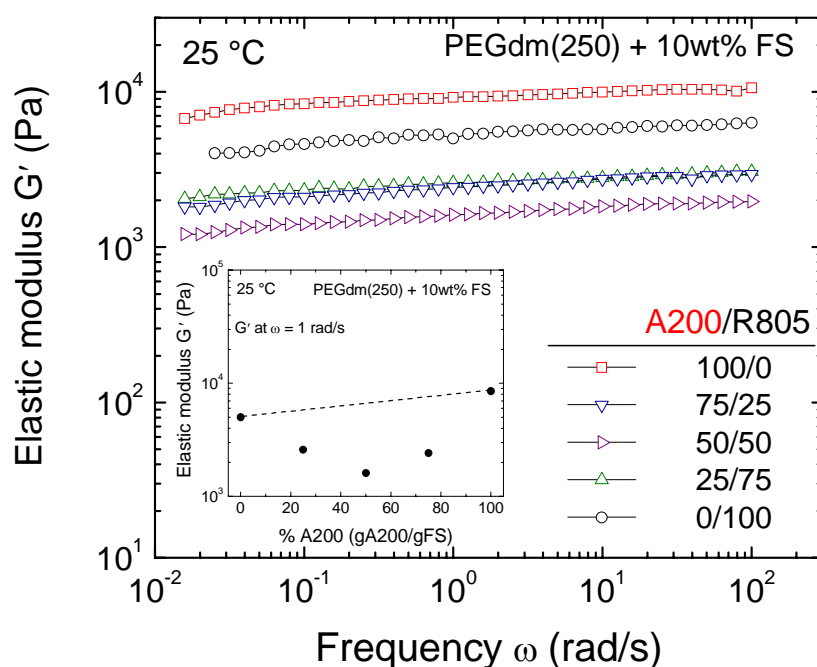


Figure 4.1. Frequency sweeps of PEGdm(250)+10wt% fumed silica at 25 °C. Results are shown for different blends of hydrophilic (A200) and hydrophobic (R805) fumed silicas. The inset shows the elastic modulus at 1 rad/s as a function of A200 content in the mixture. The dashed line represents the log-additive mixing rule.

The inset in figure 4.1 shows more clearly this dilution effect. The elastic modulus, measured at frequency of 1 rad/s, is plotted as a function of hydrophilic FS content in the mixed system and a line, representing the log-additive weight fraction of each individual component at a specific composition, is also shown as a way of illustrating the purely log-

additive behavior²⁴. It can be seen that all the mixed systems fall below the log-additive mixing rule (negative deviation), indicating antagonistic behavior of the two components in the mixture of hydrophilic and hydrophobic FS. We conclude that the two particle types seem to form independent networks which are disturbed by the presence of one another.

Another interesting feature that is worth highlighting in Figure 4.1 is the fact that substituting 25 wt% of one of the components does not seem to considerably affect the gel modulus. Only at low frequencies a slight difference is noticeable; the gel modulus of the colloid containing 75 wt% hydrophilic FS is only slightly lower than the gel modulus of the material containing 25 wt% hydrophilic FS. It seems that the strongest gel (the one containing hydrophilic FS in PEGdm(250)) is more affected by the presence of the hydrophobic FS, as its gel modulus is even lower than the value obtained for its mirror image composition containing hydrophobic FS as the major component.

4.3.2 Rheological properties of mixed fumed silicas in PEG(200)

The rheological behavior depicted in Figure 4.2 for PEG(200) is remarkably different than the one observed for PEGdm(250). First, we observe that 100% of hydrophilic fumed silica in PEG behaves liquid-like. While G' is shown for comparison purposes, in this particular case, the rheological behavior is better described by G'' as the viscous response dominates the rheological behavior within the frequency range accessible for the rheometer. This is, G'' is higher than G' and no crossover is observed up to 100 rad/s. One of the most interesting features observed in Figure 4.2 is the fact that by adding 25% of hydrophobic particles to the previously described liquid-like behaving material, causes the rheological

response to change dramatically. The 75/25 A200/R805 material behaves gel-like and its modulus is considerably higher than the 100/0 A200/R805 one. As the hydrophilic/hydrophobic fumed silica ratio decreases, the elastic modulus of the materials (all of them showing solid-like behavior) increases and goes through a maximum at 50/50 A200/R805 fumed silica. The 25/75 and 0/100 materials exhibit lower G' than the 50/50, being 0/100 the material with lowest G' between these two.

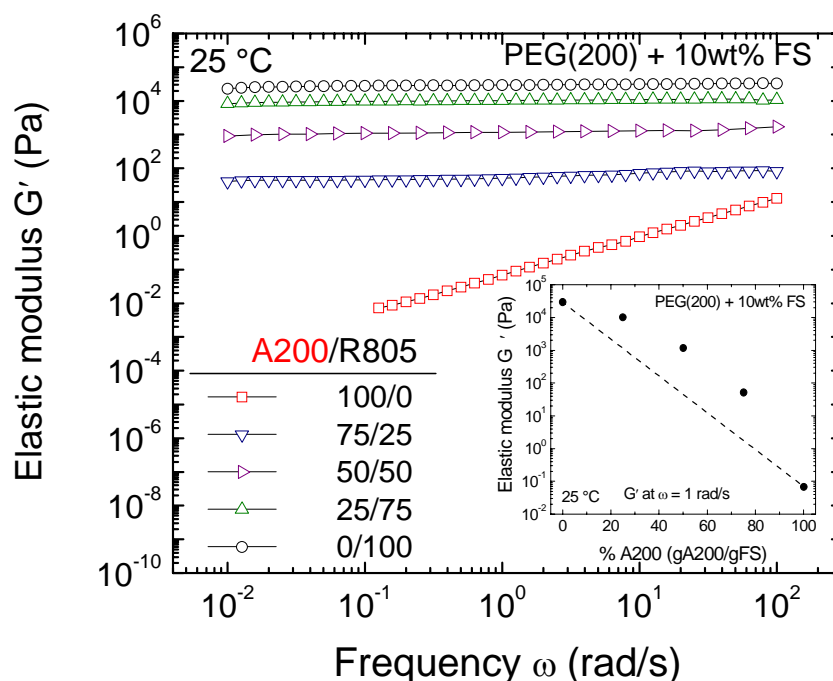


Figure 4.2. Frequency sweeps of PEG(200)+10wt% fumed silica at 25 °C. Results are shown for different blends of hydrophilic (A200) and hydrophobic (R805) fumed silicas. The inset shows the elastic modulus at 1 rad/s as a function of A200 content in the mixture. The dashed line represents the log-additive mixing rule.

It is worth noting that the elastic modulus of the mixed fumed silica in PEG(200) are above the log-additive mixing rule (indicated by the dashed line connecting the extreme

compositions on the inset in Figure 4.2). This indicates that in this particular liquid, the two fumed silicas act synergistically and the properties of the resulting material are better than the individual components. To the best of our knowledge, this result has not been published before, thus a deep understanding on this subject is lacking in the literature. We believe that the two types of particles occupy a specific place in the mixed systems microstructure. The hydrophilic particles are preferentially solvated by the PEG(200) molecules and if we (simplistically) consider the system as a hard sphere suspension with hydrodynamic interactions described by the Batchelor²⁵ relationship:

$$\eta_r = \frac{\eta}{\eta_s} = 1 + 2.5\phi + 6.2\phi^2$$

where η_r = relative viscosity

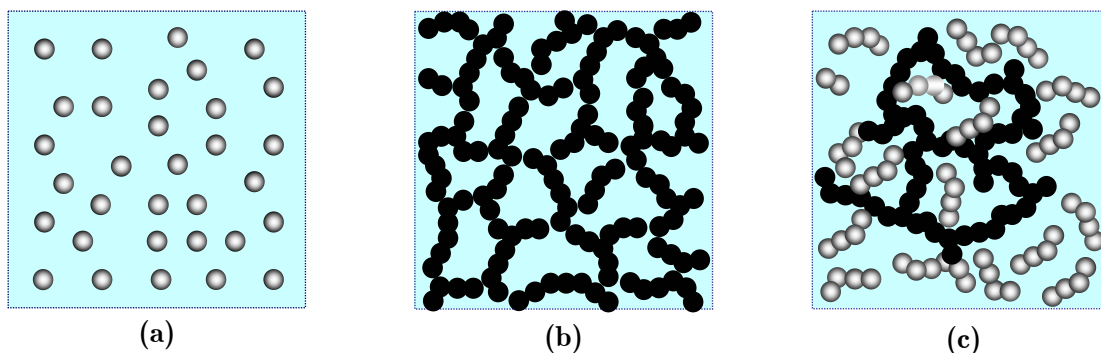
η = viscosity of the suspension

η_s = viscosity of the solvent

ϕ = particle volume fraction

we would expect the viscosity to increase as a quadratic function of the volume fraction. In reality, for fumed silica the situation is not quiet simple and if we added the hydrophobic fumed silica phase to the system, then this equation does not hold any longer. If we just intuitively think that the hydrophilic fumed silica will create an increase in viscosity and consider the fact that the aggregates of fumed silica can entrap solvent in their largely “branched” structure, we could presume for the increase in viscosity to be higher than for regular spherical particles. With this scenario in mind, the addition of hydrophobic fumed

silica particles, which interact unfavorably with the polar, strongly hydrogen bonding PEG, will cause the system to flocculate in a state where there is less solvent available (because of the entrapped fraction). The three-dimensional network will be composed of hydrophobic fumed silica particles interacting with each other through interactions between the octyl chains on the surface (mainly dispersive interactions) with spaces filled with solvent-containing hydrophilic fumed silica. Figure 4.3 shows a schematic representation of the proposed mechanism for network formation in the mixed fumed silica systems. The two types of particles, in spite of the marked differences in surface energies act synergistically and give as a result a stronger gel than if the components' properties were additive.



Hydrophilic FS in PEG(200) Hydrophobic FS in PEG(200) Mixed FS in PEG(200)

Figure 4.3. Schematic representation of the fumed silica microstructure in PEG(200), (a) hydrophilic (the spheres represent particle aggregates), (b) hydrophobic, and (c) mixed hydrophilic/hydrophobic fumed silica.

4.3.3 Effects of temperature on the rheological behavior of gels of mixed FS in PEGdm(250)

The results shown in Chapter 3 for the hydrophilic FS gels in PEGdm(250) at higher temperature, motivated the following set of experiments. We would like to learn if the gel modulus of hydrophilic FS in PEGdm(250) increases with temperature (as previously seen in §3.3.1), or if the presence of the hydrophobic fumed silica phase interferes with the adsorption/chemical reaction observed for hydrophilic fumed silica and PEGdm(250). Whether or not the concentration effect (shown to be responsible for the higher modulus in the pure hydrophilic system) is going to dominate the mixed FS gels behavior is of interest and will be discussed in the following paragraphs.

Figures 4.4 (a) and (b) show the dynamic moduli as a function of frequency for two 10 wt% mixed FS compositions in PEGdm(250) at different temperatures. The common feature in these two figures is the fact that the materials behave as gels even at higher temperatures (notice the behavior of G'' at 55 °C in Figures 4.4 (a) and 4.4 (b)). This makes these systems very attractive from the performance standpoint, as the integrity of the FS networks remains as such under external temperature fields.

A noticeable difference between the two figures is the fact that the mixed system containing less hydrophobic FS (Figure 4.4 (a)), does not show an appreciable variation in G' as the temperature increases from 25 °C to 55 °C. In contrast, the mixed FS system containing more hydrophilic FS shows an increase in G' as temperature increases. A larger contribution of the hydrophilic FS present to the overall network response can explain these

results. The silanol groups available on the surface of the hydrophilic FS have the ability to chemically react with the PEGdm(250) molecules and effectively increase the volume fraction. This gives as a result a stronger network with a higher elastic modulus. Consequently, the more hydrophilic FS available in the system (i.e. 75/25 A200/R805 case), the more pronounced the concentration effect.

Figures 4.5 (a) and (b) present the elastic modulus as a function of percent strain for 25/75 A200/R805 and 75/25 A200/R805 mixed FS gels at different temperatures. A constant G' at low strains followed by a drop at higher strains is observed in all cases. The onset of the nonlinearity (decrease in G') has been attributed to the breaking of the weak bonds in the gel network or disruption of the microstructure due to shear^{26, 27}. If the value of G' when the microstructure starts to disrupt is calculated (Figure 4.5), we observe that the trends as a function of temperature are opposite for the two mirror image compositions. While G' of the material containing more hydrophilic FS increases with temperature, the one containing more hydrophobic FS shows a decrease in G' with temperature.

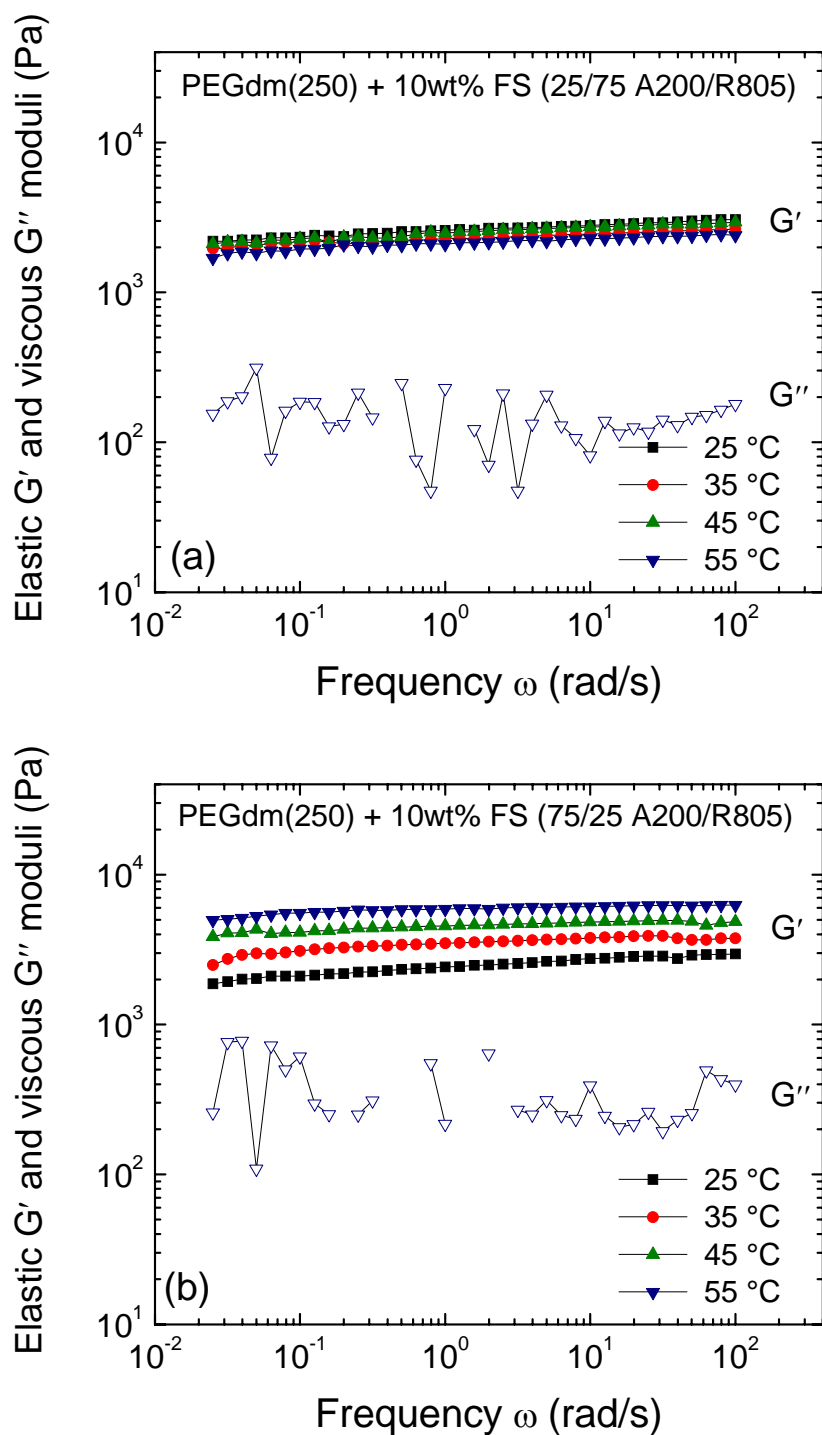


Figure 4.4. Dynamic moduli as a function of frequency at various temperatures for (a) 25/75 FS A200/R805 and (b) 75/25 FS A200/R805.

This result suggests that the gels become not only stronger but also less deformable as temperature increases. This can be explained in terms of the connectivity between the flocs or particle aggregates. If the flocs are stronger than the links among them, the connectivity is lower and the strain (or stress) at which the material starts to fail is lower than if the flocs were very well connected. A similar interpretation was given by Shih *et al*²⁷ for colloidal boehmite alumina gels. They found a scaling relationship for G' and the limit of linearity (γ_c) as a function of particle volume fraction. The authors suggest that a material whose elastic modulus increases more rapidly with concentration is in the strong-link regime, whereas that whose elastic modulus increases slowly with concentration is in the weak-link regime. The scaling of the storage modulus and limit of linearity depends on whether the interfloc links are stronger than the flocs. Therefore, if we make an analogy between concentration and temperature, our 75/25 A200/R805 material would be in the strong-link regime, where the interfloc links are stronger than the flocs.

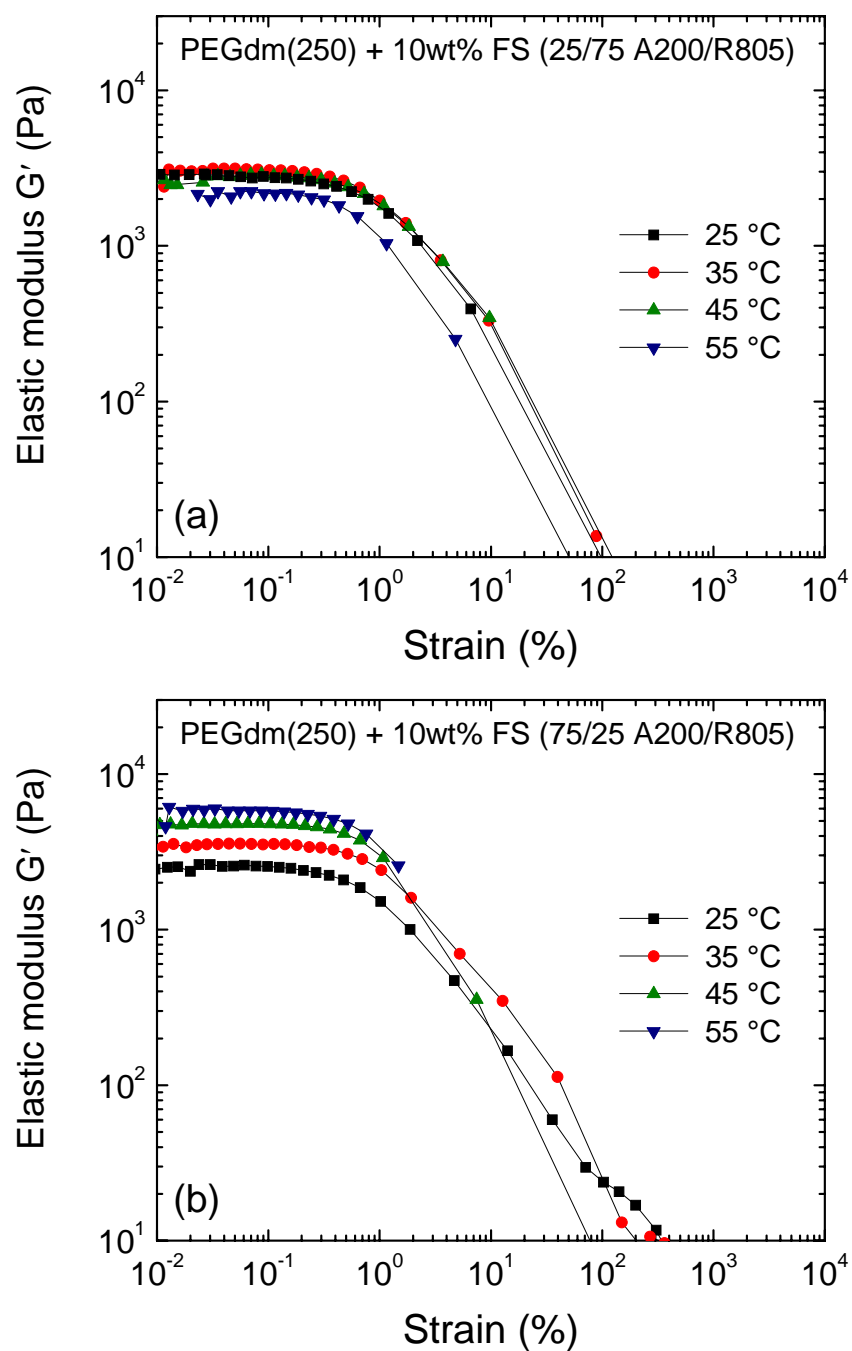


Figure 4.5. Elastic modulus as a function of strain at various temperatures for (a)25/75 FS A200/R805 and (b)75/25 FS A200/R805. Samples contain 10 wt% FS in PEGdm(250).

Following up this analogy, a scaling relationship for the 75/25 A200/R805 gel as a function of temperature has the form:

$$G' = 60 T^{1.14}$$

This indicates that the impact that temperature has on the elastic modulus for this particular mixed FS system is not as marked as the general trend observed for $G' \sim \phi^n$ (with ϕ being the volume fraction and n the power-law exponent), where n varies between 3 and 5^{15, 28, 29}. We interpret this weaker effect in terms of the amount of PEGdm(250) molecules that participate in the condensation reaction and the effective increase in volume fraction due to both adsorption and chemical reaction compared to a real increase in particle volume fraction.

When analyzing the variation of elastic modulus with temperature for the 25/75 and 50/50 A200/R805 materials, we find that the scaling behavior does not longer exist. A decrease in elastic modulus as a function of temperature is observed but does not occur in a monotonic way (see Figure 4.6).

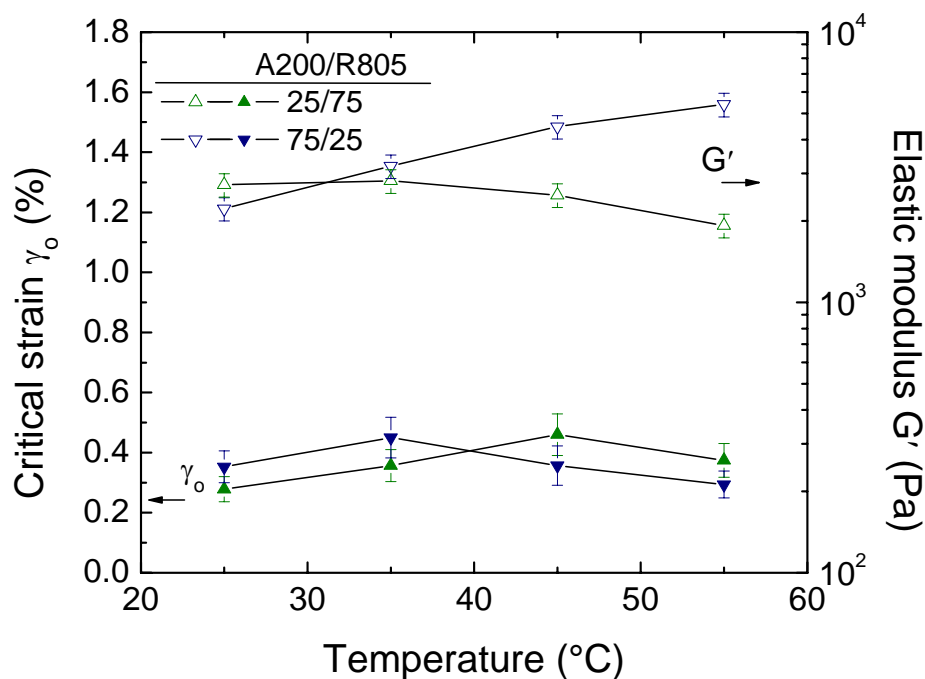


Figure 4.6. Effect of temperature on the critical strain and ultimate modulus before catastrophic failure for gels of 10 wt% mixed FS (A200/R805) in PEGdm(250).

Though there is not a scaling behavior with temperature for these compositions, our attempt to relate temperature and concentration is based on the mechanism through which the PEGdm(250) adsorbs on the silica surface and/or reacts with the silanol groups. We suggest that the scaling relationship holds only for those materials where the ratio of hydrophilic to hydrophobic FS is high enough that the concentration effect overcomes the effects caused by the presence of hydrophobic FS and its behavior with temperature.

Figure 4.6 shows that the limit of linearity (γ_c) exhibits very little variation with temperature and within the experimental error, the values can be considered the same. We speculate that the presence of the secondary FS in these mixed FS systems prevents the other component from effectively dominating the deformability of the network.

Ramsay³⁰ suggested a way of determining the work required to disrupt dispersions of aqueous dispersions of Laponite-RD. The effective work is equivalent to the cohesive energy in the flocculated structure, and the cohesive energy (E_c) is related to the stress by the following equation:

$$E_c = \int_0^{\gamma_c} \sigma d\gamma$$

where γ_c is the critical strain which results in disruption or the end of linearity in our case and σ is the stress in response and in phase with the strain γ .

If we substitute σ by $G'\gamma$ (in this case, G' corresponds to the elastic modulus in the linear region and γ to the deformation), we can integrate the previous equation within the specified limits to obtain an expression for E_c as follows:

$$E_c = \frac{1}{2} \gamma_c^2 G'$$

Figure 4.7 shows the effects of temperature on the cohesive energy for all the mixed FS in PEGdm(250) systems studied in this work. We observe that at 25 °C, the work required to disrupt the hydrophobic FS network is higher than for the hydrophilic FS network and the mixed fumed silicas. Additionally, at this temperature, the E_c values for all the blends are in between the pure components. As temperature increases, E_c for the hydrophilic FS colloids (100/0 A200/R805) dramatically increases; overcoming the values obtained for the 0/100 A200/R805 and the blends. Additionally, E_c for the mixed system containing more hydrophilic FS is almost always above the values obtained for the colloids containing 50 and 25 % hydrophobic FS. This supports the previous explanation regarding

more connectivity in those systems where the hydrophilic FS has the possibility to react with the PEGdm(250) chains (either physically or chemically).

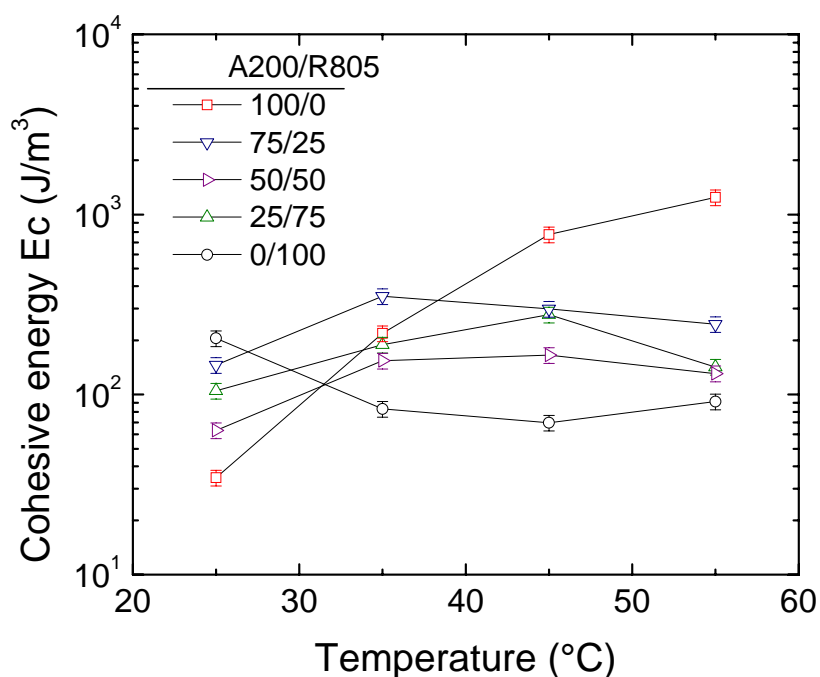


Figure 4.7. Cohesive energy as a function of temperature for various mixed FS compositions in PEGdm(250). Total content of FS in the colloid is 10 wt%.

Figure 4.6 summarizes the effects of temperature on the elastic modulus of the mixed FS systems at various temperatures. A negative deviation from the log-additive mixing rule is observed in all cases, indicating that the two types of FS particles form independent networks in PEGdm(250). The colloids containing larger amounts of hydrophilic FS tend to behave similarly to the pure component in PEGdm(250). The 50/50 A200/R805 colloid seems to be dominated by the hydrophilic FS, as the elastic modulus increases with

temperature. The dilution effect caused by the presence of a secondary FS with different interaction potential is more pronounced than for the 75/25 A200/R805 material.

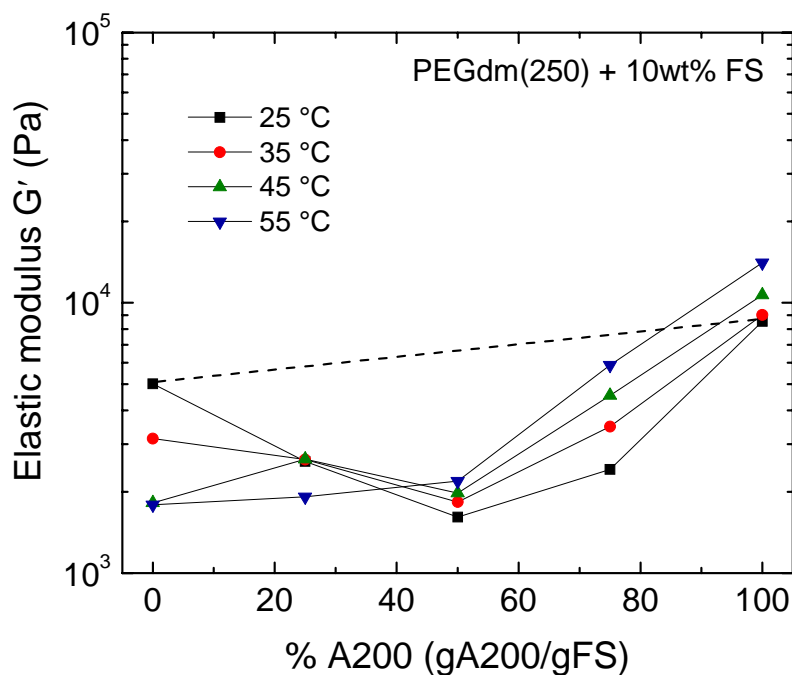


Figure 4.8. Effect of fumed silica surface chemistry on the elastic modulus of PEGdm(250)+10wt% FS at different temperatures. The concentration of FS is expressed in g of hydrophilic per g of mixed FS (hydrophilic (A200) + hydrophobic (R805)) in the colloid.

4.3.4 Effects of temperature on the rheological behavior of gels of mixed FS in PEG(200)

Figure 4.9 (a) and (b) show the elastic modulus as a function of frequency for dispersions of mixed FS in PEG(200), 25/75 A200/R805 and 75/25 A200/R805, respectively.

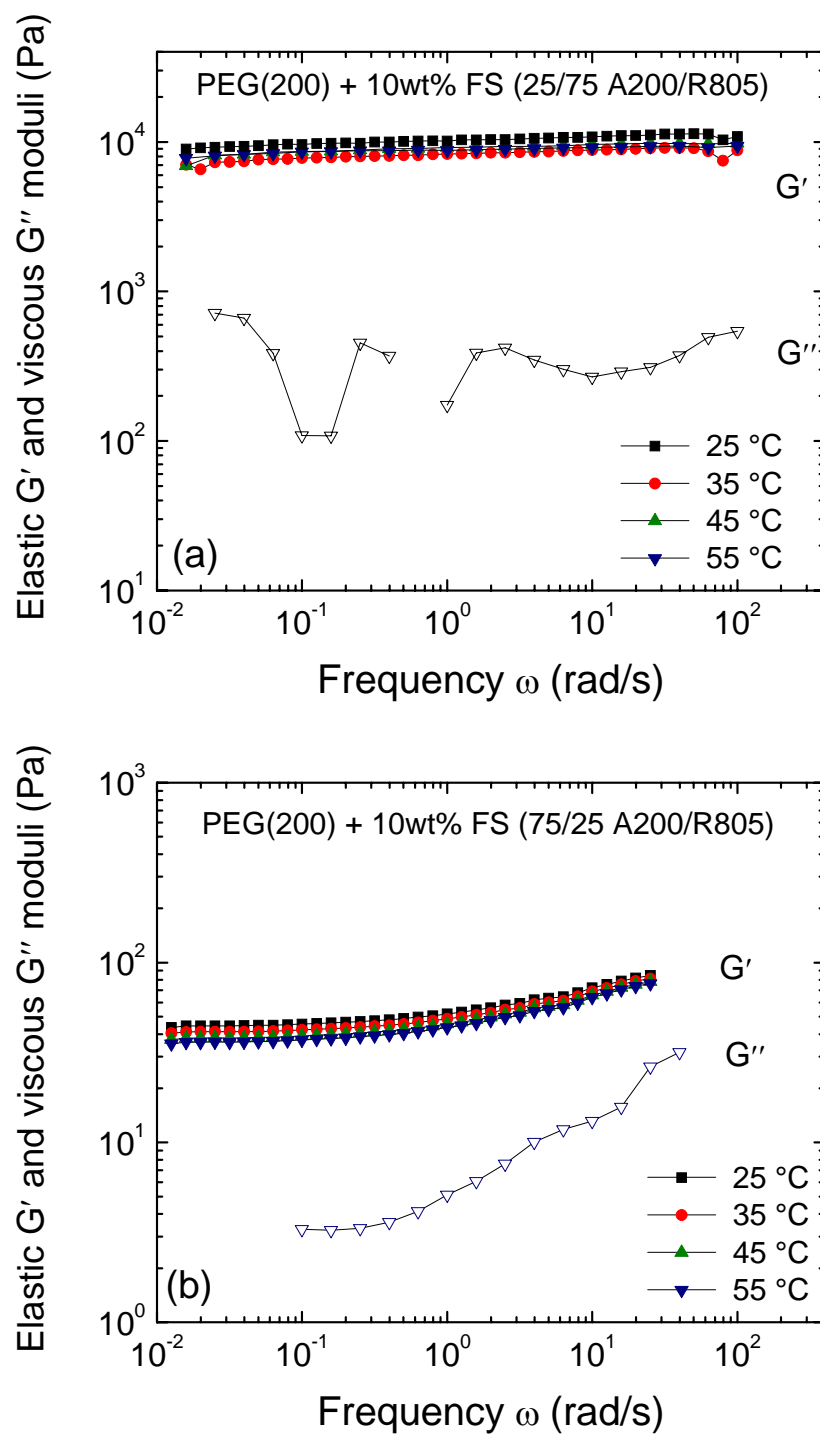


Figure 4.9. Dynamic moduli as a function of frequency at various temperatures for (a) 25/75 FS A200/R805 and (b) 75/25 FS A200/R805.

It can be seen that in both cases, temperature does not have a dramatic effect on the modulus of the colloids; on the contrary, a very mild temperature dependence is observed in all cases. The materials containing 75% of hydrophilic FS show a slightly larger change than the one containing 25% hydrophilic FS. It can be seen that as temperature increases, the elastic modulus decreases; but the modulus as a function of frequency remains the same, i.e., the materials behave solid-like even at the higher temperature evaluated. The frequency dependence for the 75/25 A200/R805 is more marked than for the 25/75 A200/R805, indicating that the major component dominates the overall behavior.

The dependence of G' with temperature for the 75/25 A200/R805 follows a power-law model of the form:

$$G' = 107 T^{-0.23}$$

As indicated by the expression above, the temperature dependence is very small and in contrast to the behavior observed for the dispersions in PEGdm(250). While in PEGdm(250) an increase of modulus with temperature is observed, the opposite is obtained with PEG(200).

Figure 4.10 summarizes the effects of temperature on the elastic modulus of different compositions. In all cases, a positive deviation of the log-additive mixing rule is obtained and the modulus goes through a maximum at 50/50 A200/R805 when the two fumed silicas can contribute the most to the rheological behavior. This result is interesting from the applications standpoint since a material can remain as a gel even at higher temperatures. and with very little hydrophobic fumed silica added to the system

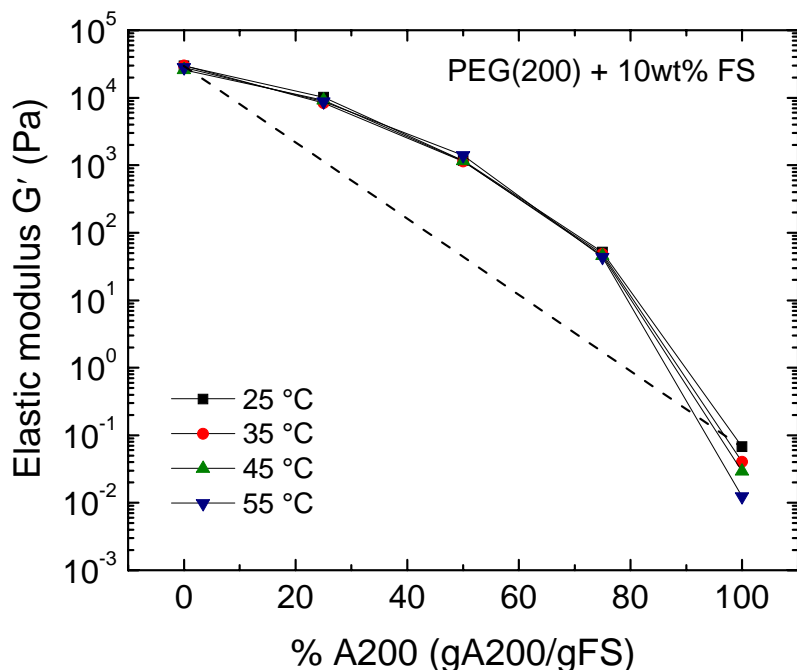


Figure 4.10. Effect of fumed silica surface chemistry on the elastic modulus of PEG(200)+10wt% FS at different temperatures. The concentration of FS is expressed in g of hydrophilic per g of mixed FS (hydrophilic (A200) + hydrophobic (R805)) in the colloid

4.4 Conclusions

The results presented here illustrate the behavior of mixed fumed silica colloidal particles differing in surface chemistry. In particular, the effects of temperature on the rheological behavior of mixed FS dispersed in PEGdm(250) and PEG(200) was studied. In PEGdm(250), the rheological behavior of the mixed systems is, for all the ratios evaluated, antagonistic as the properties of the materials lie below the log-additive mixing rule. Those samples containing larger amounts of hydrophilic FS show an increase in the elastic modulus as a function of temperature. The increase is proportional to the amount of hydrophilic FS

in the system up to 50% of A200 in the mixture. A scaling relationship between the elastic modulus and temperature was found for the 75/25 A200/R805 dispersion. This relationship is somewhat analogous to the scaling relationships between elastic modulus and particle volume fraction, and this can be explained in terms of the reaction occurring at the surface of the hydrophilic FS particles. The effective volume fraction increase resulting from exposure to higher temperatures, is more important when there are more hydrophilic FS particles in the mixture. These samples also showed a higher cohesive energy, indicating that the networks and the interfloc links are stronger.

The mixed fumed silicas dispersed in PEG(200) showed a very different behavior compared to one obtained with PEGdm(250). A positive deviation of the log-additive mixing rule indicates that the hydrophobic and hydrophilic particles organized synergistically in the polyether matrix allowing for the properties of the resulting material to be higher than the individual components. This result has not been previously published or discussed in the literature. As low as 25% hydrophobic fumed silica in the mixed systems is required to obtain a solid-like behavior in PEG(200). Moreover, the solid-like behavior does not change upon increasing temperature from 25 to 55 °C.

4.5 References

1. Larson, R. G., *The Structure and Rheology of complex Fluids*. Oxford University Press, Inc.: New York, 1999.
2. Israelachvili, J. N., *Intermolecular and Surface Forces*. 2nd ed.; Academic Press London: London, 1991; p xxi, 450.

3. Evans, D. F.; Wennerström, H., *The colloidal domain : where physics, chemistry, biology, and technology meet.* 2nd ed.; Wiley-VCH: New York, 1999; p xl, 632.
4. Fan, J.; Fedkiw, P. S., Composite electrolytes prepared from fumed silica, polyethylene oxide oligomers, and lithium salt. *Journal of the Electrochemical Society* 1997, 144, (2), 399-408.
5. Raghavan, S. R.; Riley, M. W.; Fedkiw, P. S.; Khan, S. A., Composite polymer electrolytes based on poly(ethylene glycol) and hydrophobic fumed silica: Dynamic rheology and microstructure. *Chemistry of Materials* 1998, 10, (1), 244-251.
6. Walls, H. J.; Fedkiw, P. S.; Zawodzinski, T. A.; Khan, S. A., Ion transport in silica nanocomposite electrolytes. *Journal of the Electrochemical Society* 2003, 150, (3), E165-E174.
7. Walls, H. J.; Riley, M. W.; Fedkiw, P. S.; Spontak, R. J.; Baker, G. L.; Khan, S. A., Composite electrolytes from self-assembled colloidal networks. *Electrochimica Acta* 2003, 48, (14-16), 2071-2077.
8. Walls, H. J.; Zhou, J.; Yerian, J. A.; Fedkiw, P. S.; Khan, S. A.; Stowe, M. K.; Baker, G. L., Fumed silica-based composite polymer electrolytes: synthesis, rheology, and electrochemistry. *Journal of Power Sources* 2000, 89, (2), 156-162.
9. Iler, R. K., *The Chemistry of Silica: Solubility, Polymerization, Colloid and Surface Properties, and Biochemistry.* John Wiley & Sons: New York, NY, 1979; p xxiv, 866.
10. Basic Characteristics of Aerosil; Degussa Technical Bulletin No. 11; Degussa Corp.: Akron, OH, 1993.
11. Hunt, W. J.; Zukoski, C. F., Rheology and microstructure of mixtures of colloidal particles. *Langmuir* 1996, 12, (26), 6257-6262.
12. Hunt, W. J.; Zukoski, C. F., The equilibrium properties and microstructure of mixtures of colloidal particles with long-range, soft repulsions. *Journal of Colloid and Interface Science* 1999, 210, (2), 332-342.
13. Hunt, W. J.; Zukoski, C. F., The rheology of bimodal mixtures of colloidal particles with long-range, soft repulsions. *Journal of Colloid and Interface Science* 1999, 210, (2), 343-351.

14. Anderson, B. J.; Gopalakrishnan, V.; Ramakrishnan, S.; Zukoski, C. F., Scattering of mixtures of hard spheres: comparison of total scattering intensities with model. *Physical Review E* 2006, 73, (3), 031407.
15. Khan, S. A.; Zoeller, N. J., Dynamic Rheological Behavior of Flocculated Fumed Silica Suspensions. *Journal of Rheology* 1993, 37, (6), 1225-1235.
16. Kosinski, L. E.; Caruthers, J. M., The Effect of Particle Concentration on the Rheology of Polydimethylsiloxane Filled with Fumed Silica. *Journal of Applied Polymer Science* 1989, 32, 3393-3406.
17. Kosinski, L. E.; Caruthers, J. M., Rheological Properties of Poly(Dimethylsiloxane) Filled with Fumed Silica: II. Stress Relaxation and Stress Growth. *Journal of Non-Newtonian Fluid Mechanics* 1990, 17, 69-89.
18. Raghavan, S. R.; Walls, H. J.; Khan, S. A., Rheology of silica dispersions in organic liquids: New evidence for solvation forces dictated by hydrogen bonding. *Langmuir* 2000, 16, (21), 7920-7930.
19. Raghavan, S. R.; Hou, J.; Baker, G. L.; Khan, S. A., Colloidal interactions between particles with tethered nonpolar chains dispersed in polar media: Direct correlation between dynamic rheology and interaction parameters. *Langmuir* 2000, 16, (3), 1066-1077.
20. Vincent, B.; Kiraly, Z.; Emmett, S.; Beaver, A., The Stability of Silica Dispersions in Ethanol Cyclohexane Mixtures. *Colloids and Surfaces* 1990, 49, (1-2), 121-132.
21. Vincent, B.; Emmett, S.; Jones, A.; Milling, A., The Stability of Silica Dispersions in Nonpolar-Solvents. *Abstracts of Papers of the American Chemical Society* 1990, 200, 255-COLL.
22. Raghavan, S. R. Suspensions, gels, and composite electrolytes based on fumed silica: rheology and microstructure. PhD, North Carolina State University, Raleigh, 1998.
23. Yerian, J. A. Nanocomposite polymer electrolytes: Modulation of mechanical properties using surface-functionalized fumed silica. Ph.D. Thesis, North Carolina State University, Raleigh, NC, 2003.
24. Utracki, L. A., Polymer alloys and blends : thermodynamics and rheology. Hanser: New York, NY, 1990; p xi, 356.

25. Batchelor, G. K., The stress system in a suspension of force-free particles. *Journal of Fluid Mechanics* 1970, 41, (3), 545-570.
26. Walls, H. J.; Caines, S. B.; Sanchez, A. M.; Khan, S. A., Yield Stress and Wall Slip Phenomena in Colloidal Silica Gels. *Journal of Rheology* 2003, 47, (4), 847-868.
27. Shih, W. H.; Shih, W. Y.; Kim, S. I.; Liu, J.; Aksay, I. A., Scaling Behavior of the Elastic Properties of Colloidal Gels. *Physical Review A* 1990, 42, (8), 4772-4779.
28. Buscall, R.; Mills, P. D. A.; Goodwin, J. W.; Lawson, D. W., Scaling Behavior of the Rheology of Aggregate Networks Formed from Colloidal Particles. *Journal of the Chemical Society-Faraday Transactions I* 1988, 84, 4249-4260.
29. Sonntag, R. C.; Russel, W. B., Elastic Properties of Flocculated Networks. *Journal of Colloid and Interface Science* 1987, 116, (2), 485-489.
30. Ramsay, J. D. F., Colloidal properties of synthetic hectorite clay dispersions I. Rheology. *Journal of Colloid and Interface Science* 1986, 109, (2), 441-447.

5

*Blends of Low- and High-Molecular Weight
Poly(ethylene oxide). Nanocomposites and
Composite Polymer Electrolytes*

Abstract

Blends of high- and low-molecular weight (MW) poly(ethylene oxide), PEO are prepared by using solution and extrusion methods. Various ratios PEO/PEGdm(250) were prepared to study the effects of adding a secondary low-MW component to the high-MW PEO. Fumed silica nanoparticles (hydrophobic and hydrophilic) are also employed and the differences in the rheological properties of the two sets of blends are used to quantify how the hydrophobic or hydrophilic surface chemistry affects the flocculation mechanism. It is found that by increasing the concentration of the low-MW component in the blend, the elastic and viscous moduli decrease. The blends containing hydrophilic FS are more susceptible to the presence of the low-MW component. Lower elastic modulus at low frequencies as well as moduli crossover for the 80/20 and 70/30 high- to low-MW blends in the frequency range studied, are found in the mixed-MW system containing hydrophilic FS. Additional reinforcing events taking place between the PEO segments and octyl chains on the surface of the hydrophobic fumed silica seem to explain the differences observed. Two well defined crystallization and melting endotherms are obtained for the composites in the range of compositions studied. A decrease in the crystallization and melting peak of the high-MW component is observed as the PEGdm(250) increased. Melt mixing seems to be a valuable approach as slightly higher ionic conductivities were obtained for these systems. On the other hand, higher moduli and viscosity were obtained for samples prepared in solution. The differences are attributed to possible mechanical degradation of the polymeric chains occurring during melt mixing.

To be submitted to Polymer

Authors: A.M. Sanchez and S.A. Khan

5.1 Introduction

Poly(ethylene oxide) PEO (or its low-molecular weight analog, poly(ethylene glycol) PEG) is an exceptional polymer that has the ability to solvate ionic salts such as lithium salts¹⁻³. This is a very unique feature that many researchers have recognized and exploited to prepare electrolytes which can be used in Li battery applications. Polymeric electrolytes such as those formed by adding a salt to PEO have several advantages over liquid electrolytes. They are lighter in weight, easy to process, have low volatility, and structural stability. In addition, they can be shaped through relatively simple processes and their properties controlled through those same processes. Beyond Li battery applications, high- and low-molecular weight (MW) PEOs find a special place in food and food packaging. It is also employed as plasticizer, solvent, water-soluble lubricants for rubber molds; wetting or softening agent, antistatic in the production of urethane rubber, components of detergents, among others. In medicine, PEOs are used in cosmetics, ointments, suppositories, in ophthalmic solutions and sustained-released oral pharmaceutical applications⁴. Such a versatile polymer has also been subject of numerous works related to polymeric blends, and mixtures with poly(methyl methacrylate), poly(vinyl acetate), poly(vinylpyrrolidinone), nylon, poly(vinyl alcohol), phenoxy resins, cellulose, polyethylene, poly(vinyl chloride), among others can be found in the literature⁴.

In lithium battery applications, despite its ion solvation ability and adequacy to provide mechanical strength, PEO performs poorly at low temperatures and the ionic conductivity is very low ($\sim 10^{-6} - 10^{-4}$ S/cm). This is mainly due to the relatively high degree

of crystallinity attained even with MWs as low as 105-107 g/mol, thereby shifting the optimum operating range to temperatures higher than 65 °C, the melting point of PEO. It has been suggested that the ion transport in PEO electrolytes occurs in the amorphous regions, specifically, in the interspherulitic areas where mobility is not restricted by the packets of lamellae formed upon cooling. Here the free-volume and segmental mobility are higher than in the crystalline areas and the diffusion process occurs more rapidly.

To overcome the issue of low ionic conductivity in PEO electrolytes, several approaches have been taken. Yang *et al*⁶ added plasticizers to polymer (PEO)-salt (LiCF₃SO₃) complexes in order to increase conductivity. Essentially, they attached three ethylene oxide units to the 4-position of propylene carbonate (PC) in order to maintain the high dielectric constant of PC and at the same time the good compatibility of PEG with PEO. They obtained free-standing films with good mechanical properties and a two order of magnitude increase in ionic conductivity for those samples containing 50 wt% of the modified PC with respect to the sample without either PC or modified PC. Kelly *et al*⁷ obtained higher ionic conductivities ($\sim 10^{-4}$ S/cm) for mixtures of PEO and PEGs. Among the three types of PEG employed by these researchers: poly(ethylene glycol), poly(ethylene glycol) methyl ether (PEGm), poly(ethylene glycol) dimethyl ether PEGdm, a salt complex of PEGdm showed the largest increase in ionic conductivity at 40 °C. They attributed the increase in conductivity to partial dissolution of the PEO in the salt complex additive and increased mobility of the ions in the amorphous region.

Other approaches involve the use of PEGs and inorganic fillers to overcome the detrimental effects of crystallinity on conductivity while keeping the mechanical integrity of

the electrolyte. Several inorganic fillers have been tested; these include clays⁷⁻⁹ and some forms of silicon dioxide such as fumed silica. Fumed silica (FS) has been widely employed and the gelation mechanism of such material studied in terms of its surface properties and interactions with the solvent media. Decoupling of electrochemical and mechanical properties is one of the major findings of this research¹⁰⁻¹⁶ and makes the efforts in this area worthwhile. In addition, permanent stabilization or “locking” of the fumed silica network has also been suggested as a way of improving mechanical properties of the gel electrolyte while keeping the matrix in liquid state (desired for good ion transport). In this case, crosslinkable fumed silica was dispersed in the salt-containing oligoether and UV¹⁷ or heat¹⁸ crosslinked or thereafter with the aid of acrylate monomers^{17, 19}. In both cases, gel electrolytes were obtained after the crosslinking reaction. Two important conclusions can be drawn. First, in electrolytes containing lower quantities of FS; the amount of added monomer does not significantly affect the ionic conductivity, but if the amounts of silica and acrylate monomer are larger, the ionic conductivity decreases while the gel modulus increases. Secondly, the ionic conductivity can be affected by the presence of residual monomer as lithium could react with it during cycling.

In this work, we combine a very simple, cost-effective approach of mixing two commercial polymers along with the addition of inorganic fillers to improve the mechanical strength of the mixed system at higher temperatures. Our mixed systems are composed of PEOs with very different molecular weights (200 kg/mol and 250 g/mol). The differences in MW, and on the other hand, the chemical similarities between the two structures are expected to act synergistically.

In order to have a better idea of the mechanisms dictating the rheological properties in the mixed systems, we will first study the rheological properties of several PEO/PEGdm ratios and the effects of adding fumed silica with different surface functionalities to the blends. Subsequently, the effects of salt on the rheological properties will be explored and finally, compounding methodologies will be discussed.

5.2 *Experimental*

The high-MW polymer used in this study was a poly(ethylene oxide) Polyox WSR N-80 obtained as a gift from Dow Chemicals. This water soluble resin has a number-average molecular weight of 200 kg/mol and will be referred to as PEO200k. The low-MW polymer was a poly(ethylene glycol dimethyl ether) and was obtained from Aldrich; it has a molecular weight of 250 g/mol and will be referred to as PEGdm(250). Two types of fumed silica were employed: hydrophilic A200 (surface area = 200 m²/g, and particle size = 12 nm) and octyl-modified hydrophobic R805 (surface area = 150 m²/g and particle size = 12 nm), courtesy of Degussa. Prior to use, the silicas were dried under vacuum for 3 days at 120 °C. Lithium bis(trifluoromethanesulfonyl)imide (LiN(CF₃SO₂)₂, Li Imide, LiTFSI, 3M) was also dried under vacuum at 100 °C for several days before use.

Two methods of compounding were employed:

- a) *Solution:* the appropriate amounts of PEO, PEGdm(250), FS, and LiTFSI (when used) were mixed together in acetonitrile (10:1 acetonitrile:PEO) at room temperature and homogenized in a high-shear mixer (Silverson Model SL2). The mixtures were poured in PTFE dishes and the solvent allowed to evaporate for approximately 2 days at room

temperature and pressure. The films were detached and placed in the vacuum oven (~1 kPa) for 24 h at room temperature to ensure that the samples were completely solvent free.

b) *Melt*: a twin-screw extruder (MiniLab Micro Rheology Compounder Haake) with conical co-rotating screws was employed to mix the composites in the melt. The compounding was performed at 110 rpm and 90 °C; the materials were mixed until a constant torque reading was observed (approximately 10 min).

5.2.1 Rheological Characterization

Dynamic rheological measurements were done in a stress-controlled rheometer TA AR2000, TA Instruments, using 25 mm parallel plate geometry. All the experiments were performed at 80 °C, under nitrogen flow and within the linear viscoelastic region of deformation. In all cases, the experimental error was found to be within 10%.

5.2.2 Thermal Properties

Dynamic cooling and heating scans of previously dried composites were performed in a differential scanning calorimeter (TA Instruments) DSC Q1000 at 10 °C/min from -80 to 120 °C under nitrogen atmosphere. Indium and Sapphire were employed as calibration standards. In all cases, the results presented correspond to the crystallization or heating scans collected after previously erasing the sample thermal history at 120 °C for 5 min. The glass transition temperature (T_g), melting temperature (T_m), crystallization temperature (T_c), and melting (ΔH_m) and crystallization (ΔH_c) enthalpies were determined with TA Universal Analysis software with an accuracy of ± 1 °C.

5.2.3 PEO Purification

Commercial PEO 200k contains about 2-3 wt% inorganic fillers such as calcium carbonate and silica²⁰. In order to extract these fillers, the following procedure was employed:

A 3 wt% solution of PEO200k in acetonitrile was prepared. This solution was then bubbled with carbon dioxide for 60 min while stirring. This allowed the filler particles to precipitate. The solution was centrifuged for 30 min at 4000 rpm and the supernatant filtered and poured into glass dishes to let the solvent evaporate. The purity of the PEO was confirmed by thermogravimetric analysis (TGA) TA Q500 by evaluating the weight loss resulting from a heating scan (at 10 °C/min) from 25 °C to 1000 °C. All purified samples showed a weight loss of 100%. All the experiments done for this study used the purified PEO unless otherwise noted.

5.3 Results and Discussion

We examine first the differences between the purified and as received PEO so that proper consideration is taken when analyzing the results and comparing with previous data. Figure 5.1 shows the elastic (G') and viscous (G'') moduli as a function of frequency for the as received and purified PEO 200k material at 80 °C. It can be seen that in both cases the moduli are frequency dependent, G' is lower than G'' at lower frequencies, and they crossover at higher frequencies. The crossover frequency is inversely related to the longest relaxation time of the polymer²¹, these being 3.2×10^{-2} s for the as received material and

1.3×10^{-2} s for the purified PEO. In addition, the absolute values of the moduli are higher for the as received material compared to the purified one.

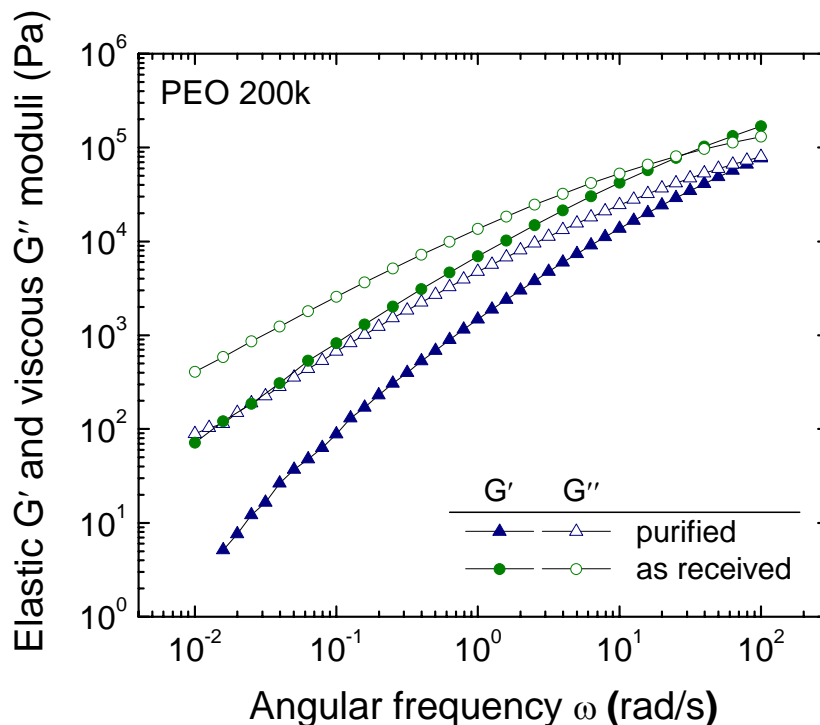


Figure 5.1. Dynamic moduli as a function of frequency for as received and purified PEO 200k at 80 °C.

The differences observed in Figure 5.1 can be attributed to the presence of inorganic filler particles in the commercial PEO. The purification process was intended to remove all inorganic fillers so that the quantities of fumed silica added in this study were absolute. Inorganic fillers such as CaCO_3 and fumed silica (as it will be illustrated later on) have the ability to increase the elasticity of polymers in the melt. In this particular case, it can be seen that not only the material has higher moduli, but also relaxes slower than the purified

PEO. Moreover, the as received PEO has a higher viscosity in the studied frequency range, shorter Newtonian regime and higher shear thinning index.

Figure 5.2 shows dynamic heating and cooling scans at 10 °C/min for the PEO 200k, as received and purified. Differences in the melting behavior and enthalpies can be observed. The purified material shows a slightly lower melting point ($T_m = 64$ °C) and higher enthalpy of melting than the as received material ($T_m = 66$ °C). Again, the presence of the inorganic fillers alters the thermal behavior of the material. In this case, it seems that the fillers act as nucleating agents during the cooling step; the lamellae formed upon crystallization from the melt have the opportunity to grow and this is reflected in T_m .

Based on the previous results, we believe that in order to quantify the effects of additives (such as fumed silica) or secondary phases (such as PEGdm(250)) in the rheological and thermal behavior of PEO, the pre-added fillers need to be removed. The results shown in the following sections correspond to purified PEO, thus the quantities of fumed silica indicated can be considered as absolute quantities.

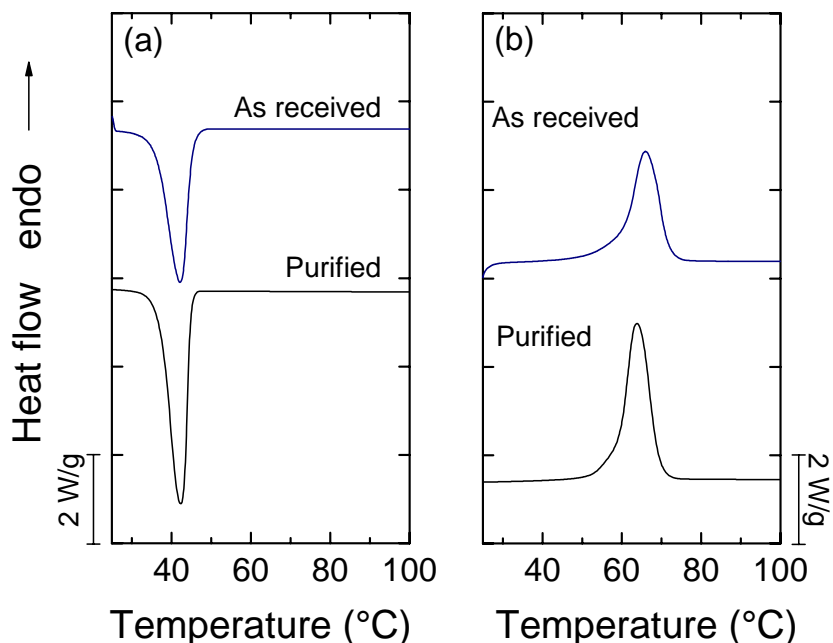


Figure 5.2. Thermal properties of the purified and as received PEO 200k. (a) DSC cooling scans and (b) DSC heating scans. In all cases, the scans were performed at 10 °C/min.

5.3.1 Rheological Properties of Mixed-MW systems

Figure 5.3 presents the rheological behavior of PEO 200k with and without fumed silica. Two types of fumed silica, hydrophilic A200 and hydrophobic R805 were employed. It can be seen that the materials containing fumed silica show a higher elastic modulus than the unfilled counterpart in the entire frequency range studied. Moreover, the frequency dependence of the filled materials is less than for the unfilled one, and the moduli crossover occurs at lower frequencies. For PEO containing FS A200, the moduli are higher than for the PEO with FS R805, and G' of A200 is essentially independent of frequency at lower frequencies. This behavior has been previously reported^{22, 23} and is attributed to the fumed silica forming a flocculated structure in the polymeric matrix. This structure delays the relaxation of the polymer molecules thus increasing viscosity and moduli.

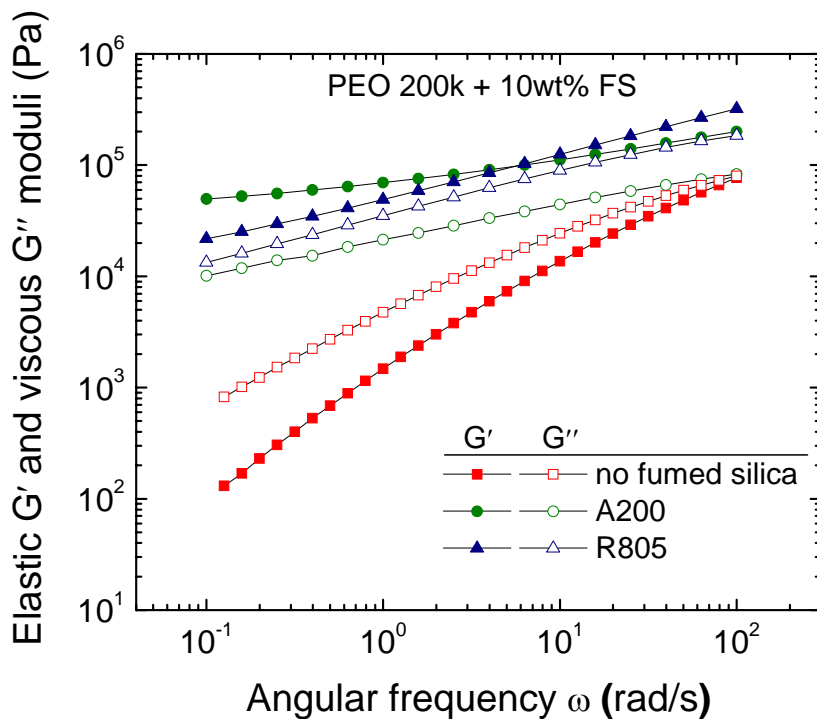


Figure 5.3. Dynamic moduli as a function of frequency for PEO 200k without fumed silica and with 10 wt% of hydrophilic (A200) or hydrophobic (R805) fumed silica. The data were collected at 80 °C.

The fact that A200 effectively shows a frequency-independent G' and that its $\tan(\delta) = G''/G'$ is lower than for R805, suggests that the silanol groups (Si-OH) on the surface of the silica particles are capable of interacting strongly (most likely through hydrogen bonding) with the PEO molecules. As a result, the material behaves more like a solid than the one containing R805. Since the Si-OH on the surface of R805 are covered with octyl chains, the probability of finding a molecule establishing molecular connection with the silica surface is much lower than for the A200 where all the Si-OH groups are available. If the ether oxygens in the PEO backbone are interacting with the silica particles,

not only contacts within the same particle are expected, but also within neighbors; therefore, the highest elasticity of the material and slower response to deformation.

So far, the effect of adding fumed silica to PEO has been discussed. It is of interest to understand the behavior of mixed PEO 200k and PEGdm(250) when fumed silica (hydrophobic or hydrophilic) is added, as the increase in the mechanical properties of filled materials seem to be considerable and suitable for industrial applications. Figure 5.4(a) shows the dynamic moduli for various PEO 200k/PEGdm(250) ratios containing hydrophilic FS. It can be seen that increasing the amount of low-MW component in the blend decreases the moduli, especially at lower frequencies. In addition, the elastic modulus becomes more frequency dependent and the moduli crossover is observed for the 80/20 and 70/30 PEO 200k/PEGdm(250) systems. A plasticization effect, caused by the presence of a larger amount of low-MW component, which has lower elasticity and lower viscosity, explains the observed trend. Figure 5.4(b) shows only elastic modulus as a function of frequency for the same compositions showed in Figure 5.4(a). Notice that the 0/100 PE0200k/PEGdm(250) composition has been added. A dramatic difference between the blends containing more of the high-MW component with respect to the low-MW material (0/100) is observed. The elastic modulus of the 0/100 material shows a perfectly frequency independent behavior, contrary to what is observed for the high-MW rich blends. This can be explained in terms of the role that plays the FS in each case. In high-MW polymers, inorganic fillers act as reinforcing fillers. If they are active fillers, i.e., if they interact with the polymer chains, the increase in modulus is related to the particles bridging each others or simply increasing the relaxation time of the chains. In the case of low-MW liquids, such as PEGmd(250) the

particles form the three-dimensional network, therefore the elasticity is not provided by the polymeric material but by the inorganic particles themselves.

Figure 5.5 illustrates the effect of hydrophobic FS in the rheological properties of mixed-MW systems. It can be seen that similarly to what is observed for the mixed-MW systems containing hydrophilic FS, the addition of the low-MW component reduces the elasticity and decreases the relaxation time of materials. Two very interesting features are observed in Figure 5.5; for the 90/10 PEO 200k/PEGdm(250) blend, contrary to what is observed for the same composition containing A200, the low frequency G' is higher than for the 100/0 composition. Secondly, the moduli of the 80/20 and 70/30 compositions do not crossover in the studied frequency range, indicating that the relaxation time is higher than 100 s. The G' of the 0/100 composition, similarly to the hydrophilic FS case, shows a very small dependence of frequency compared to the high-MW rich blends. Again, we believe that this is due to the fact that the elasticity of the material is given by the fumed silica network rather than the polymeric material, as in the case of high-MW polymer blends.

We believe that the octyl chains on the surface of the hydrophobic FS are responsible for the behavior of the mixed-MW systems containing R805. These chains, though short, can interact with the hydrophobic segments of the PEO and form temporary entanglements that increase the effective number of contact points between PEO chains and silica. This creates a more elastic system, thus a higher modulus compared to the hydrophilic FS-containing blends.

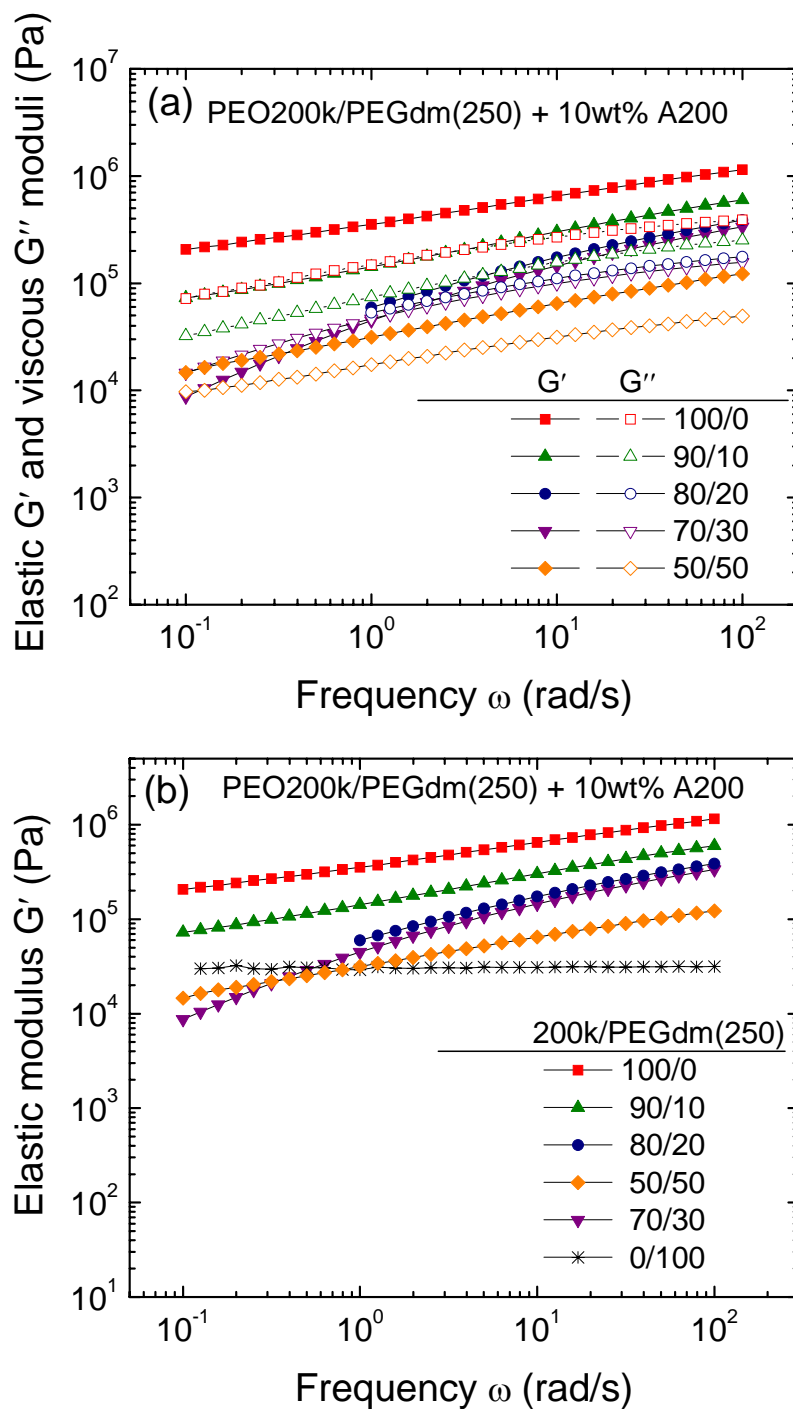


Figure 5.4. Elastic and viscous (a) and elastic (b) moduli as a function of frequency for PEO 200k/PEGdm(250) blends + 10 wt% hydrophilic (A200) FS.

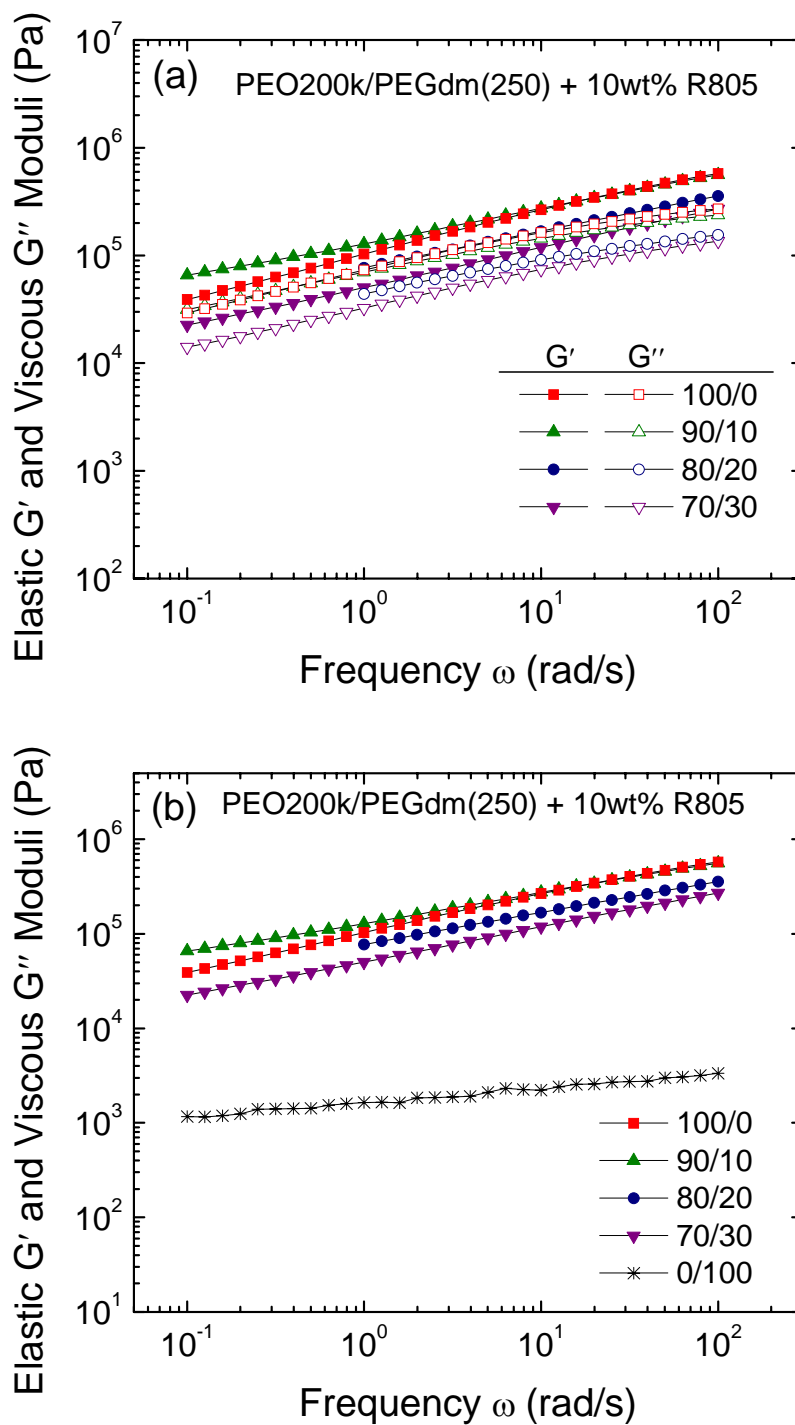


Figure 5.5. Elastic and viscous (a) and elastic (b) moduli as a function of frequency for PEO 200k/PEGdm(250) blends + 10 wt% hydrophobic (R805) FS.

Figure 5.6 summarizes the observed trend for the elastic moduli of mixed-MW systems containing hydrophobic and hydrophilic FS. As previously mentioned, the differences between hydrophilic- and hydrophobic-containing FS are more noticeable at low frequencies. As the low-MW component in the blends is increased, the mixed system containing hydrophobic FS shows higher elasticity than the mixed systems containing A200. Similar results were found by Zhang *et al*²³, who suggested that the more prominent effects at low frequencies are controlled by the fumed silica influencing the relaxation dynamics more than the plateau modulus.

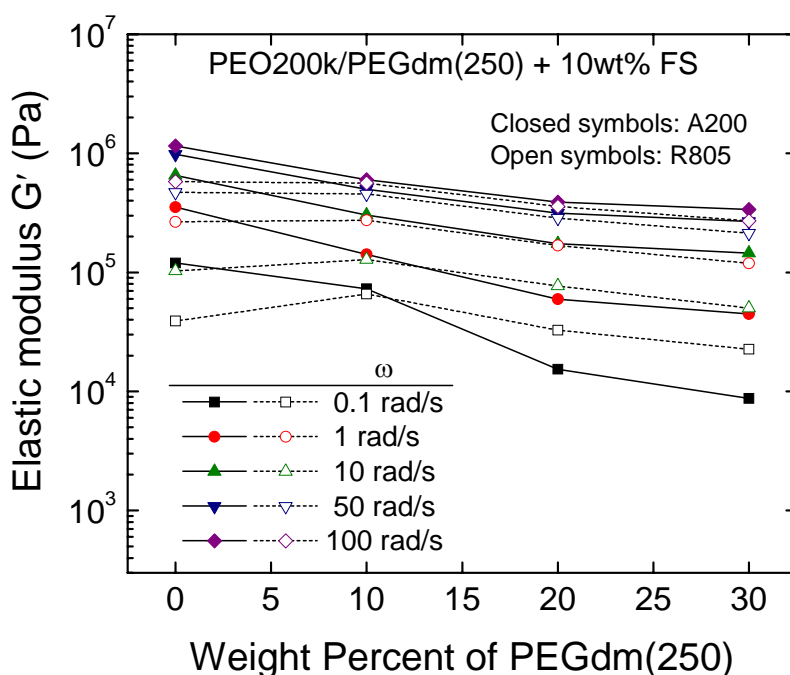


Figure 5.6. Elastic modulus as a function of PEGdm(250) content in blends of PEO 200k/PEGdm(250) + 10 wt% FS at different frequencies (ω). The closed symbols correspond to the blends containing hydrophilic FS (A200) and the open symbols to the blends containing hydrophobic FS (R805). The connecting lines are added to guide the eye.

Figure 5.7 shows oscillatory stress sweeps for the mixed systems containing hydrophilic or hydrophobic FS. Increasing the low-MW component reduces the critical stress for catastrophic failure of the gels (yielding), indicating that the connectivity between silica particles or silica particles and polymer chains, decreases due to the presence of the low-MW component. When compared to each other, the mixed-MW systems containing hydrophilic and hydrophobic FS particles do not show important differences in the yielding behavior. The contribution of the hydrophobic FS is not as important as for the behavior in the linear regime. A possible explanation for this is that if the octyl chains on the fumed silica surface do entangle with the PEO molecules, those entanglements are not capable of sustaining large deformations such as the ones imposed by the increase in stress amplitude shown in the experiments in Figure 5.7.

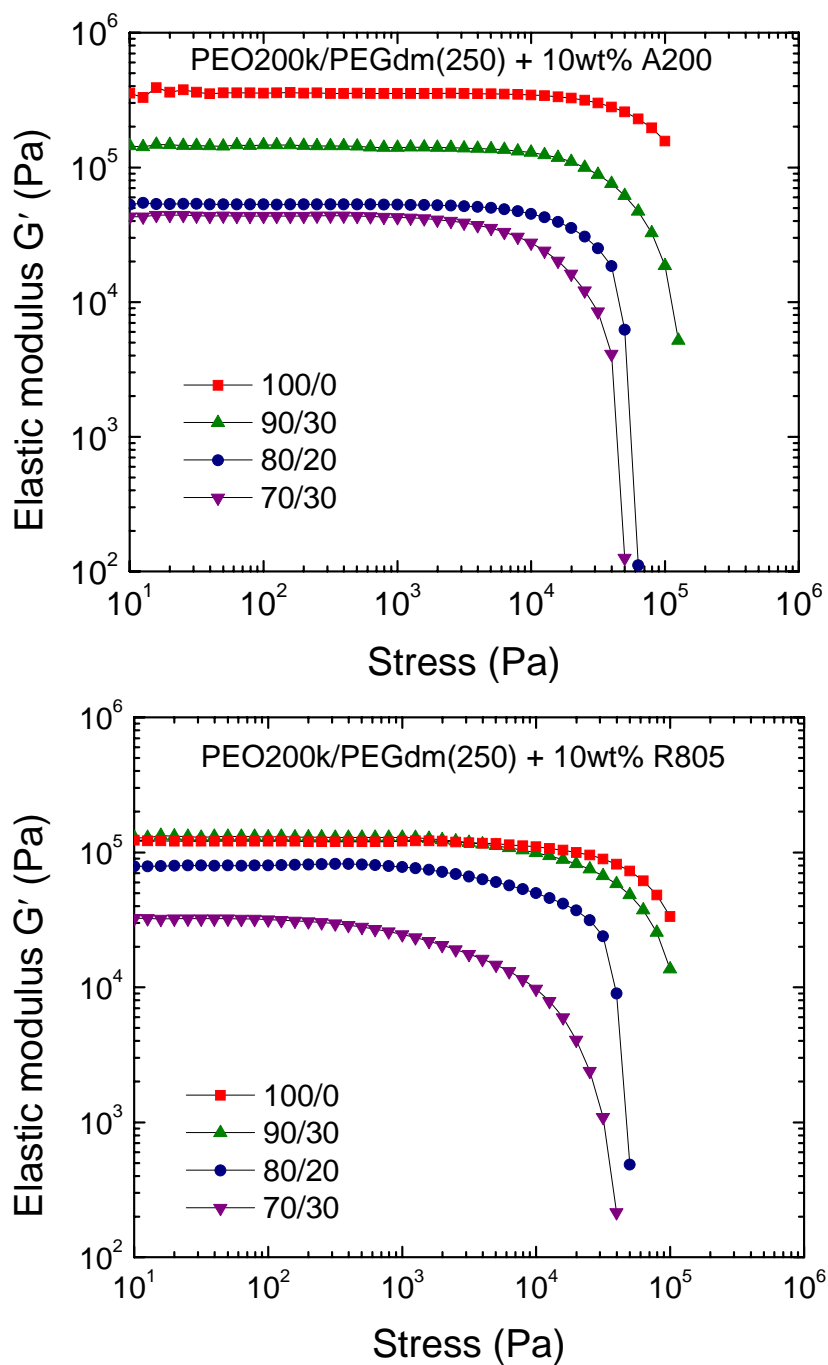


Figure 5.7. Elastic modulus versus stress amplitude for mixed systems containing hydrophilic (A200) and hydrophobic FS. Experiments were done at 80 °C.

5.3.2 Thermal Properties of Mixed-MW Systems

Figure 5.8 (a) and (b) show dynamic cooling and heating DSC scans, respectively for blends of high- and low-MW PEO200k and PEGdm(250) containing hydrophilic fumed silica. The addition of the low-MW component to the high-MW PEO causes a decrease in the crystallization and melting temperatures. The decrease in the melting point is almost linear, indicating that the mixing is additive for the composition range studied. In spite of the fact that there is a decrease in the melting and crystallization temperatures, two melting endothermic signals are observed, indicating that there is segregation of the two polymeric phases due to the marked difference in molecular weights.

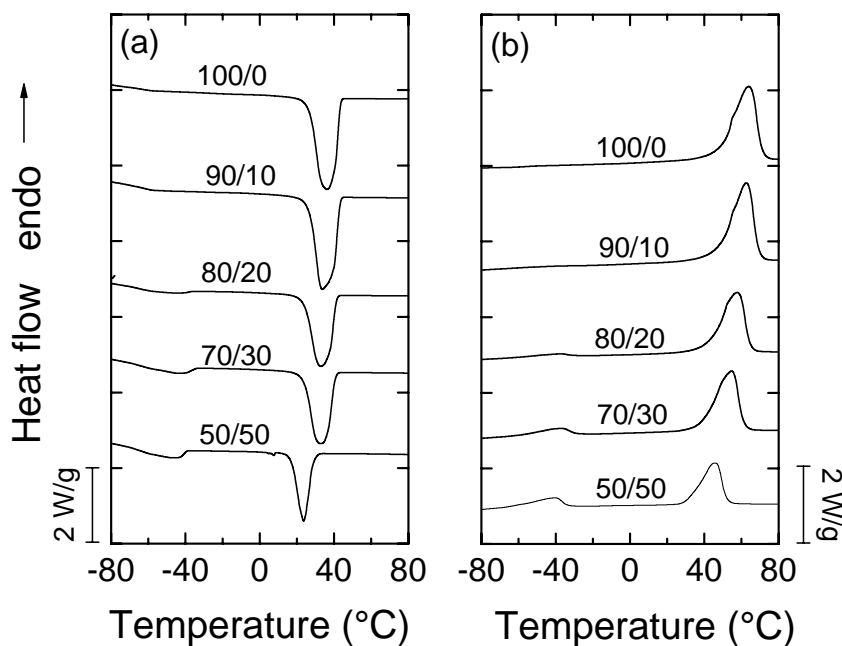


Figure 5.8. Thermal properties of different ratios of mixed-MW (PEO 200k/PEGdm(250)) containing hydrophilic FS. (a) DSC cooling scans and (b) DSC heating scans. In all cases, the scans were performed at 10 °C/min.

Although the mixing of PEO200k and PEGdm(250) is enthalpically favorable, there are several other reasons that make this system immiscible. For instance, segregation causes the two polymeric phases to crystallize in separate crystals (lamellae); this is further enhanced by the fact that the short chains of PEGdm(250) tend to crystallize in the form of extended chains while the long PEO200k chains crystallize as folded chains. Similar results have been found for blends of PEO with different molecular weights²⁴. Cimmino *et al*²⁵. observed that as the molecular weight of the low-MW component decreased, segregation was more likely to occur. They investigated three different PEO MWs and their blends: 2, 20, and 200 kg/mol. The results observed were attributed to differences in the crystallization kinetics of the two polymeric phases causing the aforementioned segregation phenomenon. If the segregation was more marked for the 2/200 kg/mol blend, our result for the 0.250/200 kg/mol blend (or PEGdm(250)/PEO200k blend) must be even more likely to observe segregation.

The previously discussed results for the crystallization and melting behavior of PEO mixed-MW blends indicate that the system is not miscible in the solid state. Whether or not the two polymeric phases are miscible in the melt is out of the reach of this project as more involved experiments such as neutron scattering in the melt phase are required to draw such conclusions.

5.3.3 Solution Mixing versus Melt mixing

The state of dispersion in filled systems as well as the morphology of polymer blends is affected by the compounding methodology²⁶. In some cases intensive shear in the melt

state is necessary to breakdown particles. In some other cases, mixing at the molecular level, such as in solution is more convenient to develop certain morphology that could not be obtained otherwise. In general, melt mixing of polymers, because of the high shear level and elevated temperatures, tends to mechanically or thermally degrade the molecules, while in solution mixing, degradation is not important.

Figure 5.9 shows the dynamic moduli for the 80/20 PEO 200k/PEGdm(250) + LiTFSI (O:Li 1:20) as a function of frequency. The blends with and without hydrophilic fumed silica were mixed in solution or in the extruder. It can be seen that in all cases, the blends mixed in the melt presented lower rheological properties, i.e. lower moduli. It is evident that mechanical and/or thermal degradation has an important contribution to the final morphology of the systems. The advantage of melt mixing over solution mixing is the fact that the materials are solvent-free and other properties of interest such as ionic conductivity can benefit from this fact.

As a way to study the effects of either solution or melt mixing in the electrochemical properties of the blends, we evaluated the ionic conductivity as a function of temperature for materials that were solution or melt mixed. Figure 5.10 illustrates the differences obtained for samples with and without hydrophilic fumed silica. It can be seen that the samples mixed in solution showed slightly lower ionic conductivity compared to the materials mixed in solution. We attribute these results to the fact that in the melt, the chains can either be broken down into smaller chains or the microstructure better dispersed. These two possibilities show as a result, a material with lower elastic moduli may possess lower degree of crystallinity or simply shorter chains with improved mobility

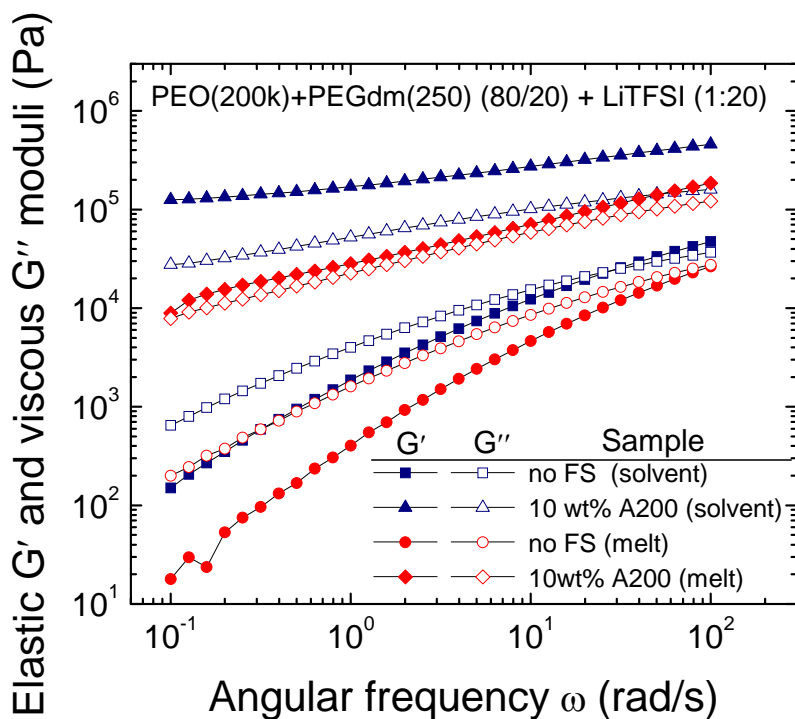


Figure 5.9. Effect of mixing method (solution versus melt mixing) on the rheological properties of mixed-MW systems. All the experiments were performed at 80 °C.

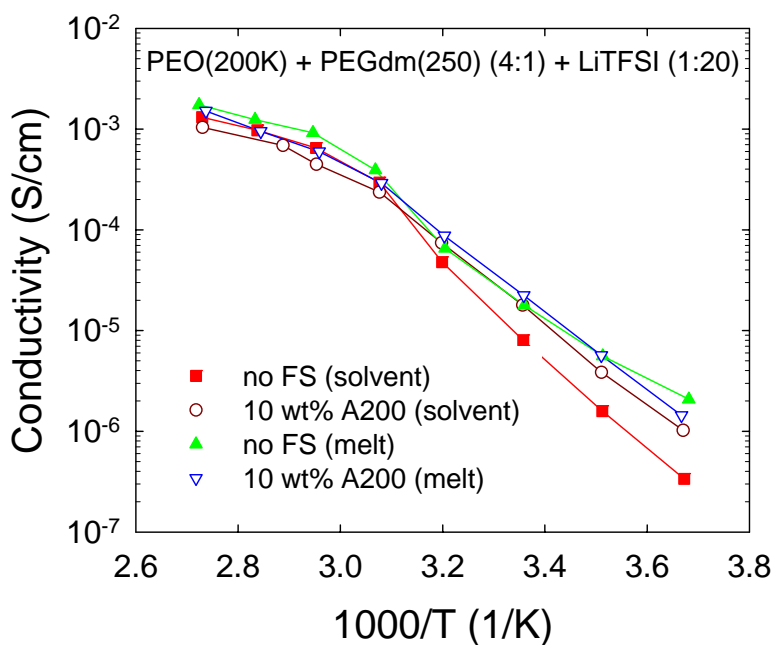


Figure 5.10. Ionic conductivity as a function of the inverse temperature.

5.4 Conclusions

Mixtures of high- and low-MW poly(ethylene oxide) and fumed silica (hydrophobic or hydrophilic) prove to be an alternative way of plasticizing the high-MW component. Adding PEGdm(250) to the PEO 200k decreases the elastic modulus. The materials containing 20 and 30 wt% PEGdm(250) and A200 show moduli crossover in the range of frequencies evaluated, whereas the materials containing R805 do not show moduli crossover. The mechanism through which the fillers reinforce the high- or low-MW PEOs is reflected in the frequency spectra. For the high-MW polymer and the high-MW rich compositions, the particles are active and increase the relaxation time of the material. On the other hand, for the low-MW component, the reinforcing occurs through an interconnected network of fumed silica particles. This network is responsible for the elasticity of the “reinforced” material.

Two well defined crystallization and melting endotherms are observed for the mixed-MW PEOs containing fumed silica in the range of compositions studied; this suggests that the systems are immiscible in the solid phase. In addition, a decrease in the crystallization and melting peaks of the high-MW component is observed as the content of the low-MW component (PEGdm(250)) increases. Crystallization and melting peaks follow an additive mixing behavior as a function of composition.

5.5 References

1. Armand, M., The History of Polymer Electrolytes. *Solid State Ionics* 1994, 69, (3-4), 309-319.
2. Baril, D.; Michot, C.; Armand, M., Electrochemistry of liquids vs. solids: Polymer electrolytes. *Solid State Ionics* 1997, 94, (1-4), 35-47.

3. Aihara, Y.; Appetecchi, G. B.; Serosati, B.; Hayamizu, K., Investigation of the ionic conduction mechanism of composite poly(ethyleneoxide) PEO-based polymer gel electrolytes including nano-size SiO₂. *Physical Chemistry Chemical Physics* 2002, 4, (14), 3443-3447.
4. Back, D. M.; Schmitt, R. L., Ethylene oxide polymers. In *Encyclopedia of polymer science and technology*, Mark, H. F., Ed. John Wiley: Hoboken, N.J., 2003; Vol. 9.
5. Yang, X. Q.; Lee, H. S.; Hanson, L.; McBreen, J.; Okamoto, Y., Development of a new plasticizer for poly(ethylene oxide)-based polymer electrolyte and the investigation of their ion-pair dissociation effect. *Journal of Power Sources Proceedings of the Seventh International Meeting on Lithium Batteries* 1995, 54, (2), 198-204.
6. Kelly, I.; Owen, J. R.; Steele, B. C. H., Mixed polyether lithium-ion conductors. *Journal of Electroanalytical Chemistry* 1984, 168, 467-478.
7. Riley, M.; Fedkiw, P. S.; Khan, S. A., Transport properties of lithium hectorite-based composite electrolytes. *Journal of the Electrochemical Society* 2002, 149, (6), A667-A674.
8. Chen, H. W.; Lin, T. P.; Chang, F. C., Ionic conductivity enhancement of the plasticized PMMA/LiClO₄ polymer nanocomposite electrolyte containing clay. *Polymer* 2002, 43, (19), 5281-5288.
9. Ramsay, J. D. F., Colloidal properties of synthetic hectorite clay dispersions I. Rheology. *Journal of Colloid and Interface Science* 1986, 109, (2), 441-447.
10. Fan, J.; Fedkiw, P. S., Composite electrolytes prepared from fumed silica, polyethylene oxide oligomers, and lithium salt. *Journal of the Electrochemical Society* 1997, 144, (2), 399-408.
11. Li, Y. X.; Fedkiw, P. S.; Khan, S. A., Lithium/V6O13 cells using silica nanoparticle-based composite electrolyte. *Electrochimica Acta* 2002, 47, (24), 3853-3861.
12. Raghavan, S. R.; Riley, M. W.; Fedkiw, P. S.; Khan, S. A., Composite polymer electrolytes based on poly(ethylene glycol) and hydrophobic fumed silica: Dynamic rheology and microstructure. *Chemistry of Materials* 1998, 10, (1), 244-251.

13. Walls, H. J.; Fedkiw, P. S.; Zawodzinski, T. A.; Khan, S. A., Ion transport in silica nanocomposite electrolytes. *Journal of the Electrochemical Society* 2003, 150, (3), E165-E174.
14. Walls, H. J.; Riley, M. W.; Fedkiw, P. S.; Spontak, R. J.; Baker, G. L.; Khan, S. A., Composite electrolytes from self-assembled colloidal networks. *Electrochimica Acta* 2003, 48, (14-16), 2071-2077.
15. Walls, H. J.; Zhou, J.; Yerian, J. A.; Fedkiw, P. S.; Khan, S. A.; Stowe, M. K.; Baker, G. L., Fumed silica-based composite polymer electrolytes: synthesis, rheology, and electrochemistry. *Journal of Power Sources* 2000, 89, (2), 156-162.
16. Zhou, J.; Fedkiw, P. S.; Khan, S. A., Interfacial stability between lithium and fumed silica-based composite electrolytes. *Journal of the Electrochemical Society* 2002, 149, (9), A1121-A1126.
17. Hou, J.; Baker, G. L., Photopolymerization of methacrylate-functionalized surface with alkyl methacrylates in low MW peo-LICLO4 matrix. *Abstracts of Papers of the American Chemical Society* 1999, 217, U499-U499.
18. Yerian, J. A.; Fedkiw, P. S.; Khan, S. A., Crosslinkable fumed silica-based nanocomposite electrolytes: role of methacrylate monomer in formation of crosslinked silica network. *Journal of Power Sources* 2004, 135, (1-2), 232-239.
19. Hou, J.; Baker, G. L., Preparation and characterization of cross-linked composite polymer electrolytes. *Chemistry of Materials* 1998, 10, (11), 3311-3318.
20. Polyox(TM) Material Safety Data Sheet. In *The Dow Chemical Company database*: 2004.
21. Macosko, C. W., *Rheology: Principles, Measurements and Applications*. VCH: New York, NY, 1994.
22. Yerian, J. A. Nanocomposite polymer electrolytes: Modulation of mechanical properties using surface-functionalized fumed silica. Ph.D. Thesis, North Carolina State University, Raleigh, NC, 2003.
23. Zhang, Q.; Archer, L. A., Poly(ethylene oxide)/silica nanocomposites: Structure and rheology. *Langmuir* 2002, 18, (26), 10435-10442.

24. Godovsky, Y. K.; Garbar, N. M.; Slonimsky, G. L., Effect of molecular-weight on crystallization and morphology of poly(ethylene oxide) fractions. *Journal of Polymer Science Part C-Polymer Symposium* 1972, 38, 1.
25. Cimmino, S.; Greco, R.; Martuscelli, E.; Nicolais, L.; Silvestre, C., Blends of poly(ethylene oxide) samples of different molecular weights: thermal and mechanical properties. *Polymer* 1978, 19, (9), 1079-1082.
26. Utracki, L. A., *Polymer alloys and blends : thermodynamics and rheology*. Hanser: New York, NY, 1990; p xi, 356.

6

Conclusions and Recommendations

6.1 Conclusions

The studies on colloidal gels of fumed silica (FS) presented in this dissertation have demonstrated the effects of particle surface chemistry and physico-chemical properties of the medium in which the particles are dispersed, on the development of a complex fluid microstructure. In particular, colloids containing fumed silica nanoparticles dispersed in polyethers, poly(ethylene oxide) PEO and blends of low-molecular weight polyethers and PEO were studied. In addition, blends of fumed silica nanoparticles with different surface chemistries were prepared and characterized as a function of temperature and in terms of their rheological properties.

6.1.1 Fumed silica forms gels that exhibit a yield stress

This work developed an approach to accurately determine the yield stress of particulate materials as well as the occurrence of wall slip. Additionally, by combining the paint line mark technique with flow visualization, yield stress and wall slip could be effectively distinguished. This is a very important finding as one of the major problems in yield stress determination is the misinterpretation due to wall slip¹⁻⁴. The suggested approach not only provided a reliable yield stress determination methodology, but also facilitated the study of the effects that the characteristics of the surface where shear occurs have on certain colloidal gels. We observed that specific interactions between the rheometer plate surfaces and the particles contained in the gel can promote or prevent wall slip. Gels containing hydrophobic nanoparticles can sustain higher stress prior to slipping if the surface where the material is sheared is hydrophobic. Moreover, the time required to observe wall

slip on this surface at a stress value within the linear viscoelastic region of deformation is longer than the one obtained with hydrophilic surfaces. This particular result expands the processability window of the material since the flow can be controlled by simply altering the surface properties.

6.1.2 Temperature affects the flow properties of fumed silica gels in an unexpected manner

In general, higher temperatures reduce the relaxation time, and this in turn decreases the rheological properties of the material, i.e., viscosity and shear modulus. Contrary to what we expected, we observed an anomalous behavior of the rheological properties of gels of hydrophilic fumed silica particles in poly(ethylene glycol) dimethyl ether PEGdm(250) with temperature. That is, the gel modulus increased as a function of temperature; in addition, the increase in elasticity was an irreversible process and the magnitude of the increase initially depended on time, and ultimately asymptoting to a constant value. In contrast, hydrophobic fumed silica does not show this anomalous behavior; the modulus of gels containing hydrophobic fumed silica particles in PEGdm(250) decreased as a function of temperature and upon cooling after heating, the modulus of the material returned to its initial value. This phenomenon opens the possibility of modifying the mechanical resistance of these hydrophilic fumed silica gels by just adding a simple, inexpensive step involving heating during their preparation.

6.1.3 Mixtures of hydrophobic and hydrophilic fumed silica particles form independent microstructures when dispersed in a liquid

Understanding mixtures of different particles remains a challenge; the results obtained here indicate that for mixtures of hydrophobic and hydrophilic fumed silica particles, unfavorable interactions make the properties of the mixed fumed silica colloids show a negative deviation from the log-additive mixing rule. Previous studies conducted by Yerian⁵ showed a similar behavior. We observed that in moderately hydrogen bonding liquids, such as PEGdm(250), hydrophobic and hydrophilic fumed silica particles form independent networks resulting in the negative deviation in the log-additive mixing rule. The behavior of these gels as a function of temperature follow the same trend as the major component; this is, gels containing high hydrophilic/hydrophobic ratio exhibited an increase in modulus as a function of temperature, whereas low hydrophilic/hydrophobic ratio showed the opposite trend. In addition, the inversion of the behavior occurred at concentrations of hydrophilic fumed silica lower than 50/50 hydrophilic FS/hydrophobic FS.

In highly polar solvents, such as poly(ethylene glycol) PEG(200), we observed that the material behaved solid-like even for compositions of hydrophilic/hydrophobic fumed silica of 75/25. This is a very interesting result that opens multiple possibilities for those applications where it is necessary to have a large concentration of silanol groups on the silica surface and at the same time obtain solid-like behavior. The presence of hydrophilic fumed silica by itself in this type of solvents is not able to provide such an elastic response; however, the presence of as low as 25% of hydrophobic particles can modify the behavior.

6.1.4 Fumed silica acts as a reinforcing filler in blends of high- to low-MW PEO ratio but forms a three-dimensional physical network as the ratio decreases

Blends of low- and high-molecular weight polymers with similar chemical structures but very different molecular weights were studied with the aim to plasticize the high-molecular weight counterpart. We found that in a composite of fumed silica (hydrophobic or hydrophilic) in PEO 200 kg/mol, adding PEGdm(250) decreased the elastic and viscous components of the modulus. This indicated plasticization of the matrix as a function of the low-molecular weight component in the blend. This result is of special interest in areas such as polymer electrolytes where the ionic conductivity may be limited by the presence of ordered structures (crystals) in the material at low temperatures. Mixing procedures have to be taken into account with regards to dispersibility, mechanical degradation, solvent evaporation or solvent interaction with the product, among others. High- and low-molecular weight PEOs were mixed in solution and in the melt. The ionic conductivity of the blend was slightly higher than that obtained for the same system mixed in solution. However, the elastic modulus of the materials mixed in solution was higher than for the melt mixed material.

6.2 Recommendations

6.2.1 Biocompatible PEO-silica hybrids

Conventional materials employed in the construction of endovascular medical devices are, for the most part, incompatible with blood and plasma proteins as they are not compatible with plasma components⁶. Surface engineering is a tool for modifying and adapting materials to specific biological applications. Among the many applications and properties of fumed silica, the ability to modify the surface of the particles by relatively simple techniques makes fumed silica a very interesting candidate for surface-modified biocompatible applications. Eglin *et al.*⁷ studied bioactive glass (CaO-P₂O₅-SiO₂) and silica-collagen composites in terms of their apatite forming ability. They conceived these hybrids for materials employed as bone substitutes; these materials should not only present the usual biocompatibility and nonantigenic properties, but also exhibit bioactive and mechanical properties matching those of implanted tissues during all steps of bone regeneration. They concluded that these hybrids exhibit *in vitro* osteoconductivity properties, whereas their components alone do not. This synergetic effect was attributed to the ability of the protein to bind calcium ions, which can further associate with silicic acid to form a bioactive layer.

In view of these results, we propose using fumed silica to prepare fumed silica-collagen hydrogels. By embedding the fumed silica in the collagen matrix, not only would the osteoconductivity properties of the material improve, but also the mechanical properties (modulus under tension and compression, ultimate fracture, and hardness) would increase with respect to the pure collagen. This improvement in mechanical properties through

interactions of the collagen and the silica at the nanometer level is highly desirable in bone-replacing materials.

6.2.2 In-depth study of the dispersibility of fumed silica in formulations to be utilized as composite polymer electrolytes

In this work, the effect of mixing in solution and in the melt showed differences not only in the rheological behavior of the materials, but also in their ionic conductivities (see Chapter 5). If the solvent in which the material is prepared has an effect on the properties of the end product, by changing either the solvent or the mixing apparatus, the mechanical and electrochemical properties could be improved. In addition, for those systems containing high-molecular weight polymers (or their blends with low-molecular weight ones), the crystallization procedure (thermal or solvent evaporation history) will have a tremendous effect on the end properties of the composites. In this sense, we propose an extensive study of the mixing (compounding) variables involved in solvent mixing, melt mixing and supercritical solvent mixing. This last method will attempt to better disperse the fumed silica in the polymeric matrix through the use of supercritical carbon dioxide. Additionally, the use of high-pressure or supercritical carbon dioxide will reduce the viscosity of the material. This would eliminate the use of volatile organic solvents or plasticizers and allow processing these materials at lower temperatures.

6.2.3 Study of the rheological properties of high- and low-molecular weight PEO blends at low temperatures

The dynamic mechanical behavior of high- and low-molecular weight (MW) PEO blends containing fumed silica is an important measure of the strength of the material. By using a dynamic mechanical temperature analyzer (DMTA) information about the properties (real and complex tensile modulus and phase angle) of the composites can be obtained at very low temperatures (~ -140 °C). In addition, if $\tan(\delta)$, i.e., the ratio between the viscous (imaginary) to the elastic (real) modulus is plotted as a function of temperature, information about the segmental mobility and the temperature at which each segment or group of segments start to move can be associated to microstructure of the composites. This piece of information is very important as some of the applications for these materials could involve performance at low temperatures. An understanding of the change in modulus as a function of temperature is needed for these systems.

6.2.4 Novel organic-inorganic hybrids for use as composite resin cements

Poly(methyl methacrylate) PMMA has been used as a cement for fixing metallic and polymeric implants to the surrounding bones and for filling bone defects. This polymer however does not bind to the bone tissue, and detachment or fracture occurs in relatively short periods of time⁸. One of the advantages of fumed silica is that surface treatment allows for the particle to be dispersible in specific matrices. This makes the inorganic filler more compatible with the polymeric matrix, which translates into higher mechanical properties and resistance to failure at the resin-filler interface. If in addition to the

reinforcing capability, the fumed silica can contain groups capable of initiating the polymerization reaction⁹ necessary for the setting of the resin during the tooth repair, an improved highly bone compatible, mechanically resistant, self-polymerizable organic-inorganic hybrid can be produced. We suggest a dual functional fumed silica particle containing PMMA-like chains and UV crosslinkable acrylate or methacrylate groups on the surface. The PMMA-like chains will improve the compatibility with the polymeric resin (usually PMMA) and the crosslinkable groups will control the curing of the composite. It is important to recognize that the curing process should involve UV light so that the material can be polymerized *in situ* and in very short periods of time.

6.3 References

1. Barnes, H. A., A Review of the Slip (Wall Depletion) of Polymer-Solutions, Emulsions and Particle Suspensions in Viscometers - Its Cause, Character, and Cure. *Journal of Non-Newtonian Fluid Mechanics* 1995, 56, (3), 221-251.
2. Russel, W. B.; Grant, M. C., Distinguishing between dynamic yielding and wall slip in a weakly flocculated colloidal dispersion. *Colloids and Surfaces a-Physicochemical and Engineering Aspects* 2000, 161, (2), 271-282.
3. Walls, H. J.; Caines, S. B.; Sanchez, A. M.; Khan, S. A., Yield Stress and Wall Slip Phenomena in Colloidal Silica Gels. *Journal of Rheology* 2003, 47, (4), 847-868.
4. Buscall, R.; McGowan, J. I.; Mortonjones, A. J., The Rheology of Concentrated Dispersions of Weakly Attracting Colloidal Particles with and without Wall Slip. *Journal of Rheology* 1993, 37, (4), 621-641.
5. Yerian, J. A. Nanocomposite polymer electrolytes: Modulation of mechanical properties using surface-functionalized fumed silica. Ph.D. Thesis, North Carolina State University, Raleigh, NC, 2003.

6. Yang, Z.; Galloway, J. A.; Yu, H., Protein interactions with poly(ethylene glycol) self-assembled monolayers on glass substrates: diffusion and adsorption. *Langmuir* 1999, 15, 8405-8411.
7. Eglin, D.; Maalheem, S.; Livage, J.; Coradin, T., In vitro apatite forming ability of type I collagen hydrogels containing bioactive glass and silica sol-gel particles. *Journal of Materials Science: materials in medicine* 2006, 17, 161-167.
8. Saha, S.; Pal, S., Mechanical properties of bone cement: A review. *Journal of Biomedical Materials Research* 1984, 18, (4), 435-462.
9. Yerian, J. A.; Fedkiw, P. S.; Khan, S. A., Crosslinkable fumed silica-based nanocomposite electrolytes: role of methacrylate monomer in formation of crosslinked silica network. *Journal of Power Sources* 2004, 135, (1-2), 232-239.